IN THE UNITED STATES PATENT AND TRADEMARK OFFICE

APPLICANT: Zhou, Ming-Ming

EXAMINER: Lucas, Zachariah

SERIAL NO.: 09/784,553

ART UNIT: 1648

Filed: February 16, 2001

For: METHODS FOR IDENTIFYING MODULATORS OF BROMODOMAINS

DECLARATION UNDER 37 C.F.R. 1.132

COMMISSIONER FOR PATENTS
P.O. BOX 1450
ALEXANDRIA, VIRGINIA 22313-1450

SIR:

I, MING-MING ZHOU, hereby declare and state that:

1. I am a Professor in the Department of Physiology and Biophysics at Mt. Sinai School of Medicine and a Director in the Translational Chemical Biology Center at Mt. Sinai School of Medicine, having received my Ph.D. degree in Chemistry from Purdue University in 1993. After that I was a postdoctoral fellow at Abbott Laboratories in Chicago, Illinois.

2. My full curriculum vitae is attached hereto as Exhibit A.

3. My principal area of research is Structural Biology, and among other positions I serve as reviewer in numerous scientific journals including Analytic Biochemistry, Biophysical Journal, EMBO Journal, European Journal of Biochemistry, FEBS Letters, GENE, JACS, Journal of Molecular Biology, Molecular Cell, Nature Structure Biology, PNAS, Protein Science, Science, and Structure. I also have served as reviewer for funding agencies, including American Cancer Society, American Heart Association, The

Israel Science Foundation, National Science Foundation, NIH and the European Commissions.

4. In the course of my activities, I have been listed as inventor on several patent applications, including the one noted above entitled "METHODS FOR IDENTIFYING MODULATORS OF BROMODOMAINS", having U.S. Serial Number 09/784,553, which claims priority to U.S. application Serial Number 09/510,314, filed on February 22, 2000.

5. I have reviewed the disclosure of the present application, with particular emphasis on the utility of the bromodomains and more particularly with respect to the use of this information for identification of small molecules that may block the interaction of the bromodomain with its ligand in support of enablement of the claims. Given the sequences provided in the present application, and the three dimensional structure of the bromodomain as well as the three dimensional structure of the bromodomain and its binding partner, it would be possible for one skilled in the art to use this information to screen for compounds or small molecules that may act to agonize or antagonize this interaction. In my opinion, the disclosures of this current application are sufficient to enable one skilled in the art to make or use the invention as described therein and concomitantly provide to the practitioner teachings that could be applied for the indicated purposes.

6. In this regard, and in corroboration of the disclosure of this current application, I have conducted additional experiments in my own laboratory to further confirm the disclosure in this application and which further supports the utility of the three dimensional structural information and of the sequences described in this application for identification of small molecule inhibitors of bromodomain binding to its ligand. Particularly, my laboratory has conducted experiments, which demonstrate a new class of small molecules that function to interfere with the binding of the bromodomain in the transcriptional coactivator PCAF with the acetylated lysine 50 in the HIV *trans*-activator

Tat. The rationale for these experiments and the results are described below and in the attached preprint (Exhibit B) from the Journal of the American Chemical Society.

7. It is known that transcription of the integrated HIV provirus is regulated by the concerted action between cellular transcription factors and a unique viral trans-activator Tat. Tat binds to a viral RNA TAR and recruits cyclin T1 and cyclin dependent kinase 9 that hyper-phosphorylates and enhances elongation efficiency of the RNA polymerase II. Tat transactivation requires acetylation of its lysine 50 and recruitment of histone lysine acetyltransferase transcriptional coactivators for remodeling nucleosome that contains the integrated proviral DNA. Our recent studies show that Tat co-activator recruitment requires its acetylated lysine 50 (AcK50) binding to the bromodomain (BRD) of the coactivator PCAF. Microinjection of anti-PCAF BRD antibody blocks Tat transactivation. These data suggest that Tat/PCAF recruitment via a BRD-AcK binding is essential for HIV transcription. Furthermore, this information points to the fact that this may serve as a new target for designing drugs that interfere with HIV replication. That is, therapeutic intervention at the stage of HIV gene expression may complement existing therapies to interfere with virus production.

8. We have used the information disclosed in the present patent application to screen for molecules that block the interaction of the bromodomain of the PCAF coactivator with the acetylated lysine 50 on the Tat molecule. In particular, we conducted NMR-based chemical screening for the BRD by monitoring ligand-induced protein signal changes in 2D ^{15}N-HSQC spectra. This screening resulted in the identification of a novel class of molecules as shown in Table 1 of the attached reference (Zeng et al.). The compounds identified bind the PCAF BRD with an affinity comparable to that of the Tat-AcK50 peptide.

9. We then synthesized a series of analogs to probe the structure activity relationship (also in Table 1). We assessed their binding to the PCAF BRD by determining the IC_{50} in an ELISA assay, whereby a compound competes against a biotinylated Tat-AcK50 peptide for binding to the GST-fusion BRD immobilized to

glutathione-coated 96 well microtiter plates. Twenty four analogs/derivatives have been identified having the R_1 and R_2 groups as shown in Table 1.

10. The results shown here provide proof of both the utility of the present application, as well as the enablement of the invention. These results fully support our earlier data provided in the present application. Furthermore, the data presented here, as well as the data provided in the present application, fully support the enablement and utility of the three dimensional structure of the bromodomain and the complex formed between the bromodomain and its ligand (acetyl lysine), as well as the sequences provided.

11. The advantages of this technology would be i) the identification of novel therapeutics for treatment of viral infections such as HIV or cancer ii) the three dimensional structure of the bromodomain and the bromodomain/ligand complex and relevant sequences for the binding sites are provided, thus allowing for computer assisted drug design and screening for small molecule agonists or antagonists.

I hereby declare that all statements made herein of my own knowledge are true and that all statements made on information and belief are believed to be true; and further, that these statements were made with the knowledge that willful false statements and the like so made are punishable by fine or imprisonment, or both, under Title 18 of the U.S. Code, Section 1001, and that such willful false statements may jeopardize the validity of this application or any patent issuing thereon.

Dated: 11/8/2004

Ming-Ming Zhou

Curriculum Vitae (updated 11/2004)

Ming-Ming Zhou, Ph.D.

Structural Biology Program
Department of Physiology and Biophysics
Mount Sinai School of Medicine
1425 Madison Avenue, Box 1677
New York, NY 10029

Phone: (212) 659-8652
Fax: (212) 849-2456
e-mail: ming-ming.zhou@mssm.edu
U.S. Citizen

EDUCATION:

1993	Ph.D.	Chemistry	Purdue University, Indiana
1988	M.S.	Chemistry	Michigan Technological University, Michigan
1984	B.S.	Chemical Engineering	East China University of Science & Technology, Shanghai, PRC

ACADEMIC APPOINTMENTS:

1993 – 1996	Postdoctoral Fellow, Abbott Laboratories, Chicago, IL (Dr. Stephen W. Fesik)
1997 – 2000	Assistant Professor, Structural Biology Program, Dept. of Physiology and Biophysics, Mount Sinai School of Medicine (MSSM), New York, NY
1999 – 2000	Assistant Professor, The Derald H. Ruttenberg Cancer Center, MSSM
2001 – 2003	Associate Professor, Structural Biology Program, Dept. of Physiology and Biophysics, and The Derald H. Ruttenberg Cancer Center, MSSM
2003 – 2004	Associate Professor with tenure, Structural Biology Program, Dept. of Physiology and Biophysics, and The Derald H. Ruttenberg Cancer Center, MSSM
2004 –	Professor with tenure, Structural Biology Program, Dept. of Physiology and Biophysics, and The Derald H. Ruttenberg Cancer Center, MSSM
2004 –	Director, Translational Chemical Biology Center, MSSM

HONORS AND AWARDS:

1999 – 2001	American Cancer Society Young Investigator Award
2003	GlaxoSmithKline Drug Discovery and Development Award

OTHER PROFESSIONAL ACTIVITIES:

Society Memberships

American Association for the Advancement of Science (1993 – present)
American Chemical Society (1999 – present)
Biophysical Society (1999 – present)
American Society for Biochemistry and Molecular Biology (2001 – present)
New York Academy of Sciences (2003 – present)

Journal Reviews

Analytic Biochemistry	GENE	PNAS
Biophysical Journal	JACS	Protein Science
EMBO Journal	Journal of Molecular Biology	Science
European Journal of Biochemistry	Molecular Cell	Structure
FEBS Letters	Nature Structure Biology	

Grant Reviews

American Cancer Society
American Heart Association
European Commissions
The Israel Science Foundation
National Science Foundation
NIH (*Ad hoc* for BBCB, BPC-B, and CDF-2Special Emphasis Panel)

Committee and Administrative Services

MSSM, Graduate Student (PhD Program) Admissions Committee (1999 – present)
MSSM, MSTP (MD/PhD Program) Admissions Committee (2000 – 2003)
MSSM, Dean's Share Research Facility Advisory Council (Mass Spectrometry) (2000)
New York Structural Biology Center, NMR Facility Negotiating Committee (2000 – 2001)
New York Structural Biology Center, NMR Operation Committee (2000 – present)
MSSM, Structural Biology Faculty Recruitment Committee (2002 – 2003)
MSSM, Steering Committee for the NIH Pharmacology Pre-doctoral Training Grant (2002 – present)
MSSM, Tenured Faculty Committee (2003 – present)
MSSM, Co-director for the BSBB program (2003 – present)
MSSM/NYU, IGERT COB Advisory Committee (2003 – present)
MSSM, Computational SRF Advisory Group Committee, MSSM (2004 – present)

TRAINING RECORD:

Name	**Position in the Zhou Lab**	**Subsequence/Current Position**
Present		
Lei Zeng	Research Assistant Professor	
Shiraz Mujtaba	Instructor	
Miklos Kuti	Postdoctoral Fellow	
Qiang Zhang	Postdoctoral Fellow	
Sachchidanand	Postdoctoral Fellow	
Chengmin Qian	Postdoctoral Fellow	
Xueqi Wang	Postdoctoral Fellow	
Kyoko Yap	Postdoctoral Fellow	
Ritesh Ramdhani	PhD Student in BSBB	
Abhas Gupta	MSTP Rotation Student	
Past		
Sakurako Tashiro	Postdoctoral Fellow	Assistant Professor at Tokyo University of Pharmacy and Life Science, Japan
Robert Ashton	Postdoctoral Fellow	Medical Resident at Albert Einstein College of Medicine, NY
Christophe Dhalluin	Postdoctoral Fellow	Research Scientist at Hoffman La Roche, Switzerland
Gaurav Chaturvedi	Postdoctoral Fellow	Postdoctoral fellow at University of Kansas
Yan He	Postdoctoral Fellow	Research Scientist at Novartis, NJ
Alexander Koch	Postdoctoral Fellow	Instructor, McGill University, Canada
Marta Murcia	Postdoctoral Fellow	Weill Medical College of Cornell University, NY
Zhiyong Wang	Visiting Professor	Professor, Univ. of Science & Tech. of China
Amjad Farooq	Postdoc. / Instructor	Assistant Professor, University of Miami, Florida
Kelly Yan	Ph.D. Student in BSBB	MSTP Student in the Medical Program at MSSM
Karishma Manzur	PhD student in MCBDS	Postdoctoral fellow at Univ. of California at Berkeley
Philipp Selenko	Visiting Student	PhD student at EMBL, Heidelberg, Germany

Björn Schwer	Visiting Student	MD student at DKFZ, Heidelberg, Germany
Edward Han	Summer Student	Williams College, Williams, MA
Oleg Broytman	Summer Student	SUNY at Binghamton, NY
Isaac Ashkenazi	Summer Student	Cooper Union, New York, NY
Linda To	Summer Student	Cornell University, Ithaca, NY

Graduate Student Advisory and Examination Committees

Saurabh Patel (1997)	Barney Yoo (2000)	Sacha Uljon (2003)
Alex Chang (1998)	Thijs Beuming (2001)	Joseph Thomas (2003)
Huayu Qi (1998)	Joshua Speidel (2002)	Matthew Diamonds (2004)
Justin Carlson (1999)	Kosj Yamoah (2002)	Jeffery James (2004)
Christopher Price (2000)	Patrick Coskren (2002)	

TEACHING ACTIVITIES:

Advanced Biophysics (MSSM), 1997, 2 lectures
Interactions and Dynamics of Biological Macromolecules (MSSM), 1997, 2 lectures
Methods in Molecular & Cellular Biophysics: Protein NMR Spectroscopy (MSSM), 1998 – 1999, 5 lectures per semester
Advanced Molecular Signaling (MSSM), 1997 – 2003, 2 lectures per semester
Molecular Therapeutics (MSSM), 1999 – 2003, 2 lectures per semester
Core II: Cell and Developmental Biology (MSSM), 1999 – 2002, 2 lectures per semester
Core III: Survey of Biophysics, Structural Biology, and Biomathematics (MSSM) 1998, 2002 and 2003, 3 lectures per semester; 2004-2005, course co-director, 5 lecture in protein NMR
Protein Folding and Diseases (Hunter College, CUNY), 2000, 2 lectures
Structural Biology and Protein NMR Spectroscopy (Skirball Institute, NYU), 2001, 1 lecture

CURRENT EXTERNAL GRANT SUPPORT (M.-M. ZHOU AS PI):

ISOA #200601 "Structure-based Design of Potentiators for Glutamate Receptors", 10/2000 – 11/2004
NIH R01 CA80938 "Structure and Function of the MAPK Phosphatase", 04/1999 – 01/2005 (NCE)
NIH R01 CA87658 "Structural Analysis of Protein Interactions in Chromatin Remodeling", 07/2000 – 06/2005
NIH S10 RR15935 "High Performance Cryogenic NMR Probe", 04/2002 – 03/2004
NIH P01 GM066531 "Structure-Based Design Paradigm: HIV Tat/PCAF Inhibitors", 08/2002 – 07/2007
GlaxoSmithKline, "Chemical Inhibitors for the HIV Tat/PCAF Complex", 11/2003 – 10/2005

PUBLICATIONS:

Peer-Reviewed Research Articles

1. Ostanin, K.V., Harms, E.H., Stevis, P.E., Kuciel, R., **Zhou, M.-M.,** & Van Etten, R.L. (1992) Overexpression, Site-Directed Mutagenesis and Mechanism of *Escherichia coli* Acid Phosphatase. *J. Biol. Chem.* **267**, 22830-36.
2. Wo, Y.-Y.P., **Zhou, M.-M.,** Stevis, P., Davis, J.P., Zhang, Z.-Y., & Van Etten, R.L. (1992) Cloning, Expression, and Catalytic Mechanism of the Low Molecular Weight Phosphotyrosyl Protein Phosphatase from Bovine Heart. *Biochemistry* **31**, 1712-21.
3. Tian, Z.P., Gu, C., Roeske, R.W., **Zhou, M.-M.,** & Van Etten, R.L. (1993) Synthesis of Phosphotyrosine-containing Peptides by the solid-Phase Method: A Re-examination of the Use of Boc-Tyr(PO_3Bzl_2)-OH. *Int. J. Peptide Protein Res.* **42**, 155-158.

4. **Zhou, M.-M.,** Davis, J.P., & Van Etten, R.L. (1993) Identification and pK_a Determination of the Histidine Residues of Human Low-Molecular-Weight Phosphotyrosyl Protein Phosphatase: A Convenient Approach Using an MLEV-17 Spectral Editing Scheme. *Biochemistry* **32**, 8479-86.
5. Davis, J.P., **Zhou, M.-M.,** & Van Etten, R.L. (1994) Spectroscopic and Kinetic Studies of the Histidine Residues of Bovine Low-Molecular-Weight Phosphotyrosyl Protein Phosphatase. *Biochemistry* **33**, 1278-86.
6. Davis, J.P., **Zhou, M.-M.,** & Van Etten, R.L. (1994) Kinetic and Site-directed Mutagenesis Studies of the Cysteine Resides of Bovine Low Molecular Weight Phosphotyrosyl Protein Phosphatase. *J. Biol. Chem.* **269**, 8734-40.
7. **Zhou, M.-M.,** Logan, T.M., Theriault, Y., Van Etten, R.L., & Fesik, S.W. (1994) Backbone ^{1}H, ^{13}C, and ^{15}N Assignments and Secondary Structure of Bovine Heart Low Molecular Weight Phosphotyrosyl Protein Phosphatase. *Biochemistry* **33**, 5221-29.
8. Logan, T.M., **Zhou, M.-M.,** Nettesheim, D.G., Meadows, R.P., Van Etten, R.L., & Fesik, S.W. (1994) Solution Structure of a Low Molecular Weight Protein Tyrosine Phosphatase. *Biochemistry* **33**, 11087-96.
9. **Zhou, M.-M.,** Meadows, R.P., Logan, T.M., Yoon, H.P., Wade, W., Ravichandran, K.S., Burakoff, S.J., & Fesik, S.W. (1995) Solution Structure of the Shc SH2 domain Complexed with a Tyrosine phosphorylated Peptide from the T-cell Receptor. *Proc. Natl. Acad. Sci. USA* **92**, 7784-88.
10. **Zhou, M.-M.,** Ravichandran, K.S., Olejniczak, E.T., Petros, A.P., Meadows, R.P., Sattler, M., Harlan, J.E., Wade, W., Burakoff, S.J., & Fesik, S.W. (1995) Structure and Ligand Recognition of the Phosphotyrosine Binding Domain of Shc. *Nature* **378**, 584-592.
11. **Zhou, M.-M.,** Harlan, J.E., Wade, W., Crosby, S., Ravichandran, K.S., Burakoff, S.J., & Fesik, S.W. (1995) Binding Affinities of Tyrosine-phosphorylated Peptides to the COOH-terminal SH2 and NH2-terminal Phosphotyrosine Binding Domain of Shc. *J. Biol. Chem.* **270**, 31119-23.
12. **Zhou, M.-M.,** Huang, B., Olejniczak, E.T., Meadows, R.P., Shuker, S.B., Miyazak, M., Trub, T., Shoelson, S.E., & Fesik, S.W. (1996) Structural Basis of IL-4 Receptor Phosphopeptide Recognition by the IRS-1 PTB Domain. *Nature Struct. Biol.* **3**, 388-393.
13. Olejniczak, E.T., **Zhou, M.-M.,** & Fesik, S.W. (1997) Changes in the NMR-Derived Motional Parameters of the Insulin Receptor Substrate 1 Phosphotyrosine Binding Domain upon Binding to an Interleukine 4 Receptor Phosphopeptide. *Biochemistry* **36,** 4118-24.
14. Ravichandran, K.S., **Zhou, M.-M.,** Pratt, J.C., Harlan, J.E., Walk, S., Fesik, S.W., & Burakoff, S.J. (1997) Evidence for a Requirement for Both Phospholipid and Phosphotyrosine Binding via the Shc Phosphotyrosine-Binding Domain In Vivo. *Mol. Cel. Biol.* **17**, 5540-49.
15. Hajduk, P.J., **Zhou, M.-M.,** Fesik, S.W. (1999) NMR-Based Discovery of Phosphotyrosine Mimetics that Bind to the Lck SH2 Domain. *Bioorganic & Medicinal Chem. Letters* **9**, 2403-06.
16. Dhalluin, C., Carlson, J.,Zeng, L., He, C., Aggarwal, A.K., & **Zhou, M.-M.** (1999) ^{1}H, ^{15}N, and ^{13}C Resonance Assignments for the Bromodomain of the Histone Acetyltransferase P/CAF. *J. Biomol. NMR* **14**, 291-292.
17. Farooq A., Plotnikova, O., Zeng, L., & **Zhou, M.-M.** (1999) Phosphotyrosine Binding Domains of IRS-1 and Shc Recognize the NPXpY Motif via a Thermodynamically Distinct Manner. *J. Biol. Chem.* **274**, 6114-21.
18. Dhalluin, C., Carlson, J.,Zeng, L., He, C., Aggarwal, A.K., & **Zhou, M.-M.** (1999) Structure and Ligand of a Histone Acetyltransferase Bromodomain. *Nature* **399**, 491-496.

19. Dhalluin, C., Yan, K., Plotnikova, O., Zeng, L., Goldfarb, M.P., & **Zhou, M.-M.** (2000) ^{1}H, ^{13}C and ^{15}N Resonance Assignments of the SNT PTB Domain in Complex with the FGFR-1 Peptide. *J. Biomol. NMR* **18**, 371-372.
20. Dhalluin, C., Yan, K., Plotnikova, O., Lee, K.W., Zeng, L., Kuti, M., Mutjaba, S., Goldfarb, M.P., & **Zhou, M.-M.** (2000) Structural Basis of SNT PTB Domain Interactions with Distinct Neurotrophic Receptors. *Mol. Cell* **6**, 921-29.
21. Farooq, A., Zeng, L., & **Zhou, M.-M.** (2001) ^{1}H, ^{13}C and ^{15}N Resonance Assignments of the ERK2 Binding Domain of MAPK Phosphatase MKP-3. *J. Biomol. NMR* **19**, 195-196.
22. Farooq, A., Chaturvedi, G., Mutjaba, S., Plotnikova, O., Zeng, L., Dhalluin, C., Ashton, R., & **Zhou, M.-M.** (2001) Solution Structure of ERK2 Binding Domain of MAPK Phosphatase MKP-3: Structural Insights into MKP-3 Activation by ERK2. *Mol. Cell* **7**, 387-399.
23. Sun, A.-Q., Arrese, M.A. Zeng, L., S., I., **Zhou, M.-M.,** Suchy, F.J. (2001) The Rat Liver Na^{+}/Bile Acid Cotransporter (Ntcp): Importance of the Cytoplasmic Tail to Function and Plasma Membrane Targeting. *J. Biol. Chem.* **276**, 6825-33.
24. Mujtaba, S., He, Y. Zeng, L., Farooq, A., Carlson, J., Ott, M., Verdin, E., & **Zhou, M.-M.** (2002) Structural Basis of HIV-1 Tat Recognition by P/CAF Bromodomain, *Mol. Cell* **9**, 575-586.
25. Dorr, A., Kiermer, V., Pedal, A., Rackwitz, H.-R., Henklein, P., Schubert, U., **Zhou, M.-M.,** Verdin, E. & Ott, M. (2002) Transcriptional synergy between at and PCAF is dependent on the binding of acetylated Tat to the PCAF bromodomain. *EMBO J.* **21**, 2715-23.
26. Yan, K.S., Kuti, M., Mujtaba, S., Farooq, A., Goldfarb, M.P., & **Zhou, M.-M.** (2002) FRS2 PTB Domain Conformation Regulates Interactions with Divergent Neurotrophic Receptors, *J. Biol. Chem.* **277**, 17088-94.
27. Zeng, L., Lu, L., Muller, M., Gouaux, E., & **Zhou, M.-M.** (2002) Structure-based functional design of chemical ligands for AMPA-subtype glutamate receptors. *J. Mol. Neuroscience **19***, 113-6.
28. Chaturvedi, G., Farooq, A., Zeng, L., & **Zhou, M.-M.** (2002) ^{1}H, ^{13}C and ^{15}N resonance assignments of the catalytic domain of human MAPK phosphatase, PAC-1. *J. Biomol. NMR* **25**, 79-80.
29. Farooq, A., Zeng, L., & **Zhou, M.-M.** (2002) ^{1}H, ^{15}N and ^{13}C resonance assignments of the PTB domain of the signaling protein Shc. *J. Biomol. NMR* **25**, 255-256.
30. Farooq, A., Plotnikova, O., Chaturvedi, G., Yan, S., Zeng, L., Zhang, Q., & **Zhou, M.-M.** (2003) Solution Structure of the Catalytic Domain of MAPK Phosphatase PAC-1: Insights into Substrate-induced Enzymatic Activation. *Structure* **11,** 155-164.
31. Sun, A.-Q., Salkar, R., Sachchidanand, Xu, S., Zeng, L., S., I., **Zhou, M.-M.**, Suchy, F.J. (2003) A 14 amino acid sequence with a beta-turn structure is required for apical membrane sorting of the rat ileal bile acid transporter. *J. Biol. Chem.* **278**, 4000-4009.
32. Manzur, K., Farooq, A., Zeng, L., Plotnikova, O., Koch, A. W., Sachchidanand, & **Zhou, M.-M.** (2003) A Dimeric Viral SET Domain Methyltransferase Specific to Lys27 of Histone H3. *Nature Struct. Biol.* **10**, 187-196.
33. Zeng, L., Chen, C.H., Muller, M., & **Zhou, M.-M.** (2003) Structure-based rational design of chemical ligands for AMPA-subtype glutamate receptors. *J. Mol. Neurosci.* **20**, 345-348.

34. Manzur, K., Farooq, A., Zeng, L., & **Zhou, M.-M.** (2003) ^{1}H, ^{13}C and ^{15}N resonance assignments of a viral SET domain histone lysine methyltransferase. *J. Biomol. NMR* **26**, 279-280.
35. Farooq, A., Zeng, L., Yan, K.S., Ravichandran, K.S., & **Zhou, M.-M.** (2003) Coupling of Folding and Binding in the PTB Domain of the Signaling Protein Shc. *Structure* **11**, 905-913.
36. Yan, K.S., Yan, S., Farooq, A., Han, A., Zeng, L., & **Zhou, M.-M.** (2003) Structure and Conserved RNA Binding of the PAZ Domain. *Nature* **426**, 469-474.
37. Mujtaba, S., He, Y., Zeng, L., Yan, S., Plotnikova, O., Sachchidanand, Sanchez, R., Zeleznik-Le, N., Ronai, Z., **Zhou, M.-M.** (2004) Structural Mechanism of the Bromodomain of the Coactivator CBP in p53 Transcriptional Activation. *Mol. Cell* **13**, 251-263.
38. Koch, A.W., Farooq, A., Zeng, L., Colman, D.R., **Zhou, M.-M.** (2004) ^{1}H, ^{13}C and ^{15}N Resonance Assignments of the N-cadherin Prodomain. *J. Biomol. NMR* **28**, 87-88.
39. Koch, A.W., Farooq, A., Shan, W.-S., Gruzglin, E., Zeng, L., Colman, D.R., **Zhou, M.-M.** (2004) Structure of the Neural (N-) Cadherin Prodomain Reveals a Cadherin Extracellular Domain-like Fold without Adhesive Characteristics. *Structure* **12**, 793-805.
40. Zhang, Y., Yan, Z., Farooq, A., Liu X., Lu, C., **Zhou, M.-M.**, & He, C. (2004) Molecular Basis of Distinct Interactions between Dok1 PTB Domain and Tyrosine-phosphorylated EGF Receptor. ***in press***.
41. Qian, C., Zeng, L., Farooq, A., & Zhou, M.-M. (2004) Resonance Assignment of the Endosomal Adaptor Protein p14. ***in press***.
42. Zhang, Q., Muller, M., Chen, C.H., Zeng, L., Farooq, A., & **Zhou, M.-M.** (2004) New insights into the catalytic Activation of the MAPK Phosphatase PAC-1 by ERK2. ***submitted***.
43. Qian, C., Zhang, Q, Zeng, L., Wang, X., Farooq, A., & Zhou, M.-M. (2004) Structure of the Adaptor Protein p14 Reveals Profilin-fold with Distinct Function. ***submitted***.
44. Zeng, L., Li, J., Muller, M., Yan, S., Mujtaba, S., Pan, C., Wang, Z., & Zhou, M.-M. (2004) Selective Small Molecules Blocking HIV-1 Tat and Coactivator PCAF Association. ***submitted***.

Invited Review Articles

1. **Zhou, M.-M.,** & Fesik, S.W. (1995) Structure and Function of the Phosphotyrosine Binding (PTB) Domain. *Prog. Biophys. Molec. Biol.* **64**, 221-235.
2. Fesik, S.W., Meadows, R.P., Olejniczak, E.T., Petros, A.P., Hajduk, P.J., Yoon, H.S., Harlan, J.E., Logan, T.M., **Zhou, M.-M.,** Nettesheim, D.G., Liang, H., & Yu, L. (1996) NMR Structures of Proteins Involved in Signal Transduction In *NMR as a Structural Tool for Macromolecules: Current Status and Future Directions*, (B.D. Rao and M.D. Kemple, Eds.) Klumer Academic, New York, pp 208-236.
3. **Zhou, M.-M.** (2000) Phosphothreonine Recognition Comes into Focus. *Nature Struct. Biol.* **7**, 1085-1087.
4. Yan, K.S., Kuti, M., **Zhou, M.-M.** (2002) PTB or not PTB – that is the question, *FEBS Lett.* **513**, 67-70.
5. Zeng, L. & **Zhou, M.-M.** (2002) Bromodomain: an acetyl-lysine binding domain. *FEBS Lett.* **513**, 124-128.
6. Yan, K.S. & **Zhou, M.-M.** (2002) TAGging the Target for Damage Control. *Nature Struct. Biol.* **9**, 638-40.

7. Yan, K.S. & **Zhou, M-M.** (2003) Examining Both Sides of a Janus PTB Domain. *Structure* **11**, 482-484.
8. Farooq, A. & **Zhou, M.-M.** (2004) Structure and Regulation of MAPK Phosphatases. *Cellular Signalling,* **16**, 769-779.

Chapters in Books

1. Farooq, A. & **Zhou, M.-M.** (2001) Structural Basis and Thermodynamics of Insulin Receptor Interactions with Phosphotyrosine Binding Domains In *Drug-Receptor Thermodynamics: Interaction and Applications* (R. B. Raffa, Ed.), John Wiley & Sons, New York, p.417-431.
2. **Zhou, M.-M.** (2002) Bromodomains In *The Encyclopedia of Molecular Medicine* (T. E. Creighton, Editor-in-Chief), John Wiley & Sons, New York, p.403-404.
3. Mujtaba, S. & **Zhou, M.-M.** (2004) Use of Nuclear Magnetic Resonance Spectroscopy to Study Structure-Function of Bromodomains In *Chromatin AND Chromatin Remodeling Enzymes, Methods in Enzymology* , 6 *Vol.* 37(C. Wu and C.D. Allis, Eds.) Elsevier Science (USA), San Diego, CA. pages 119-30.
4. Ott, M., Dorr, A., Hetzer-Egger, C., Kaehlcke, K., Schnolzer, M., Henklein, P., Cole, P., **Zhou, M.-M.**, Verdin, E. (2004) Tat acetylation: a regulatory switch between early and late phases in HIV transcription elongation. *Novartis Foundation Symposium* **259**:182-93.
5. Yan, K.S. & **Zhou, M.-M.** (2004) Bromodomains in Chromatin Remodeling and Beyond in *Protein-Protein Interactions: Biology, Chemistry, Bioinformatics and Drug Design* (G. Waksman, Ed.) Kluwer Academic/Plenum (USA), New York, NY, ***in press***.
6. Yan, K.S. & **Zhou, M.-M.** (2004) Structure and Function of the Bromodomain in *Modular Protein Domains* (Cesareni, Gimona, Sudol, Yaffe, Eds.) Wiley-VCH, Weinheim, Germany, ***in press***.

INVITED LECTURES/PRESENTATIONS:

05/1996	The University of Chicago, The Center for Molecular Oncology, Chicago, IL
03/1997	Columbia University, College of Physicians and Surgeons, NYC
12/1997	New York University, Skirball Institute of Biomolecular Medicine, NYC
02/1998	Yale University, School of Medicine, New Haven, CT
04/1998	European Molecular Biology Laboratory (EMBL), Heidelberg, Germany
02/1999	The Rockefeller University, *"The NMR Works in Progress"*, NYC
04/1999	University of Virginia, B. B. Carter Center for Immunology Research, Charlottesville, VA
07/1999	FASEB Summer Res. Conferences: *"Chromatin & Transcription"*, Snowmass Village, CO
09/1999	New York Academy of Sciences, *"New York Structural Biology Discussion Group"*, NYC
10/1999	Mount Sinai School of Medicine, Department of Microbiology, NYC
11/1999	The City College of the City University of New York (CUNY), Dept. of Chemistry, NYC
01/2000	The City College of CUNY, *"New York Structural Biology Center NMR Symposium"*
05/2000	CUNY, Hunter College, NYC
06/2000	Shanghai Institute of Organic Chemistry, Chinese Academy of Sciences, Shanghai, PRC
06/2000	East China University of Science and Technology, College of Chemistry, Shanghai, PRC
06/2000	The Second Military Medical University, Department of Neurobiology, Shanghai, PRC
06/2000	Shanghai Institute of Biochemistry, Chinese Academy of Sciences, Shanghai, PRC
06/2000	Shanghai Institute of Cell Biology, Chinese Academy of Sciences, Shanghai, PRC

08/2000 Deutsches Krebsforschungszentrum (DKFZ), Applied Tumor Virology, Heidelberg,Germany

10/2000 Institute for the Study of Aging, *"First Annual Investigators' Meeting"*, Tarrytown, NY

11/2000 Temple University School of Medicine, Department of Biochemistry, Philadelphia, PA

03/2001 Boehringer Ingelheim Symposium, Vienna, Austria

03/2001 Albert Einstein College of Medicine, Bronx, NY

04/2001 Loyola University Medical Center, Chicago, IL

08/2001 The Second Military Medical University, Department of Neurobiology, Shanghai, PRC

08/2001 Fudan University Medical School, Shanghai, PRC

10/2001 New York Academy of Sciences, *"New York Structural Biology Discussion Group"*, NYC

10/2001 Mount Sinai School of Medicine, Department of Microbiology, NYC

10/2001 15th Annual CABM Symposium *"Structural Genomics in Pharmaceutical Design"*, Princeton Technology Institute and the Center for Advanced Biotechnology and Medicine (CABM) at Rugters University, Princeton, NJ

12/2001 University of Virginia, B. B. Carter Center for Immunology Research, Charlottesville, VA

02/2002 The Johns Hopkins Univ. Med. School, Dept. of Pharmacology & Mol. Sciences, Baltimore, MD

08/2002 The University of Science & Technology of China, Chemistry Department, Hefei, PRC

08/2002 The Second Military Medical University, Department of Neurobiology, Shanghai, PRC

08/2002 The XXth Int. Conference on Magnetic Resonance in Biol. Systems (ICMRBS), Toronto, Canada

10/2002 Mount Sinai School of Medicine, The Derald H. Ruttenberg Cancer Center, NYC

10/2002 Institute for the Study of Aging, *"Third Annual Investigators' Meeting"*, Teaneck, NJ

10/2002 Mount Sinai School of Medicine, Department of Physiology and Biophysics, NYC

12/2002 Mount Sinai School of Medicine, Department of Human Genetics, NYC

06/2003 NIGMS Annual Meeting on "Groups Studying the Structure of AIDS-Related Systems", Bethesda, Maryland

10/2003 Institute for the Study of Aging, *"The Fourth Annual Investigators' Meeting"*, Teaneck, NJ

11/2003 Mount Sinai School of Medicine, "*Meeting MSSM Authors*", NYC

11/2003 2003 Eastern Analytical Society Symposium, Somerset, NJ

12/2003 New York Academy of Sciences, *"New York Structural Biology Discussion Group"*, NYC

06/2004 The Second International NMR Symposium, Wuhan, China (Co-organizer & Session Chair)

07/2004 The University of Science & Technology of China, Chemistry Department, Hefei, PRC

07/2004 The Second Military Medical University, Department of Neurobiology, Shanghai, PRC

07/2004 Shanghai University, Department of Chemistry, Shanghai, PRC

09/2004 CNIO Cancer Conference, "Structural Biology and Cancer", Madrid, Spain

11/2004 The Wistar Institute, Philadelphia, PA

11/2004 State University of New York at Albany

01/2005 The Rudin-Kase Dean's Lecture, Mount Sinai School of Medicine, NYC

04/2005 FASMB meeting "Dynamics of Protein- Protein Interactions," (Session Chair), San Diego, CA

04/2005 University of Texas Southwestern Medical Center, Dept. of Biochemistry, Dallas, TX

Selective Small Molecules Blocking HIV-1 Tat and Coactivator PCAF Association

Lei Zeng[‡], Jiaming Li[†], Michaela Muller[‡], Sherry Yan[‡], Shiraz Mujtaba[‡], Chongfeng Pan[†], Zhiyong Wang[†,*], and Ming-Ming Zhou[‡,*]

Structural Biology Program, Department of Physiology and Biophysics, Mount Sinai School of Medicine, New York University, One Gustave L. Levy Place, New York, New York 10029-6574, U.S.A., and Department of Chemistry, University of Science and Technology of China, Hefei, Anhui 230026, P.R. China

RECEIVED DATE (automatically inserted by publisher); E-mail: ming-ming.zhou@mssm.edu or zwang3@ustc.edu.cn

The replication cycle of the human immunodeficiency virus (HIV) presents several viable targets for anti-HIV chemotherapy. The current anti-HIV drugs specifically target the viral reverse transcriptase, protease and integrase.[1] However, because of the development of viral drug resistance from mutations in the targeted proteins, continuous viral production by chronically infected cells contributes to HIV-mediated immune dysfunction,[2] and there is still no cure for AIDS. A rapid growing AIDS epidemic calls for new therapeutic strategies targeting different steps in the viral life cycle. Therapeutic intervention at the stage of HIV gene expression can complement the existing therapy to interfere with virus production. Transcription of the integrated HIV provirus is regulated by the concerted action between cellular transcription factors and a unique viral *trans*-activator Tat. Tat binds to a viral RNA TAR and recruits cyclin T1 and cyclin-dependent kinase 9 that hyper-phosphorylates and enhances elongation efficiency of the RNA polymerase II.[3] Tat transactivation requires acetylation of its lysine 50 and recruitment of histone lysine acetyltransferase transcriptional coactivators for remodeling nucleosome that contains the integrated proviral DNA.[4] Our recent study shows that Tat coactivator recruitment requires its acetylated lysine 50 (AcK50) binding to the bromodomain (BRD) of the coactivator PCAF,[5a] and microinjection of anti-PCAF BRD antibody blocks Tat transactivation.[5b] These data suggest that Tat/PCAF recruitment via a BRD-AcK binding is essential for HIV transcription, and this interaction serves as a new therapeutic target for intervening HIV replication.

To validate this possible new anti-HIV therapeutic target, we aim to develop small-molecule inhibitors that block Tat/PCAF binding by targeting the BRD of PCAF. Targeting a host cell protein essential for viral reproduction, rather than a viral protein, may minimize the problem of drug resistance due to mutations of the viral counterpart as observed with protease inhibitors. Here we report the development of a novel class of N1-aryl-propane-1,3-diamine compounds using a structure-based approach that bind the PCAF BRD selectively over other structurally similar BRDs.

The bromodomain, present in chromatin associated proteins and histone lysine acetyltransferases,[6a] is an acetyl-lysine binding domain.[6b] Bromodomain/AcK binding plays an important role in control of chromatin remodeling and gene transcription.[6c] BRDs adopt the highly conserved structural fold of a left-handed four-helix bundle (αZ, αA, αB and αC), as first shown in the PCAF BRD [6b] (Figure 1A). The ZA and BC loops at one end of the bundle form a hydrophobic pocket for AcK binding. The structure of the PCAF BRD bound to a Tat-AcK50 peptide[5a] shows that AcK50 interacts with protein residues V752, Y802 and Y809, Y47(AcK-3) with V763, and R53(AcK+3) and Q54(AcK+4) with E756, conferring a

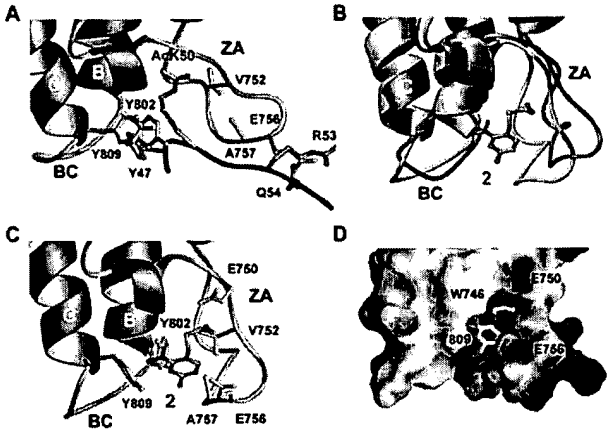

Figure 1. Structural basis of ligand recognition of the PCAF BRD. (**A**) Tat-AcK50 peptide recognition by the PCAF BRD; (**B**) Superimposition of the BRD in free (grey) and bound to the compound **2** (yellow); (**C**) Structure of the BRD/**2** complex, showing the compound **2** binding site; and (**D**) Grasp view of the compound **2** binding pocket.

specific intermolecular association. The structures of CBP BRD/p53-AcK382 and GCN5p BRD/H4-AcK16 complexes[7] show that the residues in BRDs important for AcK recognition are largely conserved, whereas sequence variations in the ZA and BC loops enable discrimination of different binding targets. Notably, as compared to the other parts of the protein, the ZA and BC loops contain significant sequence variations with amino acid deletion or insertion, supporting the notion that different sets of residues in the ZA and/or BC loops dictate BRD ligand specificity by interacting with residues flanking the acetyl-lysine in a target protein.[6c]

To develop selective small-molecule inhibitors for blocking Tat/PCAF association, we conducted NMR-based chemical screening for the BRD by monitoring ligand-induced protein signal changes in 2D ^{15}N-HSQC spectra.[8] We placed an emphasis on identifying compounds that bind selectively the BRD near but not just the AcK binding pocket, as the former may be more selective for this BRD. From screening of a few thousands of small-molecules from commercial libraries, we discovered several compounds including **1** that meet this criterion. Compound **1** binds the PCAF BRD with an affinity comparable to that of the Tat-AcK50 peptide[7a] (see below). Importantly, these compounds do not bind the structurally similar BRDs from CBP and TIF1β at millimolar concentration.

We next synthesized a series of **1** analogs to probe the structure-activity relationship (SAR) (Table 1). We assessed their binding to the PCAF BRD by measuring an IC_{50} in an ELISA assay, in which a compound competes against a biotinylated Tat-AcK50 peptide for binding to the GST-fusion BRD immobilized to glutathione-coated 96-well microtiter plate. The SAR study reveals salient features of

[‡]Mount Sinai School of Medicine
[†]University of Science and Technology of China

Table1. Structure-Activity Relationship Data for Derivatives of **1**

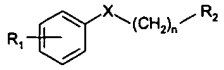

Cmpd	R_1	X	n	R_2	IC_{50} (μM)
1	2-NO_2	NH	3	-NH_3^+	5.1 ± 0.1
2	2-NO_2, 4-CH_3	NH	3	-NH_3^+	1.6 ± 0.1
3	2-NO_2, 4-CH_2-CH_3	NH	3	-NH_3^+	7.2 ± 0.1
4	2-NO_2, 3-CH_3	NH	3	-NH_3^+	5.9 ± 0.1
5	2-NO_2, 5-CH_3	NH	3	-NH_3^+	10.8 ± 0.1
6	2-NO_2, 4-Ph	NH	3	-NH_3^+	>10,000
7	2-NO_2, 4-CN	NH	3	-NH_3^+	34.9 ± 0.1
8	2-NO_2, 5-CN	NH	3	-NH_3^+	63.4 ± 0.6
9	2-CH_3, 5-NO_2	NH	3	-NH_3^+	77.8 ± 0.4
10	2-COO^-	NH	3	-NH_3^+	>10,000
11	2-$COOCH_3$	NH	3	-NH_3^+	>10,000
12	2-NO_2	O	3	-NH_3^+	125.6 ± 0.6
13	2-NO_2, 4-CH_3	O	3	-NH_3^+	180.0 ± 0.5
14	2-NO_2, 4-CH_3O	O	3	-NH_3^+	102.7 ± 0.4
15	2-NO_2, 4-Cl	O	3	-NH_3^+	215.1 ± 0.6
16	2-NO_2, 5-CH_3	O	3	-NH_3^+	203.6 ± 0.6
17	2-NO_2, 3-CH_3	O	3	-NH_3^+	164.8 ± 0.8
18	2-NO_2	CH_2	3	-NH_3^+	>10,000
19	2-NO_2	NH	4	-NH_3^+	145.9 ± 0.7
20	4-NO_2	NH	2	-NH_3^+	>2,000
21	4-NO_2	NH	4	-NH_3^+	>10,000
22	3-NH_2, 4-NO_2	NH	3	-COO^-	>2,000
23	2-NO_2, 4-Cl	NH	2	-(OH)CH_3	>10,000
24	2-Cl, 4-NO_2	NH	2	-(OH)CH_3	>10,000

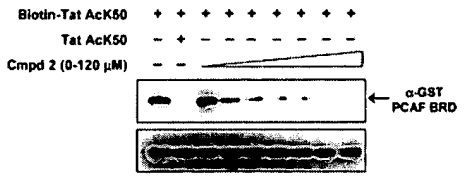

Figure 2. Inhibition of PCAF BRD/Tat AcK50 binding by **2**. In this assay, **2** inhibits the biotinylated Tat AcK50 peptide immobilized on streptavidin agarose binding to the GST-PCAF BRD, as assessed by anti-GST Western blot. Lower panel indicates an equal amount of BRD used in each assay.

BRD recognition of **1**. *First*, the BRD prefers a 4-methyl group on the aniline ring, which improves IC_{50} by 3-fold to 1.6 μM (**2** *vs.* **1**). While substitution of a 4-ethyl, 3- or 5-methyl group on the aniline ring slightly weakens the binding (**3-5** *vs.* **1**), addition of a 4-phenyl group nearly abolishes the binding (**6** *vs.* **1**). Adding a 4- or 5-cyano group weakens the binding by ~7-12-fold (**7** and **8** *vs.* **1**). *Second*, a 2-nitro group on the aniline ring is vital for the binding. Swapping of 2-nitro and 5-methyl causes a 7-fold reduction in binding (**9** *vs.* **5**). Surprisingly, substitution of 2-nitro with 2-caroxylate or 2-caroxyl ester abrogates the binding (**10** and **11** *vs.* **1**). *Third*, the functional importance of the 2-nitro is further supported by the effects of changing the NH to an O linkage in the aniline, which severely compromises the binding to the PCAF BRD (**12-17** *vs.* **1-5**). Moreover, changing to a carbon linkage eliminates the binding (**18** *vs.* **1**). *Fourth*, the BRD prefers an amino three-carbon aliphatic chain in **1** – a four-carbon chain reduces the binding by 30-fold (**19** *vs.* **1**) and a two-carbon chain nearly loses the binding (**20** *vs.* **1**). Alteration of **1** by two key elements, i.e. changing to a four-carbon chain and 4-nitro, abolishes the binding (**21** *vs.* **1**). *Finally*, the terminal amine group is also an important functional moiety for the BRD binding (**22-24** *vs.* **1**).

To understand ligand selectivity of the PCAF BRD, we solved the 3D structures of the protein bound to **1** and **2**. The two ligands are bound in the protein structure in nearly the same manner (data not shown). For clarity, the **2**-bound structure is reported, which is similar to the free structure except for the ZA and BC loops that move closer to each other by clapping onto the ligand (Figure 1B). **2** is engulfed by residues in the ZA and BC loops outside the AcK binding pocket, blocking BRD binding to AcK of a target protein (Figure 1C). The 2-nitro group of **2** likely forms a hydrogen bond with the phenolic –OH of Y809 and/or Y802, and the terminal $-NH_3^+$ interacts eletrostatically with the side-chain carboxylate of E750. The functional importance of the 2-nitro and the aniline NH result from a possible six-member ring structure formed between them. However, it is not clear why substitution of 2-nitro with 2-carboxylate abrogates the BRD binding (**10** vs. **1**). The aromatic ring of **2** is sandwiched between the side-chains of Y802 and A757 on one side, and Y809 and E756 on the other side; and the propane carbon chain is surrounded by the hydrophobic portions of the side-chains of P747, E756 and V752. Finally, the 4-methyl of **2** fills a small hydrophobic cavity formed by side-chains of A757, Y802 and Y809 (Figure 1D), contributing to a 3-fold increase over **1** in binding to the PCAF BRD. Notably, out of the ligand-interacting residues, only Y802 is conserved amongst BRDs, thus explaining the selective binding by this class of compounds to the PCAF BRD over the structurally similar CBP and TIF1β BRDs.

In summary, we have developed a class of novel small molecules that can effectively inhibit the PCAF BRD/Tat-AcK50 association *in vitro* by selectively binding to the BRD (Figure 2). The detailed SAR understanding of the lead compounds **1** and **2** will facilitate our efforts to optimize their affinity and selectivity by branching out to interact with the neighboring AcK binding pocket by the tethering techniques.[9] Such small-molecule inhibitors may be used to block lysine-acetylated HIV Tat/PCAF association that is required for HIV transcription and replication.

Acknowledgments. We think the National Institutes of Health (to M.-M.Z.) for financial support of this work.

Supporting Information Available: Full experimental procedures. This material is available free of charge via the Internet at http://pubs.acs.org.

References

(1) Garg, R.; Gupta, S. P.; Hua, G.; Babu, M. S.; Debnath, A. K.; Hansch, C. *Chem. Rev.* **1999**, *99*, 3525-601.

(2) (a) Ho, D. D; Zhang, L. *Nature. Med.* **2000**, *6*, 757-61. (b) Wei, X; Ghosh, S. K.; Taylor.; Johnson, V. A.; Emini, E. A.; Deutsch, P.; Lifson, J. D.; Bonhoeffer, S.; Nowak, M.A.; Hahn, B.H.; Saag, M. S.; Shaw, G. M. *Nature* **1995**, *373*, 117-22. (c) Richman, D. D. AIDS. Res. *Hum. Retrovirus* **1992**, *8*, 1065-71.

(3) (a) Keen, N. J; Churcher, M. J; Karn, J. EMBO. J. 1997, 16, 5260-72. (b) Karn, J. *J. Mol. Biol.* **1999**, *293*, 235-54. (c) Jones, K. A. *Genes. Dev.* **1997**, *11*, 2593-99. (d) Kao, S. Y.; Calman, A.F.; Luciw, P. A.; Peterlin, B. M. *Nature* **1987**, *330*, 489-93.

(4) (a) Ott, M.; Schnolzer, M.; Garnica, J.; Fischle, W.; Emiliani, S.; Rackwitz, H.R.; Verdin, E; *Curr. Biol.* **1999**, *9*, 1489-92. (b) Kachleke, K.; Dorr, A.; Hetzer-Egger, C.; Kiermer, V.; Henklein, P.; Schnoelzer, M.; Loret, E.; Cole, P. A.; Verdin, E.; Ott, M. *Mol. Cell* **2003**, *12*, 167-76.

(5) (a) Mujtaba, S.; He, Y.; Zeng, L.; Farooq, A.; Carison, J. E.; Ott, M.; Verdin. E.; Zhou, M-M. *Mol. Cell.* **2002**, *9*, 575-86. (b) Dorr, A; Kiermer, V.; Pedal, A.; Rackwitz, H. R.; Henklein, P.; Schubert, U.; Zhou, M-M.; Verdin, E.; Ott, M. *EMBO. J.* **2002**, *21*, 2715-33.

(6) (a) Jeanmougin, F.; Wurtz, J. M.; Douarin, B. L.; Chambon, P.; Losson, R. *Trends Biochem. Sci.* **1997**, *22*, 151-3. (b) Dhalluin, C.; Carlson, J. E.; Zeng, L.; He, C.; Aggarwal, A. K.; Zhou, M-M. *Nature* **1999**, *399*, 491-6. (c) Zeng, L.; Zhou, M.-M. *FEBS Letters* **2002**, *513*, 124-8.

(7) (a) Mujtaba, S.; He, Y.; Zeng, L.; Yan, S.; Plotnikova, O.; Sachchidanand; Sanchez, R.; Zeleznik-Le, N.J.; Ronai, Z.; Zhou, M.-M. *Mol Cell.* **2004**, *13*, 251-63. (b) Owen, D.J.; Ornaghi, P.; Yang, J.C.; Lowe, N.; Evans, P.R.; Ballario, P.; Neuhaus, D.; Filetici, P.; Travers, A.A. *EMBO J.* **2000**, *19*, 6141-9.

(8) (a) Hajduk, P.J.; Meadows, R.P.; Fesik, S.W. *Q. Rev. Biophys.* **1999**, *32*, 211-40. (b) Moore, J. M. *Curr. Opin. in Biotech.* **1999**, *10*, 54-8.

(9) (a) Hajduk, P. J.; Meadows, R. P.; Fesik, S. W. *Science* **1997**, *278*, 498-9. (b) Erlanson, D.A.; Braisted, A.C.; Raphael, D.R.; Randal, M.; Stroud, R.M.; Gordon, E.M.; Wells, J.A. *Proc. Natl. Acad. Sci. U.S.A.* **2000**, *97*, 9367-72.

Supporting Information

Selective Small Molecules Blocking HIV–1 Tat and Coactivator PCAF Association

Lei Zeng[‡], Jiaming Li[†], Michaela Muller[‡], Sherry Yan[‡], Shiraz Mujtaba[‡], Chongfeng Pan[†], Zhiyong Wang[†,*], and Ming-Ming Zhou[‡,*]

[‡] Structural Biology Program, Department of Physiology and Biophysics, Mount Sinai School of Medicine, New York University, One Gustave L. Levy Place, New York, New York 10029-6574, U.S.A.; [†]Department of Chemistry, University of Science and Technology of China, Hefei, Anhui 230026, China

E-mail: ming-ming.zhou@mssm.edu or zwang3@ustc.edu.cn

Experimental Methods:

1. Sample preparation. The PCAF bromodomain (residues 719-832) was expressed in *E. coli* BL21(DE3) cells using the pET14b vector (Novagen) [1]. Isotope-labeled proteins were prepared from cells grown on a minimal medium containing $^{15}NH_4Cl$ with or without $^{13}C_6$-glucose in either H_2O or 75% ^2H_2O. The protein was purified by affinity chromatography on a nickel-IDA column (Invitrogen), followed by the removal of poly-His tag by thrombin cleavage. GST-fusion PCAF bromodomain was expressed in *E. coli* BL21 (DE3) codon plus cells using the pGEX4T-3 vector (Pharmacia), and purified with a glutathione sepharose column. The lysine-acetylated peptide was ordered from Biosynthesis, Inc.

2. Protein structure determination by NMR. NMR samples contained the bromodomain (0.5 mM) in complex with a chemical ligand (~2 mM) in 100 mM phosphate buffer of pH 6.5, containing 5 mM perdeuterated DTT and 0.5 mM EDTA in $H_2O/^2H_2O$ (9/1) or ^2H_2O. All NMR spectra were acquired at 30°C on a Bruker 500 or 600 MHz NMR spectrometer. The backbone ^1H, ^{13}C and ^{15}N resonances were assigned using 3D HNCACB and HN(CO)CACB spectra. The

side-chain atoms were assigned from 3D HCCH-TOCSY and (H)C(CO)NH-TOCSY data. The NOE-derived distance restraints were obtained from ^{15}N- or ^{13}C-edited 3D NOESY spectra. The $^{3}J_{HN,H\alpha}$ coupling constants measured from 3D HNHA data were used to determine ϕ-angle restraints. Slowly exchanging amide protons were identified from a series of 2D ^{15}N-HSQC spectra recorded after $H_2O/^2H2O$ exchange. The intermolecular NOEs used in defining the structure of the PCAF bromodomain/ligand complex were detected in ^{13}C-edited (F_1), $^{13}C/^{15}N$- filtered (F_3) 3D NOESY spectra [2]. Protein structures were calculated with a distance geometry-simulated annealing protocol with X-PLOR [3]. Initial structure calculations were performed with manually assigned NOE-derived distance restraints. Hydrogen-bond distance restraints, generated from the H/D exchange data, were added at a later stage of structure calculations for residues with characteristic NOEs. The converged structures were used for iterative automated NOE assignment by ARIA for refinement [4]. Structure quality was assessed by Procheck-NMR [5]. The structure of the protein/ligand complex was determined using intermolecular NOE-derived distance restraints.

3. Chemical screening by NMR. A chemical library was constructed with small-molecules obtained from Chembridge Corp. (San Diego, CA), which were selected on the basis of molecular weight (<250 Da), non-reactivity, drug-like chemical framework (i.e. ring systems, linker atoms, side-chain atoms and framework), functional moieties (for hydrogen-bond or electrostatic interactions, but not reactive) and good solubility in aqueous solution. All the stock solutions of the chemical compounds are prepared in predeuterated DMSO. NMR-based screening was conducted with compounds (~1 mM) and the PCAF bromodomain (50-200 μM) using methods including 1D NOE-pumping [6] and saturation transfer difference [7, 8], as well as 2D ^{15}N-HSQC spectra [9, 10]. The latter is particularly helpful for selective screening to identify compounds that bind to a specific site of the target protein.

4. Ligand binding to the PCAF bromodomain. The ELISA assay was carried on a 96-well microplate (Nunc) that was pre-coated with anti-GST antibody (Sigma-Aldrich) overnight at 4°C in 100 μL carbonate/bicarbonate buffer, and then washed with PBS buffer supplemented with 1% Tween-20. Non-specific binding sites were minimized by treatment with PBS buffer containing 2% BSA and 1% Tween-20 for 2 hours at room temperature. GST-PCAF bromodomain (1 μg per well) was added to the plate and incubated for two hours at room temperature for binding to anti-GST antibody. The plate was washed and blocked with PBS buffer containing 10% BSA and 1% Tween-20. The biotinylated HIV Tat-AcK50 peptide (Biotin-GISYGR-AcK-KKRRQRRRP) (5 μM) and increasing concentrations of a given compound were added and allowed to bind to the PCAF bromodomain overnight at 4°C. Plate was washed with washing buffer, and bromodomain -bound peptide was determined by incubating 100 μL of a neutravidin-conjugated HRP (Pierce) solution (0.1 μg/ml) for 1 hour at room temperature, followed by washes and incubation with 100 μL of tetramethyl benzidine (Pierce) as an HRP substrate. The reaction was stopped by addition of 100 μL of 2.0 M sulfuric acid. The absorbance of the colored product was measured at 450 nm. Absorbance in each well was corrected for the blank obtained in a corresponding well subjected to the complete procedure but containing no PCAF bromodomain.

5. Chemistry. Melting points were recorded on an XT-4 micro-melting point apparatus and were uncorrected. ^{1}H and ^{13}C NMR spectra were recorded on a 300 MHz Bruker NMR spectrometer using tertramethylsilane as internal standard and the data were reported as the following: chemical shifts in ppm (δ), number of protons, multiplicity (s, singlet; d, doublet; t, triplet; m, multiplet), coupling constants in hertz. IR spectra were measured on Bruker EQUINOX55 spectrometer. Mass spectra were recorded on HRMS [LC-TOF spectrometer (micromass)] (EI/CI). Elemental analyses were recorded on Elementar Vario EL-III spectrometer. All chromatographic purifications were

performed with silica gel (100-200 mesh). All purchased materials were used without further purifications. All solvents were reagent grades.

Scheme 1 [a]

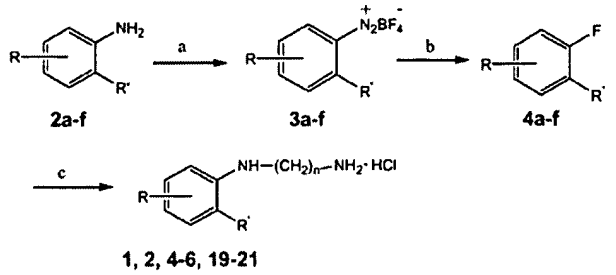

R=H, CH_3, Ph, NO_2; R'=H, NO_2; n=2, 3, 4

[a] Reagents and conditions: (a) $NaNO_2$, HBF_4, 0~5°C; (b) SiO_2/heat; (c) (i) 1,3-diaminopropane, or 1,2-diaminoethane, or 1,4-diaminobutane, 120°C; (ii) concentrated HCl, EtOH.

Scheme 2 [a]

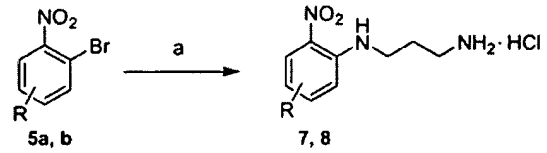

[a] Reagents and conditions: (a) (i) 1,3-diaminopropane; (ii) concentrated HCl, EtOH.

Scheme 3 [a]

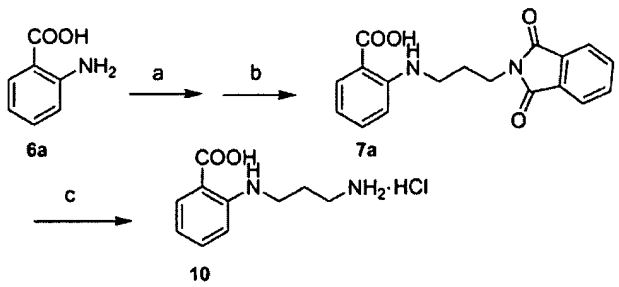

[a] Reagents and conditions: (a) potassium carbonate; (b) N-(3-bromopropyl)phthalimide, H_2O, reflux, 5h; (c) 30% NaOH, reflux, 6 h, HCl, 50 °C, 6h.

Scheme 4 [a]

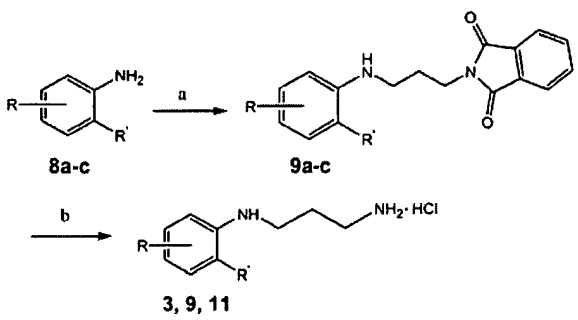

R=C_2H_5, NO_2; R'=NO_2, CH_3, $COOCH_3$.

[a] Reagents and conditions: (a) N-(3-bromopropyl)phthalimide, $(Et)_3N$, 120°C; (b) (i) $NH_2NH_2 \cdot H_2O$, EtOH, reflux, 6 h; (ii) HCl, EtOH.

Scheme 5 [a]

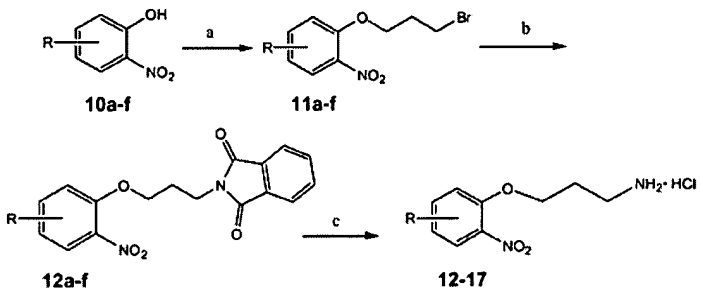

R=H, CH_3, CH_3O, Cl,

[a] Reagents and conditions: (a) 1,3-dibromopropane, NaOH, H_2O, reflux; (b) potassium phthalimide, DMF, 90~95°C, 2~3 h; (c) $NH_2NH_2 \cdot H_2O$, EtOH, reflux, 6h, or concentrated HCl, HOAc (V/V=1:1), reflux, several days.

Scheme 6 [a]

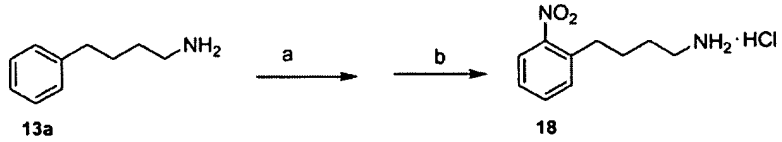

[a] Reagents and conditions: (a) (i) $(CH_3CO)_2O$, 60 °C, 1h; (ii) HNO_3 (d=1.5), 0-10 °C; (b) (i) H_2SO_4/H_2O, reflux, 5h; (ii) HCl, EtOH, yield 8%.

N_1-(2-nitro-phenyl)-propane-1,3-diamine monohydrochloride (1). Yield: 78%; mp >169°C; FTIR (KBr) $\bar{\upsilon}$ cm^{-1}: 2988.48, 1614.95, 1592.93, 1530.24, 1499.85, 1382.35, 1347.25, 1224.06, 1154.59, 1134.19, 1004.51, 918.02, 858.90, 789.80, 747.36; ^{1}H NMR (D_2O, 4.79) δ: 7.80 (1H, m, Ar-H), 7.35 (1H, m, Ar-H), 6.76 (1H, m, Ar-H), 6.50 (1H, m, Ar-H), 3.31 (2H, t, J = 6.90 Hz, 3-CH_2), 3.05 (2H, t, J = 7.40 Hz, 1-CH_2), 1.96 (2H, m, 2-CH_2); ^{13}C NMR [D_2O + acetone, acetone (CH_3):30.60] δ: 145.28, 137.35, 130.64, 126.44, 116.27, 114.44, 39.87, 37.64, 26.48; HRMS(CI) calculated for $C_9H_{13}N_3O_2$: (M+1) 196.1086, found 196.1080.

N_1-(4-methyl-2-nitro-phenyl)-propane-1,3-diamine monohydrochloride (2). Yield: 60.8%; mp 184- 186°C; FTIR (KBr) $\bar{\upsilon}$ cm^{-1}: 2964.50, 136.57, 1566.58, 1526.08, 1398.59, 1351.62, 1229.25, 1167.67, 1059.48, 851.53, 814.01, 764.74; ^{1}H NMR (D_2O, 4.79) δ: 7.79 (1H, s, 3-Ar-H), 7.36 (1H, d, J = 8.69 Hz, 5-Ar-H), 6.88 (1H, d, J = 8.67 Hz, 6-Ar-H), 3.47 (2H, t, J = 6.62 Hz, 3-CH_2), 3.15 (2H, t, J = 7.43 Hz, 1-CH_2), 2.21 (3H, s, -CH_3), 2.08 (2H, m, 2-CH_2); ^{13}C NMR [D_2O + acetone, acetone (CH_3):30.60] δ: 144.06, 139.14, 130.62, 126.21, 125.53, 114.43, 39.81, 37.67, 26.65, 19.38; HRMS(CI) calculated for $C_{10}H_{15}N_3O_2$: (M+1) 210.1243, found 210.1251.

N_1-(4-ethyl-2-nitro-phenyl)-propane-1,3-diamine monohydrochloride (3). Yield: 72.7%; mp 183- 185°C; FTIR(KBr) $\bar{\upsilon}$ cm^{-1}:2965.79, 1634.14, 1569.30, 1523.56, 1407.80, 1351.13, 1269.12, 1225.26, 1165.22, 1069.81, 817.62, 762.33; ^{1}H NMR (D_2O, 4.79)δ7.76 (1H, s, 3-Ar-H), 7.37 (1H, dd, J=7.01, 1.83Hz, 5-Ar-H), 6.87 (1H, d, J=8.87Hz, 6-Ar-H), 3.44 (2H, t, J=6.82Hz, NH-CH_2), 3.12 (2H, t, J=7.57Hz, CH_2-NH_2), 2.48 (2H, q, J=7.53Hz, Ar-CH_2), 2.05 (2H, m, 2-CH_2), 1.14 (3H, s, -CH_3); ^{13}C NMR [D_2O+acetone, acetone (CH_3):30.60] δ144.21, 138.16, 132.47, 130.58, 124.08,

114.52, 39.82, 37.65, 27.04, 26.68, 14.59; HRMS(CI) Calcd for $C_{11}H_{17}N_3O_2$: (M+1) 224.1399, found 224.1398.

N_1-(3-methyl-2-nitro-phenyl)-propane-1,3-diamine monohydrochloride (4). Yield: 81.5%; mp 180- 182°C; FTIR (KBr) $\bar{\upsilon}$ cm^{-1}: 2972.09, 1606.43, 1576.89, 1534.85, 1501.40, 1351.61, 1250.77, 1161.47, 1064.62, 1033.92, 852.11, 796.63, 769.27; ^1H NMR (D_2O, 4.79) δ: 7.35 (1H, t, J = 7.88 Hz, 5-Ar-H), 6.86 (1H, d, J = 8.50 Hz, 4-Ar-H), 6.70 (1H, d, J = 7.36 Hz, 6-Ar-H), 3.38 (2H, t, J = 6.85 Hz, 3-CH_2), 3.11 (2H, t, J = 7.41 Hz, 1-CH_2), 2.36 (3H, s, -CH_3), 2.03 (2H, m, 2-CH_2); ^{13}C NMR [D_2O + acetone, acetone (CH_3):30.60] δ141.92, 136.58, 135.56, 134.11, 121.53, 113.10, 41.22, 37.66, 26.27, 20.34; HRMS(CI) calculated for $C_{10}H_{15}N_3O_2$: (M+1) 210.1243, found 210.1251.

N_1-(5-methyl-2-nitro-phenyl)-propane-1,3-diamine monohydrochloride (5). Yield: 67.1%; mp >215 °C; FTIR (KBr) $\bar{\upsilon}$ cm^{-1}: 2925.75, 1628.10, 1577.27, 1488.41, 1408.98, 1338.69, 1252.10, 1217.79, 1182.52, 1060.46, 752.22; ^1H NMR (D_2O, 4.79) δ: 7.99 (1H, m, 3-Ar-H), 6.83 (1H, s, 6-Ar-H), 6.58 (1H, d, J = 6.76 Hz, 4-Ar-H), 3.52 (2H, t, J = 6.64 Hz, 3-CH_2), 3.17 (2H, t, J = 7.60 Hz, 1-CH_2), 2.36 (3H, s, -CH_3), 2.10 (2H, m, 2-CH_2); ^{13}C NMR [D_2O + acetone, acetone (CH_3):30.60] δ: 150.00, 145.91, 129.12, 126.62, 118.14, 113.71, 39.64, 37.65, 26.59, 21.68; HRMS(CI) calculated for $C_{10}H_{15}N_3O_2$: (M+1) 210.1243, found 210.1234.

N_1-(3-nitro-biphenyl-4-yl)-propane-1,3-diamine monohydrochloride (6). mp >190 °C; FTIR (KBr) $\bar{\upsilon}$ cm^{-1}:3435.01, 2971.02, 1635.79, 1561.44, 1404.99, 1359.55, 1241.99, 1222.08, 1169.70, 158.97, 698.40; ^1H NMR (D_2O, 4.79) δ: 8.34 (1H, d, J=2.01Hz, Ar-H), 7.83 (1H, m, Ar-H), 7.64

(2H, d, J=7.26Hz, Ar-H), 7.50 (2H, m, Ar-H), 7.42 (1H, m, Ar-H), 7.08 (1H, d, J=9.02Hz, Ar-H), 3.53 (2H, t, J=6.96Hz, 3-CH_2), 3.13 (2H, t, J=7.59Hz, 1-CH_2), 2.08 (2H, m, 2-CH_2); ^{13}C NMR (DMSO-d_6) δ: 144.19, 144.06, 138.05, 134.84, 131.49, 129.07, 127.15, 127.11, 125.80, 123.36, 115.45, 36.44, 36.35, 26.16; HRMS(CI) calculated for $C_{15}H_{17}N_3O_2$: (M+1) 272.1399, found 272.1390.

N_1-(4-cyano-2-nitro-phenyl)-propane-1,3-diamine monohydrochloride (7). mp >230°C; FTIR (KBr) $\bar{\upsilon}$ cm^{-1}: 3364.13, 2929.80, 2222.94, 1625.89, 1561.22, 1524.98, 1410.25, 1364.46, 1261.01, 1176.10, 921.75, 819.69; ^{1}H NMR (D_2O, 4.79) δ: 8.58 (1H, d, J=1.54Hz, 3-Ar-H), 7.73 (1H, dd, J=1.70, 9.13Hz, 5-Ar-H), 7.12 (1H, d, J=9.15Hz, 6-Ar-H), 3.58 (2H, t, J=6.91Hz, 3-CH_2), 3.13 (2H, t, J=8.01Hz, 1-CH_2), 2.08 (2H, m, 2-CH_2); ^{13}C NMR (DMSO-d_6) δ: 146.68, 137.58, 131.90, 131.01, 118.22, 115.90, 96.29, 36.06, 29.78, 25.77; HRMS(CI) calculated for $C_{10}H_{12}N_4O_2$: (M+1) 221.1039, found 221.1040.

N_1-(5-cyano-2-nitro-phenyl)-propane-1,3-diamine monohydrochloride (8). mp >185°C; FTIR (KBr) $\bar{\upsilon}$ cm^{-1}: 3234.94, 2228.70, 1602.69, 1470.61, 1308.98, 1266.12, 1158.97, 1070.74, 874.89, 829.64, 750.00; ^{1}H NMR (D_2O, 4.79) δ: 8.20 (1H, d, J=8.73Hz, 3-Ar-H), 7.91 (1H, brs, Ar-NH), 7.66 (1H, s, 6-Ar-H), 7.04 (1H, dd, J=1.38, 8.76Hz, 4-Ar-H), 3.52 (2H, t, J=6.39Hz, 3-CH_2), 2.86 (2H, brs, 1-CH_2), 1.86 (2H, m, 2-CH_2); ^{13}C NMR (DMSO-d_6) δ: 144.15, 133.43, 127.68, 119.35, 118.11, 117.65, 116.81; 36.43, 30.61, 25.96; HRMS(CI) calculated for $C_{10}H_{12}N_4O_2$: (M+1) 221.1039, found 221.1045.

N_1-(2-methyl-5-nitro-phenyl)-propane-1,3-diamine monohydrochloride (9). Yield: 81%; mp >152 °C; FTIR(KBr) $\bar{\upsilon}$ cm^{-1}: 3246.44, 2984.42, 1627.55, 1534.15, 1510.90, 1349.34, 1167.14, 1130.54, 917.28, 853.18, 737.04; ^1H NMR (D_2O, 4.79)δ7.77 (1H, dd, J=2.15, 8.24Hz, 4-Ar-H), 7.70 (1H, d, J=1.94Hz, 6-Ar-H), 7.38 (1H, d, J=8.27Hz, 3-Ar-H), 3.43 (2H, t, J=7.27Hz, 3-CH_2), 3.14 (2H, t, J=7.51Hz, 1-CH_2), 2.32 (3H, s, -CH_3), 2.10 (2H, m, 2-CH_2); ^{13}C NMR [D_2O+acetone, acetone (CH_3):30.60] δ146.78, 137.91, 132.96, 121.03, 114.10, 45.80, 37.24, 24.59, 17.36; HRMS(CI) calculated for $C_{10}H_{15}N_3O_2$: (M+1) 210.1243, found 210.1238.

N_1-(2-carboxyl-phenyl)-propane-1,3-diamine monohydrochloride (10). Yield: 51%; mp >135°C; FTIR (KBr) $\bar{\upsilon}$ cm^{-1}: 3328.13, 3045.98, 1687.79, 1605.86, 1579.99, 1379.37, 1198.87, 1158.54, 755.76; ^1H NMR (DMSO-d_6) δ7.69 (1H, d, J=7.73Hz, 3-Ar-H), 7.41 (1H, t, J=7.35, 8.02Hz, 5-Ar-H), 7.15 (1H, d, J=8.02Hz, 6-Ar-H), 7.08 (1H, t, J=7.73, 7.35Hz, 4-Ar-H), 3.47 (2H, t, J=6.27Hz, 3-CH_2), 3.31 (2H, t, J=4.89Hz, 1-CH_2), 1.69 (2H, m, 2-CH_2); ^{13}C NMR (DMSO-d_6) δ167.28, 131.92, 128.45, 122.23, 121.14, 116.86, 114.13, 58.59, 36.50, 32.19; HRMS(CI) calculated for $C_{10}H_{14}N_2O_2$: (M+1) 195.1134, found 195.1119.

N_1-(2-carboxymethyl-phenyl)-propane-1,3-diamine monohydrochloride (11). mp 141-143°C; FTIR(KBr) $\bar{\upsilon}$ cm^{-1}:3344.52, 2952.20, 1697.49, 1605.34, 1574.36, 1508.79, 1438.17, 1258.09, 1222.79, 1169.82, 1088.74, 751.55, 706.79; ^1H NMR (D_2O, 4.79)δ7.95 (1H, dd, J=1.49, 8.03Hz, 3-Ar-H), 7.52 (1H, t, J=8.53Hz, 5-Ar-H), 6.92 (1H, d, J=8.45Hz, 4-Ar-H), 3.89 (3H, s, -OCH_3), 3.40 (2H, t, J=6.83Hz, 3-CH_2), 3.14 (2H, t, J=7.64Hz, 1-CH_2), 2.05 (2H, m, 2-CH_2); ^{13}C NMR [D_2O+acetone, acetone (CH_3): 30.60] δ170.31, 150.60, 135.69, 132.17, 116.13, 112.46, 110.80, 52.26, 39.78, 37.83, 26.72; HRMS(CI) calculated for $C_{11}H_{16}N_2O_2$: (M^+) 208.1212, found 208.1228.

3-(2-nitro-phenoxy)-1-propylamine monohydrochloride (12). Yield 79%; mp 160-162°C; FTIR (KBr) $\bar{\upsilon}$ cm^{-1}:2957.52, 1612.32, 1581.01, 1525.19, 1398.45, 1339.86, 1271.26, 1254.75, 1167.97, 1059.83, 854.61, 740.78; ^1H NMR (D_2O, 4.79) δ: 8.06 (1H, d, J = 8.19 Hz, 3-Ar-H), 7.75 (1H, t, J = 8.28 Hz, 5-Ar-H), 7.34 (1H, d, J = 8.51 Hz, 4-Ar-H), 7.21 (1H, t, J = 7.99 Hz, 6-Ar-H), 4.42 (2H, t, J = 5.45 Hz, 3-CH_2), 3.34 (2H, t, J = 6.40 Hz, 1-CH_2), 2.30 (2H, m, 2-CH_2); ^{13}C NMR [D_2O + acetone, acetone (CH_3): 30.60] δ: 152.26, 138.47, 136.33, 126.42, 121.41, 115.20, 68.13, 38.36, 26.47; HRMS(EI) Calcd for $C_9H_{12}N_2O_3$: (M+1) 197.0926, found 197.0928.

3-(4-methyl-2-nitro-phenoxy)-1-propylamine monohydrochloride (13). Yield 83%; mp 158-160°C; FTIR(KBr) $\bar{\upsilon}$ cm^{-1}: 2952.95, 1628.51, 1572.03, 1533.89, 1399.08, 1340.97, 1265.53, 1249.95, 1162.89, 1060.92, 910.02809.57, 792.09; ^1H NMR (D_2O, 4.79) δ: 7.85 (1H, t, J = 1.5 Hz, 3-Ar-H), 7.55 (1H, tt, J = 1.64, 6.33Hz, 5-Ar-H), 7.20 (1H, d, J = 8.66 Hz, 6-Ar-H), 4.36 (2H, t, J = 5.53 Hz,3-CH_2), 3.34 (2H, t, J = 6.52 Hz, 1-CH_2), 2.36 (3H, s, Ar-CH_3), 2.28 (2H, m, 2-CH_2); ^{13}C NMR [D_2O + acetone, acetone (CH_3): 30.60] δ: 150.21, 138.38, 136.71, 131.59, 126.03, 115.31, 68.03, 38.19, 26.65, 19.61; HRMS(EI) calculated for $C_{10}H_{14}N_2O_3$: (M+1) 211.1083, found 211.1076.

3-(4-methoxy-2-nitro-phenoxy)-1-propylamine monohydrochloride (14). Yield 73.5%; mp 154-156 °C; FTIR (KBr) $\bar{\upsilon}$ cm^{-1}: 2950.19, 1576.28, 1342.42, 1286.70, 1265.19, 1222.72, 1157.96, 1059.63, 1040.04, 871.77, 823.40, 792.10; ^1H NMR (D_2O, 4.79) δ: 7.45 (1H, d, J = 2.94Hz, 3-Ar-H), 7.22-7.06 (2H, m, 5,6-Ar-H), 4.22 (2H, t, J = 5.58Hz, 3-CH_2), 3.75 (3H, s, -OCH_3), 3.21 (2H, t, J = 6.39Hz, 1-CH_2), 2.15 (2H, m, 2-CH_2); ^{13}C NMR [D_2O + acetone, acetone (CH_3): 30.60]

δ: 152.86, 146.75, 138.38, 122.40, 116.89, 110.63, 68.59, 56.38, 38.30, 26.62; HRMS(EI) calculated for $C_{10}H_{14}N_2O_4$: (M+1) 227.1032, found 227.1027.

3-(4-chloro-2-nitro-phenoxy)-1-propylamine monohydrochloride (15). Yield 82%; mp 184-186°C; FTIR (KBr) $\bar{\upsilon}$ cm^{-1}: 2970.91, 1614.90, 1530.26, 1343.08, 1291.04, 1266.11, 1161.89, 1063.10, 883.30, 818.43; ^1H NMR (D_2O, 4.79) δ: 8.11 (1H, t, J = 2.61 Hz, 3-Ar-H), 7.76-7.71 (1H, m, 5-Ar-H),7.34-7.30 (1H, m, 6-Ar-H), 4.40 (2H, t, J = 5.49 Hz, 3-CH_2), 3.32 (2H, t, J = 6.51 Hz, 1-CH_2), 2.29 (2H, m, 2-CH_2); ^{13}C NMR [D_2O + acetone, acetone (CH_3): 30.60] δ: 151.22, 138.67, 135.78, 125.94, 125.54, 116.83, 68.47, 38.20, 26.48; HRMS(EI) calculated for $C_9H_{11}ClN_2O_3$: (M+1) 231.0536, found 231.0528.

3-(5-methyl-2-nitro-phenoxy)-1-propylamine monohydrochloride (16). Yield 80.6%; mp 211-213 °C; FTIR (KBr) $\bar{\upsilon}$ cm^{-1} :2954.26, 1611.32, 1589.03, 1513.38, 1341.30, 1272.89, 1182.24, 1059.49, 897.54, 817.55; ^1H NMR (D_2O, 4.79) δ: 7.93 (1H, d, J = 8.39Hz, 2-Ar-H), 7.11 (1H, s, 6-Ar-H), 6.96 (1H, d, J = 8.28 Hz, 4-Ar-H), 4.34 (2H, t, J = 5.20 Hz, 3-CH_2), 3.30 (2H, t, J = 5.69 Hz, 1-CH_2), 2.41 (3H, s, Ar-CH_3), 2.24 (2H, m, 2-CH_2); ^{13}C NMR [D_2O + acetone, acetone (CH_3): 30.60] δ: 152.83, 149.43, 135.89, 126.90, 122.39, 115.66, 68.53, 38.83, 26.71, 21.74; HRMS(EI) Calcd for $C_{10}H_{14}N_2O_3$: (M+1) 211.1083, found 211.1080.

3-(3-methyl-2-nitro-phenoxy)-1-propylamine monohydrochloride (17). Yield 77%; mp 160-162°C; FTIR (KBr) $\bar{\upsilon}$ cm^{-1}: 2892.96, 1628.38, 1581.93, 1534.27, 1476.82, 1369.63, 1279.42, 1091.30, 852.71, 776.96, 747.35; ^1H NMR (D_2O, 4.79) δ: 7.45 (1H, t, J = 7.94Hz, 5-Ar-H), 7.08 (1H, d, J = 8.23 Hz, 4-Ar-H), 7.01 (1H, d, J = 7.38 Hz, 6-Ar-H), 4.28 (2H, t, J = 5.34Hz, 3-CH_2),

3.22 (2H, t, J = 6.84Hz, 1-CH_2), 2.19 (2H, m, 2-CH_2); ^{13}C NMR [D_2O + acetone, acetone (CH_3): 30.60] δ: 148.93, 140.68, 131.36, 130.72, 122.77, 111.06, 66.36, 36.79, 25.95, 15.70; HRMS (EI) Calcd for $C_{10}H_{14}N_2O_3$: (M+1) 211.1083, found 211.1084.

4-(2-nitro-phenyl)-butylamine monohydrochloride (18). Yield 8%; oil; FTIR (film) $\bar{\upsilon}$ cm^{-1}:2927.59, 1526.99, 1455.22, 1346.86, 1276.80, 1123.55, 1076.11, 779.06; ^1H NMR (D_2O, 4.79) δ:7.97 (1H, d, J=6.16Hz, 3-Ar-H), 7.68 (1H, t, J=5.67Hz, 5-Ar-H), 7.52-7.45 (2H, m, Ar-H), 3.08 (2H, t, J=5.16Hz, -CH_2NH_2), 2.93(2H, t, J=5.73Hz, Ar-CH_2), 1.78 (4H, m, CH_2-CH_2); ^{13}C NMR [D_2O + acetone, acetone (CH_3): 30.60] δ:148.80, 136.83, 133.90, 132.19, 127.55, 124.85, 39.42, 31.72, 26.91, 26.71; HRMS (CI) Calcd for $C_{10}H_{14}N_2O_2$: (M+1) 195.1089, found 195.1085.

N_1-(2-nitro-phenyl)-butane-1,4-diamine monohydrochloride (19) Yield: 50.4%; mp 173-176°C; FTIR (KBr) $\bar{\upsilon}$ cm^{-1}:3380.74, 2938.61, 1625.67, 1573.05, 1516.63, 1417.23, 1358.38, 1256.09, 1229.27, 1158.77, 1036.31, 732.93; ^1H NMR (D_2O, 4.79) δ8.11 (1H, m, Ar-H), 7.52 (1H, m, Ar-H), 7.01 (1H, m, Ar-H), 6.72 (1H, m, Ar-H), 3.43 (2H, m, 4-CH_2), 3.06 (2H, m, 1-CH_2), 1.80 (4H, m, 2,3-CH_2); ^{13}C NMR [D_2O+acetone, acetone (CH_3): 30.60] δ146.12, 137.56, 130.82, 126.69, 116.05, 114.65, 42.20, 39.66, 25.66, 24.84; HRMS (CI) Calcd for $C_{10}H_{15}N_3O_2$: (M+1) 210.1234, found 210.1237.

N_1-(4-nitro-phenyl)-ethane-1,2-diamine monohydrochloride (20). Yield: 67%; mp 198°C; FTIR (KBr) $\bar{\upsilon}$ cm^{-1}:3272.73, 3069.16, 1601.46, 1543.80, 1504.85, 1469.89, 1328.32, 1118.56, 934.92, 835.07, 803.03, 750.56; ^1H NMR (D_2O, 4.79) δ7.99 (2H, dd, J=1.90, 5.37Hz, 3,5-Ar-H), 6.66 (2H, dd, J=1.98, 5.29Hz, 2, 6-Ar-H), 3.61 (2H, t, J=5.96Hz, 2-CH_2), 3.27 (2H, t, J=6.07Hz, 1-CH_2); ^{13}C

NMR [D_2O+acetone, acetone (CH_3):30.60] δ154.33, 137.09, 126.97, 111.68, 40.09, 38.57; HRMS (CI) Calcd for $C_8H_{11}N_3O_2$: (M+1) 182.0930, found 182.0922.

N_1-(4-nitro-phenyl)-butane-1,4-diamine monohydrochloride (21) Yield: 70.5%; mp 183-185°C; FTIR (KBr) $\bar{\upsilon}$ cm^{-1}: 3273.67, 2954.13, 1605.10, 1543.48, 1500.61, 1434.47, 1329.48, 1118.68, 896.13, 833.95, 754.75; ^1H NMR (D_2O, 4.79) δ8.06 (2H, d, J=9.28Hz, 3,5-Ar-H), 6.68 (2H, d, J=9.38Hz, 2, 6-Ar-H), 3.29 (2H, t, J=6.44Hz, 4-CH_2), 3.05 (2H, t, J=7.16Hz, 1-CH_2), 1.76 (4H, m, 2,3-CH_2); ^{13}C NMR [D_2O+acetone, acetone (CH_3): 30.60] δ154.66, 136.54, 127.16, 111.95, 42.67, 39.59, 25.37, 24.77; HRMS (CI) Calcd for $C_{10}H_{15}N_3O_2$: (M+1) 210.1234, found 210.1242.

Compounds (22, 23, 24) were purchased from Chembridge Corp. (San Diego, CA).

6. Structure coordinates: Coordinates for the three-dimensional NMR structure of the PCAF bromodomain in complex with the lead compound **2** are being deposited in the Brookhaven Protein Data Bank.

References:

1. Dhalluin, C., J.E. Carlson, L. Zeng, C. He, A.K. Aggarwal, and M.-M. Zhou. Structure and ligand of a histone acetyltransferase bromodomain. Nature **1999**, *399*, 491-496

2. Clore, G.M. and A.M. Gronenborn. Multidimensional heteronuclear nuclear magnetic resonance of proteins. Meth. Enzymol. **1994**, *239*, 249-363

3. Brunger, A.T., *X-PLOR Version 3.1: A system for X-Ray crystallography and NMR*. version 3.1 ed. 1993, New Haven, CT: Yale University Press.

4. Nilges, M. and S. O'Donoghue. Ambiguous NOEs and automated NOE assignment. Prog. NMR Spectroscopy **1998**, *32*, 107-139

5. Laskowski, R.A., J.A. Rullmannn, M.W. MacArthur, R. Kaptein, and J.M. Thornton. AQUA and PROCHECK-NMR: Programs for checking the quality of protein structures solved by NMR. J. Biomol. NMR **1996**, *8*, 477-486

6. Chen, A. and M.J. Shapiro. NOE pumping: a novel NMR technique for identification of compounds with binding affinity to marcomolecules. J. Am. Chem. Soc. **1998**, *120*, 10258-10259

7. Kwak, S.P. and J.E. Dixon. Nultiple dual specificity protein tyrosine phosphatases are expressed and regulated differentially in liver cell lines. J. Biol. Chem. **1995**, *270*, 1156-1160

8. Klein, J., R. Meinecker, M. Mayer, and B. Mayer. Detecting binding affinity to immobilized receptor proteins in compound libraries in HR-MAS STD NMR. J. Am. Chem. Soc. **1999**, *121*, 5336-5337

9. Hajduk, P.J., R.P. Measdows, and S.W. Fesik. NMR-based screening in drug discovery. Quarterly Reviews of Biophysics **1999**, *32*, 211-240

10. Moore, J.M. NMR screening in drug discovery. Curr. Opin. in Biotech. **1999**, *10*, 54-58

Table S1. NMR Structural Statistics for the PCAF BRD/Ligand 2 Complex

Total Experimental Restraints		3375
Total NOE Distance Restraints		3273
Total Ambiguous		112
Total Unambiguous		3161
Manually assigned		3040
ARIA assigned		121
Intra-residue		1266
Inter-residue		1895
Sequential	($\|i - j\| = 1$)	613
Medium	($2 \leq \|i - j\| \leq 4$)	568
Long range	($\|i - j\| > 4$)	714
Intermolecular		48
Hydrogen Bond Restraints		44
Dihedral Angle Restraints		58
Final Energies (kcal·mol^{-1}) [a]		
E_{Total}		236.2 ± 14.5
E_{NOE}		35.3 ± 8.5
$E_{Dihedral}$		0.005 ± 0.02
E_{L-J} [b]		-604.5 ± 18.3
Ramachandran Plot (%)	Full Protein	2nd Structure
Most Favorable Region	81.6 ± 2.2	96.8 ± 1.9
Additionally Allowed Region	15.9 ± 2.3	3.2 ± 1.9
Generously Allowed region	2.4 ± 1.3	0.0 ± 0.0
Disallowed Region	0.05 ± 0.24	0.0 ± 0.0
Cartesian coordinate RMSDs (Å) [c]		
Backbone atoms (N, Cα, C')	0.49 ± 0.05	0.38 ± 0.05
Heavy atoms [d]	0.97 ± 0.08	0.84 ± 0.07

Notes:

[a] The Lennard-Jones potential was not used during any refinement stage.

[b] None of these final structures exhibit NOE-derived distance restraint violations greater than 0.3 Å or dihedral angle restraint violations greater than 5°.

[c] Protein residues 723-830.

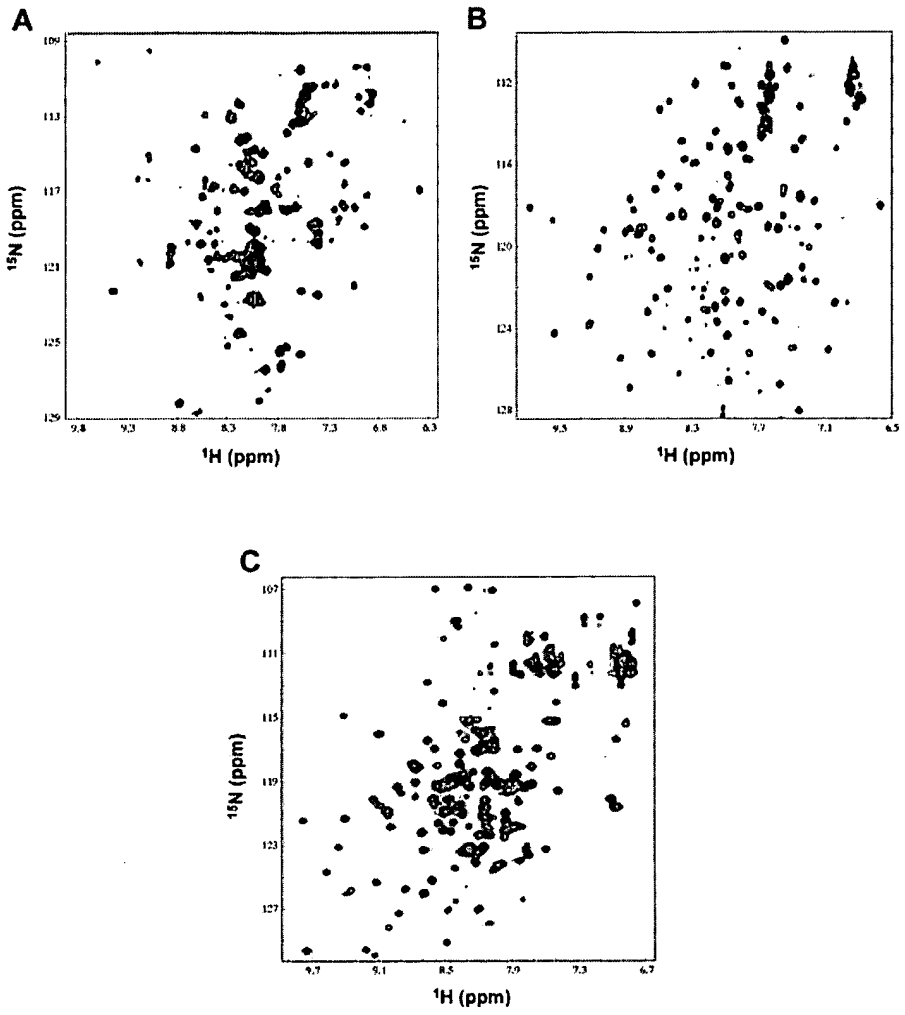

Figure S1. Selective binding of the lead compound **1** by (**A**) the PCAF bromodomain but not (**B**) the CBP bromodomain and (**C**) the tandem PHD finger and bromodomain of TIF1β. The 2D ^{1}H-^{15}N HSQC spectra of the bromodomain show changes of backbone amide resonances of the protein in the presence (red) or absence (black) of the chemical ligand.

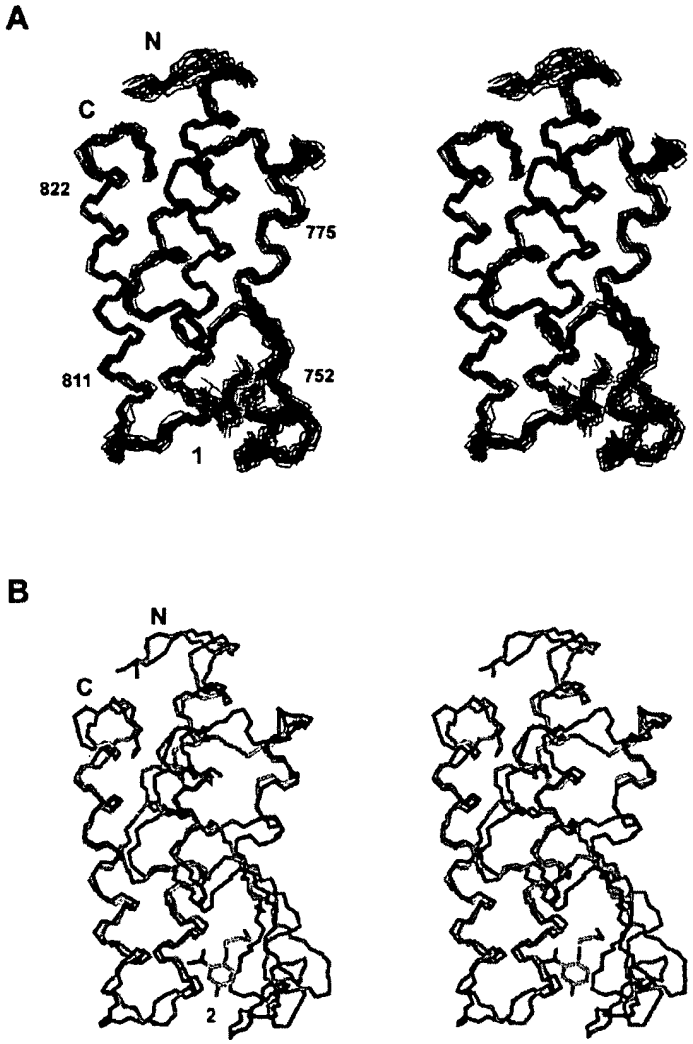

Figure S2. Three-dimensional structure of the PCAF bromodomain, as determined by NMR. (**A**) Superimposition of the backbone atoms (N, C_α and C') of the final 20 NMR structures of the bromodomain in complex with the lead compound **2** (highlighted in red). (**B**) Superimposition of the final representative structures of the bromodomain in the free (yellow) and when bound to the lead compound **2** (blue).

Molecular Cell, Vol. 9, 575–586, March, 2002, Copyright ©2002 by Cell Press

Structural Basis of Lysine-Acetylated HIV-1 Tat Recognition by PCAF Bromodomain

Shiraz Mujtaba,[1] Yan He,[1] Lei Zeng,[1]
Amjad Farooq,[1] Justin E. Carlson,[1] Melanie Ott,[2]
Eric Verdin,[3] and Ming-Ming Zhou[1,4]
[1]Structural Biology Program
Department of Physiology and Biophysics
Mount Sinai School of Medicine
New York University
New York, New York 10029
[2]Applied Tumor Virology
Deutsches Krebsforschungszentrum
Im Neuenheimer Feld, 242
Heidelberg, D-69120
Germany
[3]Gladstone Institute of Virology and Immunology
University of California, San Francisco
365 Vermont Street
San Francisco, California 94103

Summary

The human immunodeficiency virus type 1 (HIV-1) *trans*-activator protein Tat stimulates transcription of the integrated HIV-1 genome and promotes viral replication in infected cells. Tat transactivation activity is dependent on lysine acetylation and its association with nuclear histone acetyltransferases p300/CBP (CREB binding protein) and p300/CBP-associated factor (PCAF). Here, we show that the bromodomain of PCAF binds specifically to HIV-1 Tat acetylated at lysine 50 and that this interaction competes effectively against HIV-1 TAR RNA binding to the lysine-acetylated Tat. The three-dimensional solution structure of the PCAF bromodomain in complex with a lysine 50-acetylated Tat peptide together with biochemical analyses provides the structural basis for the specificity of this molecular recognition and reveals insights into the differences in ligand selectivity of bromodomains.

Introduction

The human immunodeficiency virus type 1 (HIV-1) protein Tat is an atypical *trans*-activator of transcription which functions through binding to an RNA element known as the transactivation responsive region (TAR), located in the retroviral long-terminal repeat (LTR) (Cullen, 1998; Jeang et al., 1999; Karn, 1999). Tat binds to TAR RNA with high affinity but transiently (Keen et al., 1997; Rana and Jeang, 1999). Dissociation of Tat from TAR RNA facilitates Tat association with the assembled RNA polymerase II (RNAPII) complex (Deng et al., 2000; Kiernan et al., 1999). The latter process enables the transcriptional machinery complex to elongate efficiently on the viral DNA template in order to produce full-length HIV transcripts during viral productive replication in infected cells (Adams et al., 1994; Garber and Jones, 1999).

While the detailed molecular mechanisms underlying Tat dissociation from TAR RNA and its transactivation of transcription of the integrated HIV-1 genome remain elusive, increasing lines of evidence suggest that Tat activity requires its association with several multiprotein complexes, which include the cyclinT1/cyclin-dependent kinase 9 (CDK9) complex (Jones, 1997; Wei et al., 1998) and histone acetyltransferase (HAT) transcriptional coactivators, p300/CBP (CREB binding protein), and p300/CBP-associated factor (PCAF) (Benkirane et al., 1998; Deng et al., 2000; Hottiger and Nabel, 1998). Recruitment of CDK9 through the N-terminal cysteine-rich region of Tat results in hyperphosphorylation of the C-terminal domain of RNAPII that increases elongation efficiency of HIV-1 transcription (Wei et al., 1998). Recently, it has been shown that Tat activity is dependent on acetylation by p300/CBP at K50 located in the C-terminal arginine-rich motif (ARM) (Kiernan et al., 1999; Ott et al., 1999), a region that is also important for TAR RNA binding and nuclear localization. Mutation of K50 to arginine, a conserved amino acid substitution that retains the positive charge but prevents acetylation by p300, markedly decreases the synergistic activation of the HIV-1 promoter by Tat and p300 (Kiernan et al., 1999; Ott et al., 1999). Tat acetylation at K50 results in its dissociation from TAR RNA and promotes formation of a multiprotein complex comprised of Tat, p300/CBP, and PCAF (Benkirane et al., 1998; Deng et al., 2000). Furthermore, it has been shown that the HAT activity of PCAF is preferentially required for Tat transactivation of transcription of the integrated but not the unintegrated HIV-1 LTRs (Benkirane et al., 1998).

Protein lysine acetylation is emerging as a central mechanism in regulation of chromatin remodeling and transcriptional activation (Jenuwein and Allis, 2001; Kouzarides, 2000; Strahl and Allis, 2000). Bromodomains, an extensive family of conserved protein modules found in many chromatin-associated proteins and in nearly all nuclear histone acetyltransferases (Brownell and Allis, 1996; Haynes et al., 1992; Jeanmougin et al., 1997; Tamkun et al., 1992), have been recently discovered to function as acetyl-lysine binding domains (Dhalluin et al., 1999; Hudson et al., 2000; Jacobson et al., 2000; Owen et al., 2000). This new finding suggests a novel mechanism for regulating protein-protein interactions via lysine acetylation (Dyson et al., 2001; Jenuwein and Allis, 2001; Strahl and Allis, 2000; Winston and Allis, 1999). This new mechanism supports the hypothesis that bromodomains could contribute to highly specific histone acetylation by tethering transcriptional HATs to specific chromosomal sites (Brownell and Allis, 1996; Manning et al., 2001; Travers, 1999), and to the assembly and activity of multiprotein complexes of chromatin remodeling such as SAGA and NuA4 (Brown et al., 2001; Sterner et al., 1999). However, because no specific, biologically relevant binding sites had been reported for any particular bromodomain, the major question of ligand specificity of bromodomains still remains unanswered.

[4]Correspondence: zhoum@inka.mssm.edu

In efforts to determine the mechanisms of action of Tat in transactivation of HIV-1 transcription, we investigated whether the interaction of the activated, lysine-acetylated Tat with the nuclear HAT transcriptional cofactors p300/CBP and PCAF involves any of the bromodomains of the latter proteins. Here, we report that the bromodomain of PCAF but not CBP can specifically recognize the lysine-acetylated Tat at K50 (not K51 or K28), and this interaction competes effectively against TAR RNA binding to the acetylated Tat. We have also determined the three-dimensional structure of the PCAF bromodomain in complex with a lysine-acetylated peptide derived from Tat at K50 by using nuclear magnetic resonance (NMR) spectroscopy. NMR structural and biochemical analyses were further used to gain structural insights into this important molecular recognition as well as the differences in ligand selectivity of different bromodomains.

Results and Discussion

PCAF Bromodomain Recognition of Lysine-Acetylated HIV-1 Tat at K50

To test whether Tat-p300/CBP-PCAF association involves bromodomains of the histone acetyltransferase transcriptional coactivators, we performed an in vitro binding assay by using recombinant and purified GST-fusion bromodomains and lysine-acetylated peptides derived from known acetylation sites in Tat at K28 and K50. A lysine-acetylated Tat peptide containing AcK50 (SYGR-AcK-KRRQR, where AcK is an N^{ϵ}-acetyl-lysine) showed no detectable interactions with either bromodomains or bromodomain and PHD finger (Aasland et al., 1995) tandem modules from CBP or TIF1β (transcriptional intermediary factor 1β, also named KAP-1 and KRIP-1) (Friedman et al., 1996) (Figure 1A). Strikingly, the same Tat peptide bound tightly to the bromodomain of PCAF, which shares high sequence homology to CBP bromodomain (Jeanmougin et al., 1997). The binding is dependent on acetylation of K50 on Tat. Neither of these bromodomains interacted with an acetylated Tat peptide derived from K28 (TNCYCK-AcK-CCFH) (data not shown), highlighting the selective nature of PCAF bromodomain recognition of the Tat AcK50 sequence.

We performed an NMR study in order to determine the specificity of PCAF bromodomain binding to lysine-acetylated Tat. As anticipated, PCAF bromodomain did not bind to Tat AcK28 peptide, nor did CBP bromodomain to either Tat AcK28 or AcK50 peptide. In contrast, PCAF bromodomain bound to Tat AcK50 peptide with high affinity and caused extensive chemical shift perturbations of protein amide resonances, significantly greater than those seen with an acetylated peptide derived from histone H4 at K16, as shown in 2D ^{1}H-^{15}N heteronuclear single quantum coherence (HSQC) spectra (Figure 1B). This observation agrees with the differences in dissociation constants (K_D), determined by NMR titration to be ~10 μM and >300 μM for the former and latter complexes, respectively. These results argue that PCAF bromodomain binding to H4 peptide is largely limited to the acetyl-lysine, whereas its recognition of Tat most likely involves additional interactions with residues flanking AcK50.

To assess the biological relevance of the PCAF bromodomain and Tat interaction to the activation of Tat transcriptional activity by PCAF and p300/CBP (Benkirane et al., 1998; Kiernan et al., 1999), we performed cell transfection experiments and measured their combined effect on the activity of the HIV-1 promoter using an HIV-1 LTR-luciferase reporter gene assay (Bieniasz et al., 1998; Madore and Cullen, 1993). As shown in Figure 1C, synergistic activation of Tat-mediated transcription of the HIV-1 promoter in human 293T cells is dependent upon both PCAF and CBP. The latter HAT transcriptional coactivator has been recently shown to be responsible for lysine acetylation of Tat at K50 that is required for Tat activation (Kiernan et al., 1999; Ott et al., 1999). More importantly, our data show that cotransfection of the PCAF bromodomain but not the CBP bromodomain resulted in a significant reduction of the synergistic activation of Tat by PCAF and CBP, likely due to an effective competition of the PCAF bromodomain against the full-length PCAF binding to Tat. Collectively, our in vivo transfection study further confirms the highly specific nature of PCAF bromodomain/Tat recognition and highlights the functional importance of this bromodomain interaction in the synergistic PCAF- and CBP-induced activation of Tat transcriptional activity in HIV-1 gene expression.

Structure of the PCAF Bromodomain/Tat Peptide Complex

To understand the structural basis of this molecular recognition, we determined the three-dimensional structure of the PCAF bromodomain in complex with Tat AcK50 peptide from a total of 2903 NMR-derived restraints. The structure for the protein (residues 723–830) and the peptide (residues 47–54) complex was well defined by the NMR data (Figure 2A, Table 1). The structure of the bromodomain when complexed to the Tat peptide consists of a left-handed four-helix bundle (helices α_Z, α_A, α_B, and α_C) and is similar to its free form structure (Dhalluin et al., 1999), except for the ZA and BC loops that comprise the acetyl-lysine binding site and undergo local conformational changes to accommodate peptide binding (see below). The Tat peptide adopts an extended conformation and lies across a pocket formed between the ZA and BC loops (Figure 2B). The side chain of the acetyl-lysine intercalates into the protein hydrophobic cavity and interacts extensively with residues F748, V752, Y760, I764, Y802, and Y809 (Figure 2C). Peptide residues flanking the acetyl-lysine contact the protein. Particularly, G(AcK−2), R(AcK−1), and R(AcK+3) showed intermolecular NOEs to the protein, and extensive interactions were observed between the side chains of Y(AcK−3) and V763 and between Q(AcK+4) and E756. These specific interactions confer a highly selective association between PCAF bromodomain and Tat.

Structural comparison of PCAF bromomdomain in the free and ligand-bound forms reveals that structural changes of the protein, largely localized in the ZA and BC loops, are directly coupled with the peptide binding (Figure 2D). These structural changes are supported by extensive NMR data, which include changes of chemical shifts and NOE patterns for the backbone amides, side chain methyl groups, and aromatic rings of many protein

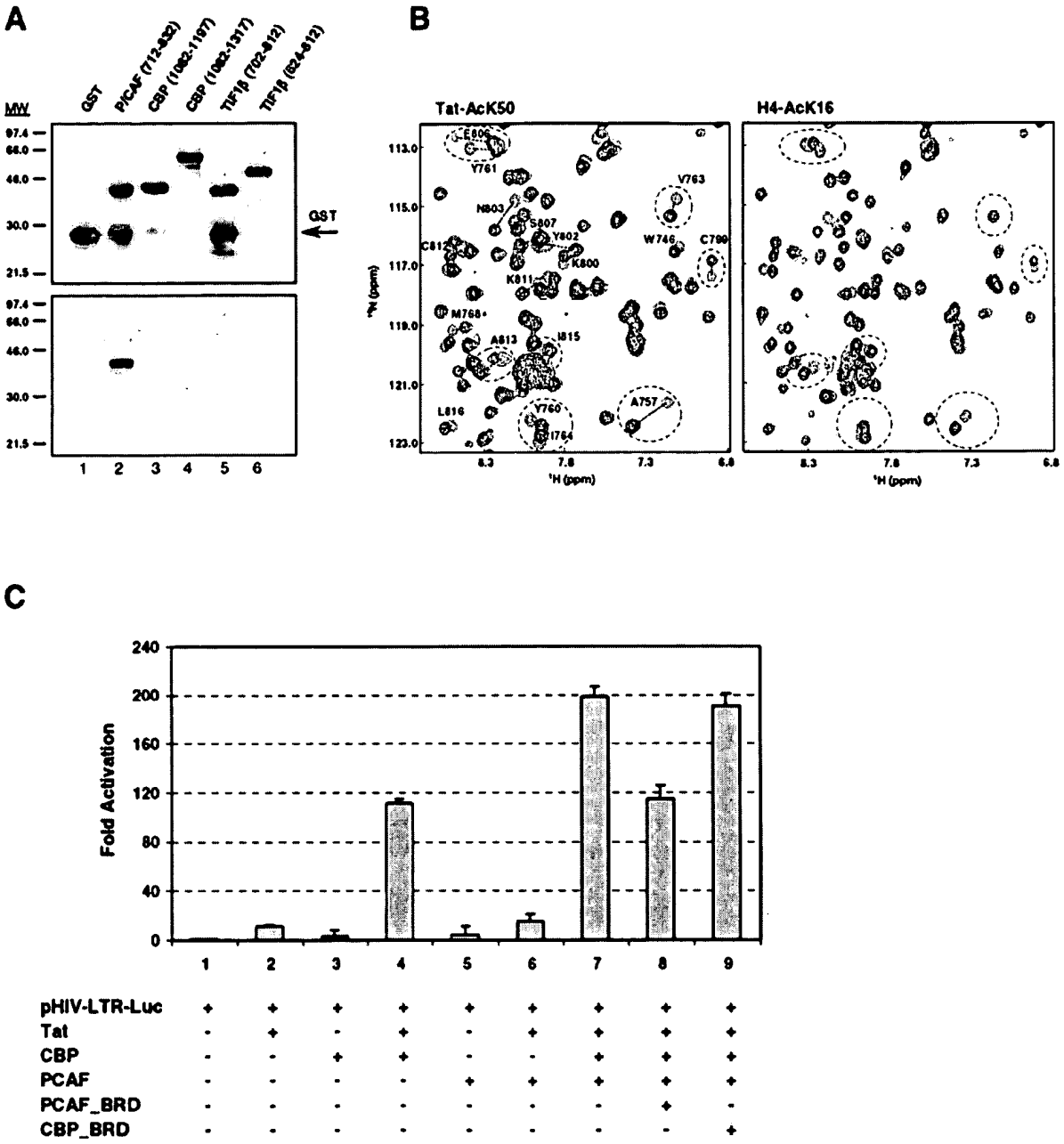

Figure 1. Recognition of Lysine-Acetylated HIV-1 Tat by PCAF Bromodomain

(A) Binding of bromodomains alone from PCAF, CBP, and TIF1β or in combination with PHD fingers from CBP and TIF1β to a biotinylated and lysine-acetylated Tat AcK50 peptide immobilized on streptavidin agarose beads. The upper panel shows purity of the GST-fusion bromodomains used in the assay, separated by SDS-PAGE and stained with Coomassie blue. The lower panel depicts Western blot with anti-GST antibodies, showing specific interaction between PCAF bromodomain and Tat AcK50 peptide.

(B) Comparison of PCAF bromodomain binding to lysine-acetylated peptide derived from HIV-1 Tat at K50 (SYGR-AcK-KRRQR) (left) versus one derived from histone H4 at K16 (SGRGKGGKGLGKGGA-AcK-RHRK) (right). The protein samples were completely titrated with the lysine-acetylated peptide of Tat or H4 with molar ratio 1:1.5 or 1:6, respectively. The 2D ^{1}H-^{15}N HSQC spectra of the bromodomain show changes of backbone amide resonances of the protein in the presence (red) or absence (black) of the peptide ligand. Blue dashed cycles highlight protein residues that exhibited major chemical shift perturbations upon Tat AcK50 peptide binding (left), significantly greater than those observed upon addition of the histone H4 peptide (right).

(C) Functional contribution of PCAF bromodomain and Tat interaction to synergistic stimulation of Tat transcriptional activity by PCAF and CBP. The plasmids used in various combinations in transfections with human 293T cells are as indicated below the graph. The amounts of the plasmids used in transfection experiments are pHIV-LTR-Luc (100 ng), pcTat (100 ng), pRSV-HA-CBP (2.0 ug), pCI-FLAG-PCAF (2.0 ug), pCMV-HA-PCAF_BRD (0.5 ug), and pCMV-FLAG-CBP_BRD (0.5 ug). Total amounts of DNA for transfections were kept constant with addition of empty control vector. Luciferase activities of the cell cytoplasmic extracts were measured using a luciferase-based assay (Promega) 24 hr after transfection and normalized to the β-galactosidase plasmid uptake as described in the Experimental Procedures. Fold activation in 293T cells is expressed relative to the basal expression of pHIV-LTR-Luc set as 1. Mean values of the luciferase activities represent at least three independent transfection experiments.

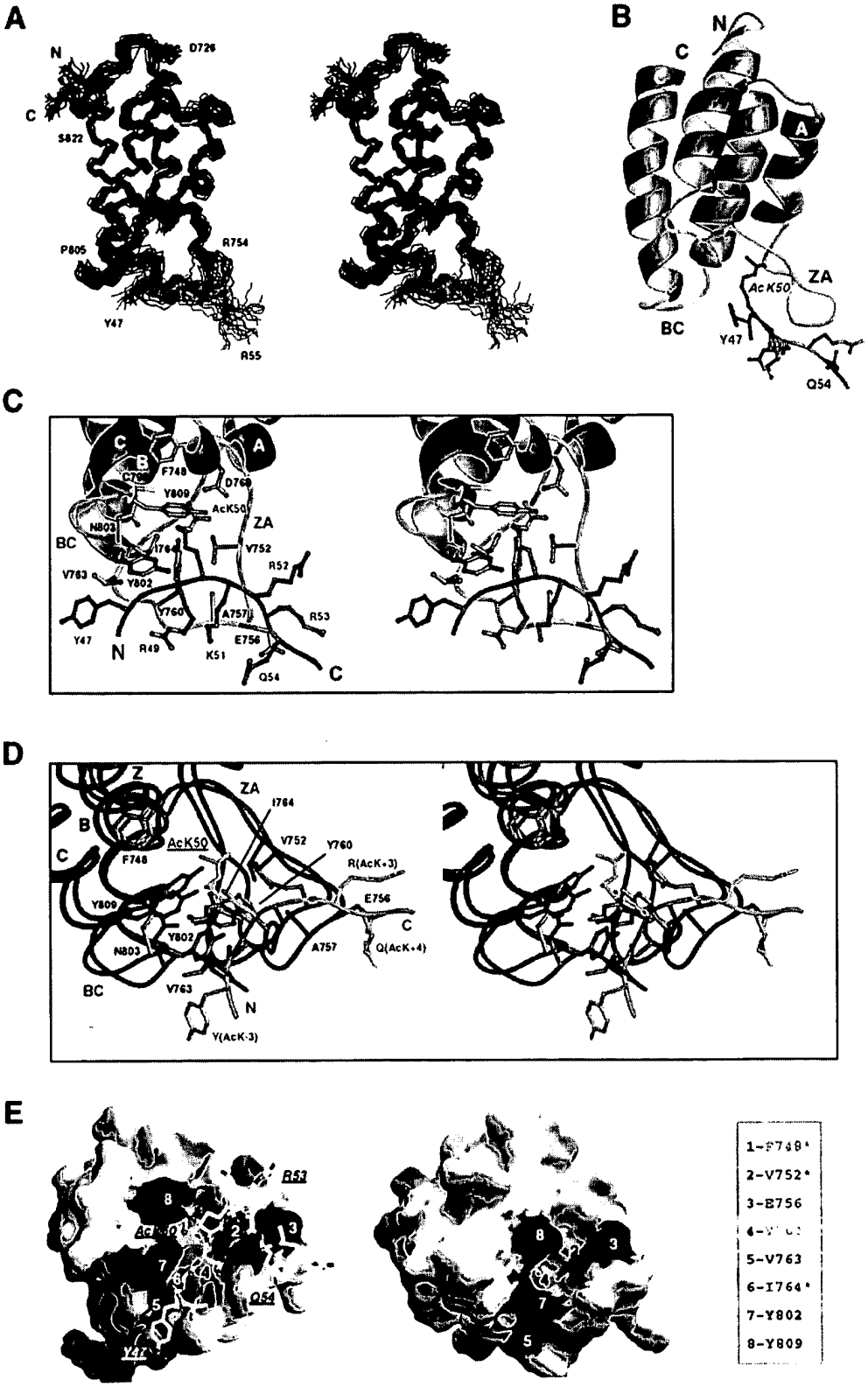

Figure 2. NMR Structure of the PCAF Bromodomain/Tat AcK50 Peptide Complex

(A) Stereoview of the backbone atoms (N, Cα, and C′) of 25 superimposed NMR-derived structures of the PCAF bromodomain (black) (showing residues 719–830) in complex with the Tat AcK50 peptide (green) (showing residues 46–55). Note that amino acid residues in the Tat peptide are described either according to their relative positions with respect to the acetyl-lysine in the sequence or for clarity numbered by their specific positions in the protein sequence of Tat.

Table 1. Summary of NMR Structural Statistics

Total Experimental Restraints	2903	
Total NOE Distance Restraints[a]	2822	
Protein		
Total ambiguous	122	
Total unambiguous	2590	
Intraresidue	1093	
Interresidue		
Sequential ($\|i - j\| = 1$)	480	
Medium ($2 \leq \|i - j\| \leq 4$)	547	
Long range ($\|i - j\| > 4$)	470	
Peptide	32	
Intermolecular	78	
Hydrogen Bond Restraints	28	
Dihedral Angle Restraints	53	
Final Energies (kcal·mol^{-1})		
E_{Total}	366.4 ± 31.1	
E_{NOE}	58.0 ± 12.6	
$E_{Dihedral}$	0.6 ± 0.3	
E_{L-J}[b]	−569.5 ± 22.4	
	Protein/Peptide Complex[f]	Secondary Structure
Ramachandran Plot (%)		
Most favorable region	72.1 ± 2.3	92.0 ± 3.0
Additionally allowed region	22.9 ± 2.4	7.4 ± 3.1
Generously allowed region	3.6 ± 1.4	0.6 ± 0.1
Disallowed region	1.3 ± 0.6	0.0 ± 0.0
Cartesian coordinate RMSDs (Å)[c]		
Backbone atoms (N, Cα, and C′)[d]	0.66 ± 0.14	0.39 ± 0.05
Heavy atoms[d]	1.25 ± 0.18	0.96 ± 0.08
Backbone atoms (N, Cα, and C′)[e]	0.50 ± 0.16	
Heavy atoms[e]	1.83 ± 0.50	
Backbone atoms (N, Cα, and C′)[f]	0.72 ± 0.15	0.54 ± 0.09
Heavy atoms[f]	1.39 ± 0.20	1.25 ± 0.16

[a] Of the total 2822 NOE-derived distance restraints, 341 were obtained by using ARIA program, of which 122 are classified as ambiguous NOEs. The latter NOE signals in the NMR spectra match with more than one proton atom in both the chemical shift assignment and the final NMR structures.
[b] The Lennard-Jones potential was not used during any refinement stage.
[c] None of these final structures exhibit NOE-derived distance restraint violations greater than 0.3 Å or dihedral angle restraint violations greater than 5°.
[d] Protein residues 723–830.
[e] Peptide residues 47–52 and 53–54.
[f] Protein residues 723–830 and peptide residues 47–52 and 53–54.

residues (Figure 1B; see Supplemental Figure S1 at http://www.molecule.org/cgi/content/full/9/3/575/DC1). For instance, aromatic protons of Y802 in the BC loop and Y760 in the ZA loop show numerous long-range NOEs in the free form, which become completely absent in the peptide-bound form (see Supplemental Figures S2A, S2B, and S2C at http://www.molecule.org/cgi/content/full/9/3/575/DC1). These changes of NOE patterns are reflected in a ~90° rotational flip of the aromatic ring of Y802, which opens a channel lined by the ZA and BC loops to grasp the peptide through intermolecular interactions such as those observed between Y(AcK-3) and V763 (Figure 2D). Changes of loop conformation in the ZA and BC loops also result in exposing otherwise almost completely buried protein residues such as F748, V752, and I764 for direct peptide recognition (Figure 2E). Supporting NMR data include: (1) the methyl group (δ1) of I764 in the ZA loop shows a NOE cross peak to H^{α} of Y802, only in the free but not in the complex form; and (2) the methyl group of A757 in the ZA loop changes its spatial position from being close to the aromatic ε protons of Y802 (Y802.ε) in the free form to being proximal to Y761.ε upon binding to the Tat peptide (see Supplemental Figures S2D and S2E at

(B) Ribbons (Carson, 1991) representation of the average minimized NMR structure of the PCAF bromodomain/Tat peptide complex.
(C) Stereoview of the Tat binding site in the bromodomain showing side chains of the protein (green) and peptide (blue) residues that are directly involved intermolecular interactions.
(D) Stereoview of superimposition of the free (green) and ligand-bound (blue) structures of PCAF bromodomain showing side chain conformation of the residues in the Tat peptide binding site. The residues of the Tat peptide are colored in orange.
(E) Surface representation of the Tat binding site of the bromodomain in ligand-bound (left) and free form (right). Protein residues important in ligand recognition are colored with the same color scheme in both structures. Residues indicated by an asterisk are almost completely buried in the free form structure.

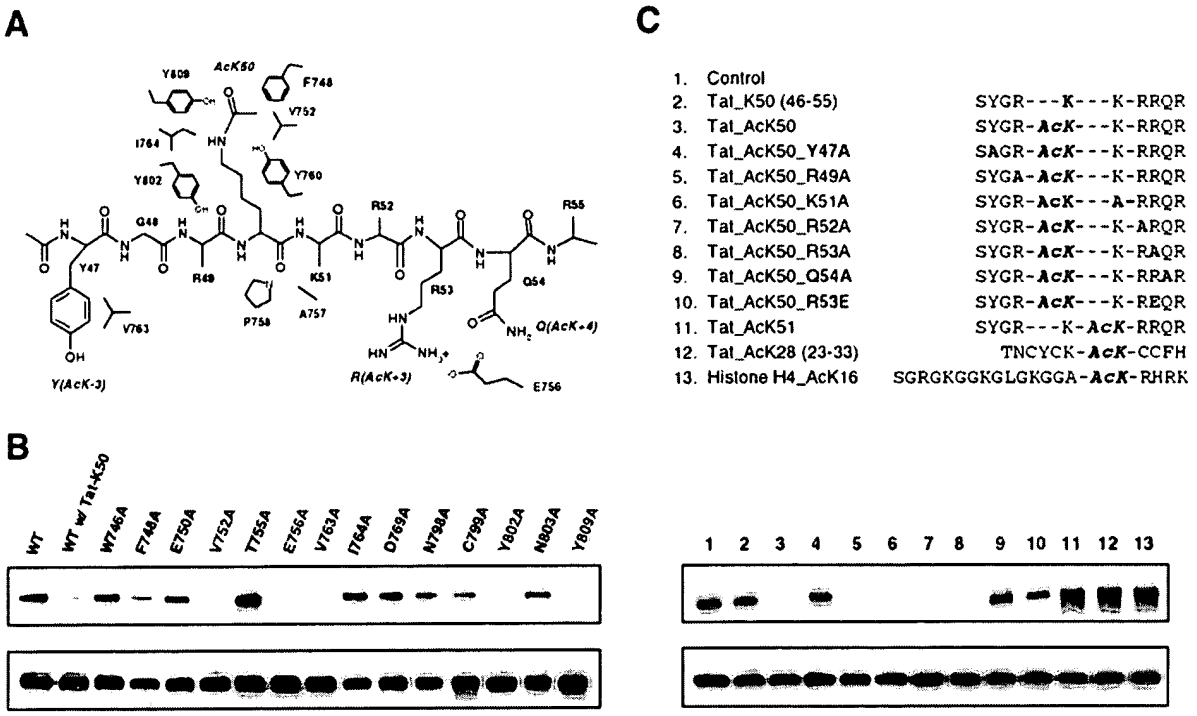

Figure 3. Mutational Analyses of PCAF Bromodomain Binding to HIV-1 Tat

(A) Schematic diagram showing amino acid residues involved in the protein/peptide interface.

(B) Effect of point mutation of protein residues on Tat AcK50 peptide binding. Western blot with anti-GST antibodies shows binding of the GST-fusion PCAF bromodomain proteins to the biotinylated Tat AcK50 peptide immobilized on streptavidin agarose beads (upper panel). The lower panel indicates a relatively equal amount of bromodomain proteins used in each binding experiment. Protein residues highlighted in red exhibited a significant reduction in binding to the Tat AcK50 peptide due to an alanine substitution.

(C) Mutational analysis of Tat peptide residues. Mutation effect was assessed by a peptide competition assay using anti-GST Western blot, in which a nonbiotinylated peptide competes with the biotinylated wild-type Tat AcK50 peptide for binding to the GST-fusion PCAF bromodomain. Numerals above the upper panel indicate a specific peptide used in the competition assay. The numerals in red refer to mutant Tat peptides that showed a significant reduction in binding to the bromodomain in the competition assay. The lower panel shows the relatively equal amount of bromodomain proteins used in each study. For clarity, the peptide residues are numbered according to their positions in the Tat protein sequence.

http://www.molecule.org/cgi/content/full/9/3/575/DC1). Together, our NMR data strongly suggest that conformational changes of protein residues in the ligand binding site are directly coupled with the highly selective interactions between PCAF bromodomain and acetylated Tat.

Specificity of PCAF Bromodomain and Tat Recognition

To determine the relative contributions of bromodomain residues in Tat binding site (Figure 3A), we examined its mutant proteins for binding to an N-terminal biotinylated Tat AcK50 peptide immobilized onto streptavidin agarose beads. Mutation of bromodomain residues W746, E750, T755, I764, D769, N798, C799, or N803 to alanine did not affect peptide binding, whereas proteins containing an alanine mutation at F748, V752, Y802, or Y809 showed a major reduction or nearly complete loss in Tat binding (Figure 3B). Moreover, alanine substitution of V763 or E756 almost completely abrogated peptide association, underlining the importance of their specific interactions with peptide residues Y(AcK−3) and Q(AcK+4). It is important to note that since both V763 and E756 are solvent exposed and located in loop regions of the structure (Figure 2D), their individual mutation to alanine unlikely causes major conformational disruption of the protein. Mutation results of these protein residues are consistent with the NMR structure of the complex and confirm their direct interactions with the acetyl-lysine and/or its flanking residues in the Tat peptide.

To further identify determinants in Tat sequence for PCAF bromodomain recognition, we synthesized mutant peptides and tested their binding to the protein in a peptide competition assay. Because of the high sensitivity of this detection method, the binding study was performed at a protein concentration (10 μM) much lower than that required for NMR study (~200 μM), ensuring specificity of protein-peptide interactions. As anticipated, lysine-acetylated peptides derived from Tat at K51 or K28 (lanes 11 and 12 in Figure 3C) or from histone H4 at K16 (lane 13) showed almost no competition against Tat AcK50 peptide in PCAF bromodomain binding, demonstrating that the latter interaction is of high affinity and specificity. Alanine substitution of resi-

dues R(AcK−1), K(AcK+1), R(AcK+2), or R(AcK+3) in Tat AcK50 peptide slightly weakened its binding to the bromodomain. Conversely, change of Y(AcK−3) (lane 4) or Q(AcK+4) (lane 9) to alanine caused a nearly complete loss of bromodomain binding, confirming the importance of their pairwise interactions with V763 and E756 for Tat-PCAF association. Finally, while mutation of R(AcK+3) to alanine (lane 8) did not significantly alter Tat binding to the bromodomain, its substitution to glutamic acid (lane 10) exhibited a marked reduction in the protein/peptide interaction. The effect of the latter mutation is likely due to an electrostatic repulsion between the glutamate and E756 of the protein. Together, these results explain the structural basis for the highly selective nature of PCAF and lysine-acetylated Tat association, which requires specific interactions of the bromodomain with AcK50 and its flanking residues, including Y(AcK−3), R(AcK+3), and Q(AcK+4).

PCAF Bromodomain Competing against TAR RNA for Binding to Lysine-Acetylated Tat

The arginine-rich motif containing R52 and R53 in Tat is also known to interact with the HIV-1 TAR RNA element (Aboul-ela et al., 1995; Long and Crothers, 1999; Rana and Jeang, 1999). Tat acetylation at K50 by p300/CBP promotes Tat dissociation from TAR RNA in early transcriptional elongation (Deng et al., 2000; Kiernan et al., 1999). To determine whether lysine acetylation directly affects Tat association with TAR RNA, we performed an NMR study of a 27 nucleotide HIV-1 TAR RNA binding to Tat peptides containing either K50 or AcK50. Our results showed that TAR RNA bound to the nonacetylated Tat peptide with a subnanomolar affinity (K_D), in agreement with results reported previously (Aboul-ela et al., 1995; Long and Crothers, 1999), and that K50 acetylation of Tat resulted in a significant reduction of its affinity to TAR RNA (data not shown). More strikingly, we found that PCAF bromodomain competes effectively against TAR RNA for binding to Tat AcK50 peptide (Figures 4A and 4B), suggesting that the binding affinity (K_D) of the latter interaction is on the order of low micromolar. This observation may be explained by possible conformational change of the peptide residues due to acetylation at K50 or involvement of R53 of Tat in both interactions. These results strongly imply that the PCAF bromodomain interaction with AcK50 on Tat not only contributes to Tat-PCAF association but also to the release of lysine-acetylated Tat from TAR RNA association, leading to Tat-mediated HIV-1 transcriptional activation.

Differences of Ligand Selectivity of Bromodomains

Structural comparison of bromodomains from PCAF and other proteins extends our understanding of differences in ligand selectivity. Recent structures of bromodomains from human GCN5 (Hudson et al., 2000) and *Saccharomyces cerevisiae* GCN5p (Owen et al., 2000), and the double bromodomain module of human $TAF_{II}250$ (Jacobson et al., 2000), reinforce the notion that the left-handed four-helix bundle fold of the PCAF bromdomain is conserved in the bromodomain family (Dhalluin et al., 1999). Structural similarity is high for the four helices with pairwise root-mean-square deviations of 0.7–1.8 Å for the backbone Cα atoms. The majority of structural deviations are localized in the loop regions, particularly in the ZA and BC loops (see Supplemental Figure S3 at http://www.molecule.org/cgi/content/full/9/3/575/DC1).

The crystal structure of scGCN5p bromodomain solved in complex with an acetylated peptide derived from histone H4 at K16 (A-AcK-RHRKILRNSIQGI) reveals that the mechanism of acetyl-lysine recognition is highly conserved in bromodomains—it involves a nearly identical set of corresponding conserved residues in the PCAF and scGCN5p bromodomains (Figures 5A and 5B) (Owen et al., 2000). In addition to the acetyl-lysine, scGCN5p bromodomain has a limited number of contacts with two residues at (AcK+2) and (AcK+3) in the H4 peptide. Binding of H(AcK+2) to aromatic rings of Y406 and F367 in scGCN5p is reminiscent of PCAF bromodomain recognition of Tat Y(AcK−3) through interactions with Y802 and V763, which are equivalent to the two scGCN5p residues. Because of this similar mode of molecular interaction, the two aromatic residues in the Tat and H4 peptides, which are located in very different positions with respect to the acetyl-lysine, are bound in a nearly identical position in the corresponding bromodomain structures (Figure 5A). High conservation of these residues in bromodomains (Figure 5B) suggests that selection of an aromatic or hydrophobic residue neighboring the acetyl-lysine is possibly conserved for many members of the bromodomain family.

It is important to note that while the major binding determinant in scGCN5p bromodomain-H4 complex is the acetyl-lysine (Owen et al., 2000), the highly specific association of PCAF bromodomain and Tat peptide is dependent on its interactions not only with the acetyl-lysine and Y(AcK−3) but also with residues on the other side of the acetyl-lysine at (AcK+3) and (AcK+4) (Figures 3B and 3C). These differences in the extent of ligand interactions explain why the Tat AcK50 peptide competes effectively against a similar histone H4 AcK16 peptide for binding to the PCAF bromodomain (Figure 3C, lane 13). Moreover, these differences in ligand selectivity provide an explanation for the striking differences in location and orientation of the bound peptides in the two bromodomains—the backbones of the Tat and H4 peptides lie in the two corresponding structures nearly antiparallel to each other (Figure 5A). Binding of A757 and E756 in the ZA loop to R(AcK+3) and Q(AcK+4) of the Tat peptide, which are completely lacking in the scGCN5 bromodomain-H4 complex, further explains why the PCAF bromodomain undergoes more extensive conformational changes in the ligand site than those seen in the GCN5 bromodomains (see Supplemental Figure S3 at http://www.molecule.org/cgi/content/full/9/3/575/DC1). While the biological relevance of the scGCN5 and histone H4 AcK16 interaction remains to be determined, a growing body of evidence, including previous reports (Benkirane et al., 1998; Deng et al., 2000), our present study of NMR structure and in vitro mutagenesis, and results from in vivo functional studies of Tat-mediated HIV-1 transcriptional activation (Figure 1C and M.O. and E.V., unpublished data), strongly support the biological relevance and importance for the highly selective association of PCAF bromodomain and acetylated Tat.

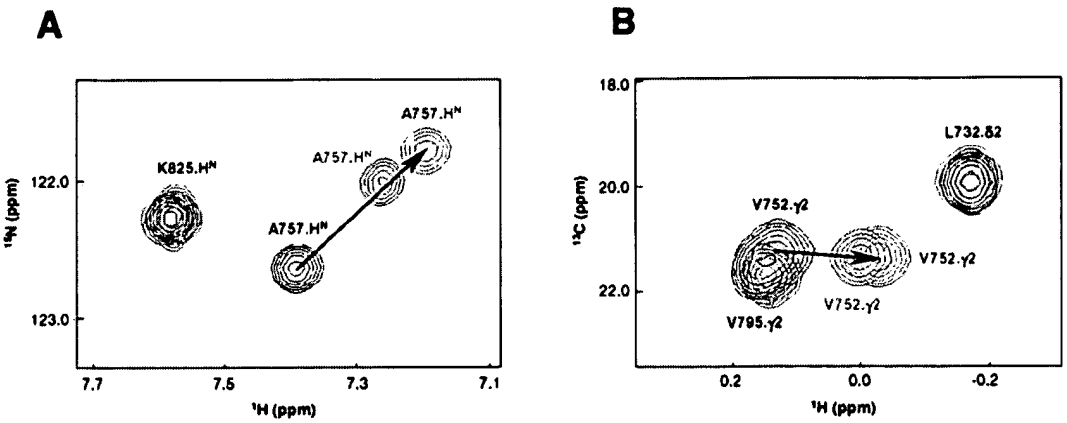

Figure 4. PCAF Bromodomain Competing against TAR RNA for Binding to Tat AcK50 Peptide

(A) Superimposition of a selected region of 2D ^{1}H-^{15}N HSQC spectra of a $^{13}C/^{15}N$-labeled PCAF bromodomain protein in the free form (black), in the presence of Tat AcK50 peptide (molar ratio of 1:1.2) (red), and in the presence of Tat AcK50 peptide and TAR RNA (molar ratio of 1:1.2:1 for protein:peptide:RNA) (blue). The spectra show chemical shift changes of the backbone amide resonances of protein residues due to peptide binding.

(B) Superimposition of 2D ^{1}H-^{13}C HSQC spectra of the PCAF bromodomain collected under the same conditions as described in (A). The NMR spectra exhibit chemical shift changes of the side chain methyl group resonances of protein residues due to peptide binding. The same color-coding scheme was used as in (A). Arrows indicate chemical shift changes of protein NMR resonances from the free form (black) to the Tat AcK50 peptide-bound form (red). Note that only the bromodomain residues (i.e., A757 and V752) that directly interact with the Tat peptide, as shown in the three-dimensional structure, exhibited major chemical shift changes upon peptide binding or in competing against TAR RNA for binding to the Tat peptide. More importantly, addition of TAR RNA causes only small shifts of the protein signals from the Tat peptide-bound position toward the free form position, suggesting that the PCAF bromodomain competes effectively against TAR RNA for binding to the lysine-acetylated Tat peptide. We observed by NMR no significant nonspecific interactions between the protein and TAR RNA under these conditions.

Since bromodomain residues important for acetyl-lysine recognition are largely conserved, binding of acetyl-lysine on a protein is likely a general biochemical function for bromodomains. However, differences in ligand selectivity may be attributed to a few but important differences in bromodomain sequences (Figure 5B), which include (1) variations in the ZA loop such as relatively low sequence conservation and amino acid deletion or insertion; and (2) variation of bromodomain residues that are involved in direct interactions with residues surrounding acetyl-lysine in a target protein. For instance, E756 in the bromodomain of PCAF is unique and only present in a small subset of bromodomains including GCN5. An analogous residue in the structurally similar bromodomain of CBP or p300 (Y.H. and M.-M.Z., unpublished data) is a leucine followed by a 2 amino acid insertion, which are present in a small subfamily of bromodomains (Figure 5B) (Jeanmougin et al., 1997). Moreover, a short helix corresponding to the AWPFM sequence in the ZA loop of PCAF (residues 745–749) is likely completely missing in TIF1β bromodomain due to amino acid deletion, and E756 of PCAF is substituted with a two residue AT motif in the sequence. Together, these findings explain why bromodomains from CBP and TIF1β did not interact with Tat AcK50 peptide (Figure 1A).

Human GCN5-S, a shorter version of hGCN5 that contains only the HAT domain and the bromodomain but lacks the N-terminal p300/CBP binding domain due to an alternative RNA splicing (Schiltz and Nakatani, 2000; Yamauchi et al., 2000), has been recently reported to interact with HIV Tat in vitro (Col et al., 2001). This Tat interaction involves both the HAT domain and the bromodomain of hGCN5-S. While the specific binding site on Tat by the hGCN5 bromodomain and the question of whether this bromodomain interaction is dependent on Tat lysine acetylation remain to be determined, our data reported here suggest that the hGCN5 bromodomain may possess ligand selectivity similar to that of the structurally homologous bromodomain of PCAF.

Conclusion

Tat-stimulated transcriptional activation of integrated HIV-1 genomes defines the rate-limiting step for viral replication (Adams et al., 1994; Benkirane et al., 1998). Tat synergy with histone acetyltransferases and its recruitment of PCAF via a bromodomain interaction, as we described in this study, support the notion that Tat transactivation of HIV-1 chromosomal transcription proceeds via chromatin remodeling (Deng et al., 2000; Kiernan et al., 1999; Ott et al., 1999). Our findings may explain why deletion of the PCAF C-terminal region comprising the bromodomain potently abrogated Tat transactivation of integrated but not unintegrated HIV-1 LTR (Benkirane et al., 1998). Our study reinforces the concept that bromodomain and acetyl-lysine recognition could serve as a pivotal mechanism for controlling protein-protein interactions in chromatin remodeling as well as other cellular processes including viral life cycle (Dyson et al., 2001; Winston and Allis, 1999), and that differences

A

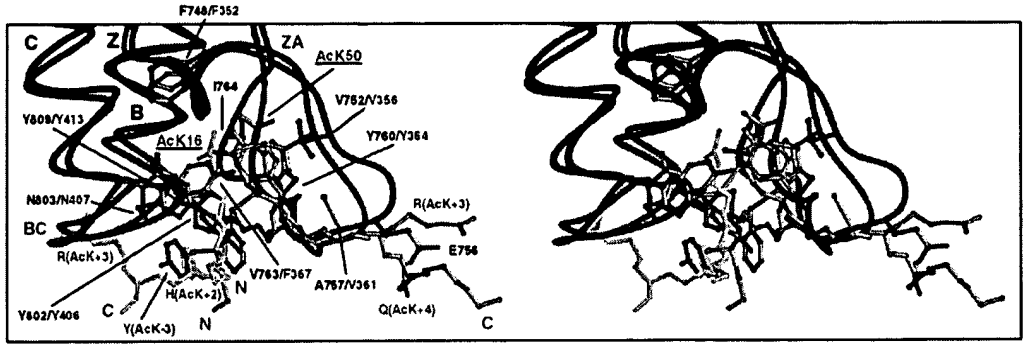

B

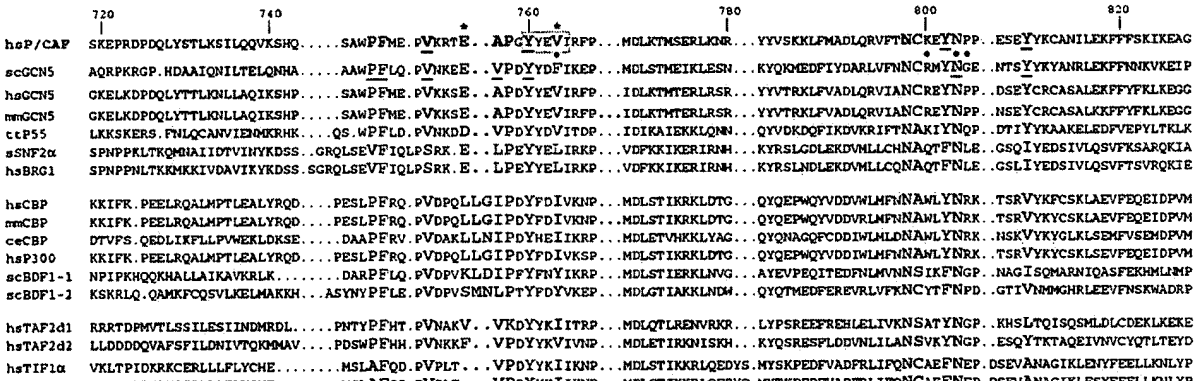

Figure 5. Differences in Ligand Selectivity of Bromodomains

(A) Stereoview of superimposition of the structures of the PCAF bromodomain-Tat peptide complex (blue) and the scGCN5 bromodomain-H4 peptide complex (red) showing conformational differences of protein residues in the peptide binding sites. The lysine-acetylated peptides of HIV-1 Tat and histone H4 are shown in green and orange, respectively. The residues of the PCAF and scGCN5 bromodomains are numbered according to protein sequences and color-coded in black and red, respectively. The corresponding conserved residues in the two bromodomains are annotated together. The amino acid residues of the Tat and H4 peptides are described according to their position with respect to the acetyl-lysine in the corresponding peptide sequences. The structures were superimposed on the four helices of the two bromodomains in Insight and the figure was prepared with Ribbons.

(B) Sequence alignment of a selected number of bromodomains. The sequences were aligned based on the experimentally determined three-dimensional structures of five bromodomains, highlighted in yellow. Note that in the PCAF bromodomain, a short helix in the ZA loop comprising the YYEVI sequence (residues 760–764) (boxed by dashed lines) was only observed in the free form but not in the Tat peptide-bound form. The predicted secondary structures in the corresponding regions of other bromodomains are shown in green. Because of relatively high variations in amino acid sequence in the ZA loop, prediction of secondary structures was omitted. Bromodomains are grouped on the basis of the predicted sequence and/or structural similarities. Residue numbers of the PCAF bromodomain are indicated above its sequence. Three absolutely conserved residues, corresponding to P751, P767, and N803 in the PCAF bromodomain, are shown in purple. Highly conserved residues are colored in blue. The residues in the PCAF bromodomain that directly interact with the Tat peptide, as determined by intermolecular NOEs, are displayed in a larger font size. The residues essential for the acetyl-lysine binding are underlined, and the residues important for ligand selectivity through interactions with the peptide residues flanking the acetyl-lysine are highlighted by red asterisks. The protein residues contacting the acetyl-lysine in the scGCN5 bromodomain-H4 peptide complex are underlined, and residues contacting other parts of the peptide are indicated by red dots.

in ligand selectivity of conserved protein modular domains can be achieved by evolutionary changes of amino acid sequences in the ligand binding site. The new knowledge of the structural basis of PCAF bromodomain and Tat recognition should aid in the design of small molecules that can be used to block this specific

interaction in order to disrupt HIV-1 transcriptional activation and replication.

Experimental Procedures

Sample Preparation

The PCAF bromodomain (residues 719–832) was expressed in *Escherichia coli* BL21(DE3) cells using the pET14b vector (Novagen) (Dhalluin et al., 1999). Isotope-labeled bromodomain proteins were prepared from cells grown on a minimal medium containing $^{15}NH_4Cl$ with or without $^{13}C_6$-glucose in either H_2O or 75% ^2H_2O. The protein was purified by affinity chromatography on a nickel-IDA column (Invitrogen), followed by the removal of poly-His tag by thrombin cleavage. GST-fusion bromodomains from PCAF, CBP, and TIF1β were expressed in *E. coli* BL21 (DE3) codon plus cells using the pGEX4T-3 vector (Pharmacia) and purified with a glutathione sepharose column. NMR spectra of the recombinant CBP and TIF1β proteins were acquired to ensure that they were properly folded and functional (see Supplemental Figure S4 at http://www.molecule.org/cgi/content/full/9/3/575/DC1). The acetyl-lysine-containing peptides were prepared on a MilliGen 9050 peptide synthesizer (Perkin Elmer) using Fmoc/HBTU chemistry. Acetyl-lysine was incorporated using the reagent Fmoc-Ac-Lys with HBTU/DIPEA activation. The HIV-1 TAR RNA was obtained from Dharmacon Research, Inc. (Lafayette, CO).

NMR Spectroscopy

NMR samples contained a protein/peptide complex of 0.5 mM in 100 mM phosphate buffer (pH 6.5) containing 5 mM perdeuterated DTT and 0.5 mM EDTA in $H_2O/^2H_2O$ (9/1) or ^2H_2O. All NMR spectra were acquired at 30°C on a Bruker 500 or 600 MHz NMR spectrometer. The ^1H, ^{13}C, and ^{15}N resonances of the protein backbone and side chain atoms were assigned by using a standard set of triple-resonance experiments (Sattler et al., 1999) with a uniformly $^{13}C/^{15}N$-labeled and 75% deuterated protein in complex with an unlabeled peptide. The distance restraints were obtained from ^{13}C- or ^{15}N-edited three-dimensional nuclear Overhauser enhancement spectroscopy (NOESY) spectra (Clore and Gronenborn, 1994). ϕ-angle restraints were determined based on the $^3J_{HN,H\alpha}$ coupling constants measured in a 3D HNHA spectrum (Clore and Gronenborn, 1994). Slowly exchanging amide protons were identified from a series of 2D ^{15}N-HSQC spectra recorded after the H_2O buffer was changed to a ^2H_2O buffer, which were used together with the initial structures calculated with only NOE-derived distance restraints to generate hydrogen-bond distance restraints in final structure calculations. The intermolecular NOEs were detected in ^{13}C-edited (F_1), $^{13}C/^{15}N$-filtered (F_3) 3D NOESY spectrum (Clore and Gronenborn, 1994). All NMR spectra were processed with the NMRPipe program (Delaglio et al., 1995) and analyzed using NMRView (Johnson and Blevins, 1994). NMR binding studies of Tat peptides and TAR RNA interactions were performed in the phosphate buffer (pH 6.5) containing 200 mM NaCl to minimize any nonspecific interactions.

Structure Calculations

Structures of the protein/peptide complex were calculated with a distance geometry-simulated annealing protocol using the X-PLOR program (Brunger, 1993). A total of 2359 manually assigned NOE-derived distance restraints were used in initial structure calculations. The ARIA (Nilges and O'Donoghue, 1998)-assigned distance restraints agree with the structures calculated using only the manually determined NOE distance restraints, 28 hydrogen-bond distance restraints, and 53 ϕ angle restraints. The final structure calculations employed a total of 2903 NMR experimental restraints from the manual and the ARIA-assisted assignments, including 2700 unambiguous intramolecular and 78 intermolecular NOE distance restraints. The distance restraint force constant was 50 kcal mol^{-1} $Å^{-2}$, and no NOE was violated by more than 0.3 Å. The torsion restraint force constant was 200 kcal mol^{-1} rad^{-2}, and no dihedral angle restraint was violated by more than 5°. While only the covalent geometry terms, NOE, torsion, and repulsive van der Waals terms were used in the structure refinement, a large, negative Lennard-Jones potential energy was observed (−569.5 ± 22.4 kcal mol^{-1}), indicating good nonbonded geometry of the structure. Procheck (Laskowski et al., 1996) analysis indicated that over 98% of the protein and peptide residues are in allowed regions of the Ramachandran map.

Mutational Analysis

Site-directed mutant proteins of PCAF bromodomain were prepared with the QuickChange kit (Stratagene). DNA sequencing confirmed the desired mutations. The GST-fusion bromodomains (10 μM) of PCAF, CBP, or TIF1β were incubated with an N-terminal biotinylated and lysine-acetylated Tat peptide (50 μM) in 50 mM Tris buffer (pH 7.5), containing 50 mM NaCl, 0.1% BSA, and 1 mM DTT at 22°C for 2 hr. Streptavidin agarose (10 μL) was added to the mixture, and the beads were washed in the Tris buffer containing 500 mM NaCl and 0.1% NP-40. Proteins eluted from the agarose beads were separated by SDS-PAGE and visualized by Western blotting using anti-GST antibody (Sigma) and horseradish-peroxidase-conjugated goat anti-rabbit IgG. Peptide competition assay was performed by incubating a nonbiotinylated peptide with the PCAF bromodomain and the biotinylated Tat AcK50 peptide. The molar ratio of the former and latter peptides in the mixture was kept at 1:2.

Plasmid Constructs

The mammalian expression vectors for the PCAF and CBP bromodomains were constructed as follows. Coding sequence for the PCAF bromodomain (residues 719–832) was subcloned into EcoRI-XhoI sites of pCMV-HA vector (Clontech). The CBP bromodomain (residues 1082–1197) was subcloned into BamHI-XhoI sites of pCMV-FLAG vector (Stratagene). The expression vectors for the full-length PCAF (pCI-FLAG-PCAF) (Li et al., 2000), the full-length CBP (pRSV-HA-CBP) (Kwok et al., 1996), HIV-1 Tat (pcTat), and the HIV-1 LTR-luciferase reporter construct (pHIV-LTR-Luc) (Bieniasz et al., 1998; Madore and Cullen, 1993) have been previously described.

Cell Culture and Transfections

Human 293T cells were propagated in Dulbecco's modified Eagle's medium with 10% fetal calf serum and transfected using the calcium phosphate coprecipitation method. Amounts of plasmid DNA used in cell transfections are as described in the legend to Figure 1C. The transfected 293T cells were lysed 24 hr after transfection and assayed for luciferase activity of the cell extracts using a luciferase-based assay system (Promega) (Bieniasz et al., 1998; Madore and Cullen, 1993). Luciferase activities derived from HIV-1 LTR were normalized to a cotransfected vector expressing β-galactosidase. The expression level of the transfected proteins was examined by Western blotting using monoclonal antibodies to HA (Roche Diagnostics), FLAG (Stratagene), or β-actin (Sigma), and rabbit polyclonal antibodies to the PCAF bromodomain or the CBP bromodomain (see Supplemental Figure S5 at http://www.molecule.org/cgi/content/full/9/3/575/DC1).

Acknowledgments

We thank P.D. Bieniasz for providing the pcTat and HIV-1 LTR-luc constructs, M.J. Walsh and R.L. Schiltz for the PCAF expression plasmids, and N. Zeleznik-Le for the full-length CBP construct. We also thank I. Wolf for peptide synthesis, C. Dhalluin, O. Plotnikova, and S. Yan for technical advice and support, A. Koch, K. Manzur, and K.S. Yan for critical reading of the manuscript, and A.K. Aggarwal, D.E. Logothetis, and H. Weinstein for helpful suggestions to the study. This work was supported by a National Institutes of Health grant to M.-M. Z.

Received September 18, 2001; revised January 9, 2002.

References

Aasland, R., Gibson, T.J., and Stewart, A.F. (1995). The PHD finger: implications for chromatin-mediated transcriptional regulation. Trends Biochem. Sci. *20*, 56–59.

Aboul-ela, F., Karn, J., and Varani, G. (1995). The structure of the human immunodeficiency virus type-1 TAR RNA reveals principles of RNA recognition by Tat protein. J. Mol. Biol. *253*, 313–332.

Adams, M., Sharmeen, L., Kimpton, J., Romeo, J.M., Garcia, J.V.,

Peterlin, B.M., Groudine, M., and Emerman, M. (1994). Cellular latency in human immunodeficiency virus-infected individuals with high CD4 levels can be detected by the presence of promoter-proximal transcripts. Proc. Natl. Acad. Sci. USA *91*, 3862–3866.

Benkirane, M., Chun, R.F., Xiao, H., Ogryzko, V.V., Howard, B.H., Nakatani, Y., and Jeang, K.-T. (1998). Activation of integrated provirus requires histone acetyltransferase: p300 and P/CAF are co-activators for HIV-1 Tat. J. Biol. Chem. *273*, 24898–24905.

Bieniasz, P.D., Grdina, T.A., Bogerd, H.P., and Cullen, B.R. (1998). Recruitment of a protein complex containing Tat and cyclin T1 to TAR governs the species specificity of HIV-1 Tat. EMBO J. *17*, 7056–7065.

Brown, C.E., Howe, L., Sousa, K., Alley, S.C., Carozza, M.J., Tan, S., and Workman, J.L. (2001). Recruitment of HAT complexes by direct activator interactions with the ATM-related Tra1 subunit. Science *292*, 2333–2337.

Brownell, J.E., and Allis, C.D. (1996). Special HATs for special occasions: Linking histone acetylation to chromatin assembly and gene activation. Curr. Opin. Genet. Dev. *6*, 176–184.

Brunger, A.T. (1993). X-PLOR Version 3.1: A System for X-Ray Crystallography and NMR, Version 3.1 edn (New Haven, CT: Yale University Press).

Carson, M. (1991). Ribbons 2.0. J. Appl. Crystallogr. *24*, 958–961.

Clore, G.M., and Gronenborn, A.M. (1994). Multidimensional heteronuclear nuclear magnetic resonance of proteins. Methods Enzymol. *239*, 249–363.

Col, E., Caron, C., Seigneurin-Berny, D., Gracia, J., Favier, A., and Khochbin, S. (2001). The histone acetyltransferase, hGCN5, interacts with and acetylates the HIV transactivator. Tat. J. Biol. Chem. *276*, 28179–28184.

Cullen, B.R. (1998). HIV-1 auxiliary proteins: making connections in a dying cell. Cell *93*, 685–692.

Delaglio, F., Grzesiek, S., Vuister, G.W., Zhu, G., Pfeifer, J., and Bax, A. (1995). NMRPipe: a multidimensional spectral processing system based on UNIX pipes. J. Biomol. NMR *6*, 277–293.

Deng, L., de la Fuente, C., Fu, P., Wang, L., Donnelly, R., Wade, J.D., Lambert, P., Li, H., Lee, C.-G., and Kashanchi, F. (2000). Acetylation of HIV-1 Tat by CBP/P300 increases transcription of integrated HIV-1 genome and enhances binding to core histones. Virology *277*, 278–295.

Dhalluin, C., Carlson, J.E., Zeng, L., He, C., Aggarwal, A.K., and Zhou, M.-M. (1999). Structure and ligand of a histone acetyltransferase bromodomain. Nature *399*, 491–496.

Dyson, M.H., Rose, S., and Mahadevan, L.C. (2001). Acetylation-binding and function of bromodomain-containing proteins in chromatin. Front. Biosci. *6*, 853–865.

Friedman, J.R., Fredericks, W.J., Jensen, D.E., Speicher, D.W., Huang, X.P., Neilson, E.G., and Rauscher, F.J., III. (1996). KAP-1, a novel corepressor for the highly conserved KRAB repression domain. Genes Dev. *10*, 2067–2078.

Garber, M.E., and Jones, K.A. (1999). HIV-1 Tat: coping with negative elongation factors. Curr. Opin. Immunol. *11*, 460–465.

Haynes, S.R., Dollard, C., Winston, F., Beck, S., Trowsdale, J., and Dawid, I.B. (1992). The bromodomain: a conserved sequence found in human, *Drosophila* and yeast proteins. Nucleic Acids Res. *20*, 2603.

Hottiger, M.O., and Nabel, G.J. (1998). Interaction of human immunodeficiency virus type 1 Tat with the transcriptional coactivators p300 and CREB binding protein. J. Virol. *72*, 8252–8256.

Hudson, B.P., Martinez-Yamout, M.A., Dyson, H.J., and Wright, P.E. (2000). Solution structure and acetyl-lysine binding activity of the GCN5 bromodomain. J. Mol. Biol. *304*, 355–370.

Jacobson, R.H., Ladurner, A.G., King, D.S., and Tjian, R. (2000). Structure and function of a human TAFII250 double bromodomain module. Science *288*, 1422–1425.

Jeang, K.-T., Xiao, H., and Rich, E.A. (1999). Multifaceted activities of the HIV-1 transactivator of transcription. Tat. J. Biol. Chem. *274*, 28837–28840.

Jeanmougin, F., Wurtz, J.M., Douarin, B.L., Chambon, P., and Losson, R. (1997). The bromodomain revisited. Trends Biochem. Sci. *22*, 151–153.

Jenuwein, T., and Allis, C.D. (2001). Translating the histone code. Science *293*, 1074–1080.

Johnson, B.A., and Blevins, R.A. (1994). NMRView: a computer program for the visualization and analysis of NMR data. J. Biomol. NMR *4*, 603–614.

Jones, K.A. (1997). Taking a new TAK on Tat transactivation. Genes Dev. *11*, 2593–2599.

Kam, J. (1999). Tackling Tat. J. Mol. Biol. *293*, 235–254.

Keen, N.J., Churcher, M.J., and Kam, J. (1997). Transfer of Tat and release of TAR RNA during the activation of the human immunodeficiency virus type-1 transcription elongation complex. EMBO J. *16*, 5260–5272.

Kieman, R.E., Vanhulle, C., Schiltz, L., Adam, E., Xiao, H., Maudoux, F., Calomme, C., Burny, A., Nakatani, Y., Jeang, K.-T., et al. (1999). HIV-1 Tat transcriptional activity is regulated by acetylation. EMBO J. *18*, 6106–6118.

Kouzarides, T. (2000). Acetylation: a regulatory modification to rival phosphorylation? EMBO J. *19*, 1176–1179.

Kwok, R.P., Laurance, M.E., Lundblad, J.R., Goldman, P.S., Shih, H., Connor, L.M., Marriott, S.J., and Goodman, R.H. (1996). Control of cAMP-regulated enhancers by the viral transactivator Tax through CREB and the co-activator CBP. Nature *380*, 642–646.

Laskowski, R.A., Rullmannn, J.A., MacArthur, M.W., Kaptein, R., and Thornton, J.M. (1996). AQUA and PROCHECK-NMR: programs for checking the quality of protein structures solved by NMR. J. Biomol. NMR *8*, 477–486.

Li, S.D., Aufiero, B., Schiltz, R.L., and Walsh, M.J. (2000). Regulation of the homeodomain CCAAT displacement/*cut* protein function by histone acetyltransferase p300/CREB-binding protein (CBP)-associated factor and CBP. Proc. Natl. Acad. Sci. USA *97*, 7166–7171.

Long, K.S., and Crothers, D.M. (1999). Characterization of the solution conformations of unbound and Tat peptide-bound forms of HIV-1 TAR RNA. Biochemistry *38*, 10059–10069.

Madore, S.J., and Cullen, B.R. (1993). Genetic analysis of the cofactor requirement for human immunodeficiency virus type 1 Tat function. J. Virol. *67*, 3703–3711.

Manning, E.T., Ikehara, T., Ito, T., Kadonaga, J.T., and Kraus, W.L. (2001). p300 forms a stable, template-committed complex with chromatin: role for the bromodomain. Mol. Cell Biol. *21*, 3876–3887.

Nilges, M., and O'Donoghue, S. (1998). Ambiguous NOEs and automated NOE assignment. Prog. NMR Spectroscopy *32*, 107–139.

Ott, M., Schnolzer, M., Garnica, J., Fischle, W., Emiliani, S., Rackwitz, H.-R., and Verdin, E. (1999). Acetylation of the HIV-1 Tat protein by p300 is important for its transcriptional activity. Curr. Biol. *9*, 1489–1492.

Owen, D.J., Ornaghi, P., Yang, J.C., Lowe, N., Evans, P.R., Ballario, P., Neuhaus, D., Eiletici, P., and Travers, A.A. (2000). The structural basis for the recognition of acetylated histone H4 by the bromodomain of histone acetyltransferase gcn5p. EMBO J. *19*, 6141–6149.

Rana, T.M., and Jeang, K.-T. (1999). Biochemical and functional interactions between HIV-1 Tat protein and TAR RNA. Arch. Biochem. Biophys. *365*, 175–185.

Sattler, M., Schleucher, J., and Griesinger, C. (1999). Heteronuclear multidimensional NMR experiments for the structure determination of proteins in solution employing pulsed field gradients. Prog. NMR Spectroscopy *34*, 93–158.

Schiltz, R.L., and Nakatani, Y. (2000). The PCAF acetylase complex as a potential tumor suppressor. Biochim. Biophys. Acta *1470*, M37–M53.

Sterner, D.E., Grant, P.A., Roberts, S.M., Duggan, L.J., Belotserkovskaya, R., Pacella, L.A., Winston, F., Workman, J.L., and Berger, S.L. (1999). Functional organization of the yeast SAGA complex: distinct components involved in structural integrity, nucleosome acetylation, and TATA-binding protein interaction. Mol. Cell. Biol. *19*, 86–98.

Strahl, B.D., and Allis, C.D. (2000). The language of covalent histone modifications. Nature *403*, 41–45.

Tamkun, J.W., Deuring, R., Scott, M.P., Kissinger, M., Pattatucci, A.M., Kaufman, T.C., and Kennison, J.A. (1992). brahma: a regulator of *Drosophila* homeotic genes structurally related to the yeast transcriptional activator SNF2/SWI2. Cell *68*, 561–572.

Travers, A. (1999). Chromatin modification: how to put a HAT on the histones. Curr. Biol. *9*, 23–25.

Wei, P., Garber, M.E., Fang, S.M., Fischer, W.H., and Jones, K.A. (1998). A novel CDK9-associated C-type cyclin interacts with HIV-1 Tat and mediates its high-affinity, loop-specific binding to TAR RNA. Cell *92*, 451–462.

Winston, F., and Allis, C.D. (1999). The bromodomain: a chromatin-targeting module? Nat. Struct. Biol. *6*, 601–604.

Yamauchi, T., Yamauchi, J., Kuwata, T., Tamura, T., Yamashita, T., Bae, N., Westphal, H., Ozato, K., and Nakatani, Y. (2000). Distinct but overlapping roles of histone acetylase PCAF and of the closely related PCAF-B/GCN5 in mouse embryogenesis. Proc. Natl. Acad. Sci. USA *97*, 11303–11306.

Accession Numbers

Coordinates for the NMR three-dimensional structure of the PCAF bromodomain/HIV-1 Tat peptide complex have been deposited in the Brookhaven Protein Data Bank under the accession code 1JM4.

Molecular Cell, Vol. 13, 251–263, January 30, 2004, Copyright ©2004 by Cell Press

Structural Mechanism of the Bromodomain of the Coactivator CBP in p53 Transcriptional Activation

Shiraz Mujtaba,[1,4] Yan He,[1,4] Lei Zeng,[1]
Sherry Yan,[1] Olga Plotnikova,[1] Sachchidanand,[1]
Roberto Sanchez,[1] Nancy J. Zeleznik-Le,[3]
Ze'ev Ronai,[2] and Ming-Ming Zhou[1,*]
[1]Structural Biology Program
Department of Physiology and Biophysics
[2]Derald H. Ruttenberg Cancer Center
Mount Sinai School of Medicine
New York University
1425 Madison Avenue
New York, New York 10029
[3]Loyola University Medical Center
2160 South First Avenue
Maywood, Illinois 60153

Summary

Lysine acetylation of the tumor suppressor protein p53 in response to a wide variety of cellular stress signals is required for its activation as a transcription factor that regulates cell cycle arrest, senescence, or apoptosis. Here, we report that the conserved bromodomain of the transcriptional coactivator CBP (CREB binding protein) binds specifically to p53 at the C-terminal acetylated lysine 382. This bromodomain/acetyl-lysine binding is responsible for p53 acetylation-dependent coactivator recruitment after DNA damage, a step essential for p53-induced transcriptional activation of the cyclin-dependent kinase inhibitor p21 in G1 cell cycle arrest. We further present the three-dimensional nuclear magnetic resonance structure of the CBP bromodomain in complex with a lysine 382-acetylated p53 peptide. Using structural and biochemical analyses, we define the molecular determinants for the specificity of this molecular recognition.

Introduction

The human tumor suppressor protein p53 plays a pivotal role in cellular response to numerous stress signals in cell cycle arrest, senescence, DNA repair, or apoptosis (Ko and Prives, 1996; Levine, 1997; Prives and Hall, 1999; Vogelstein et al., 2000). The indispensable functions of p53 are underscored by the fact that *p53* is one of the most frequently mutated cellular genes and its mutations occur in nearly 50% of all human cancers (Vogelstein et al., 2000). p53 functions as a sequence-specific transcription factor that induces or represses transcription of a large number of genes, including p21/WAF1/CIP1, Mdm2, GADD45, Bax, cyclin G, and PAC-1 (Attardi et al., 1996; El-Deiry et al., 1993; Miyashita and Reed, 1995; Yin et al., 2003). Alteration of transcription of these genes has been directly linked to p53-mediated cell cycle arrest or apoptosis in response to DNA damage (Yin et al., 2003; Zhao et al., 2000). Interestingly, the biological functions of p53 itself are dependent upon the expression of the genes that it regulates.

p53 contains 393 amino acids, consisting of several functional domains, including an N-terminal activation domain, a PXXP region, a sequence-specific DNA binding domain, and C-terminal tetramerization and basic regions. The biological activity of p53 is tightly regulated by posttranslational modifications in its N- and C-terminal regions (Alarcon-Vargas and Ronai, 2002; Prives and Hall, 1999). Upon DNA damage, p53 is extensively phosphorylated within the N-terminal activation domain, which relieves it from association with the negative regulator Mdm2, resulting in p53 stabilization and activation as a transcription factor (Fuchs et al., 1998b; Haupt et al., 1997; Kubbutat et al., 1997; Momand and Zambetti, 1997). In addition, phosphorylation occurs in the C terminus of p53, which has been shown to enhance its DNA binding in vitro (Hupp and Lane, 1994; Wang and Prives, 1995).

In response to DNA damage, p53 becomes acetylated on multiple lysine residues in its C terminus (Gu and Roeder, 1997; Liu et al., 1999; Sakaguchi et al., 1998). Particularly, it has been reported that transcriptional coactivator histone acetyltransferases (HATs) p300/CBP (CREB binding protein) and p300/CBP-associated factor (PCAF) acetylate K373 and K382 (to a lesser extent K372 and K381) and K320, respectively. Lysine acetylation or deacetylation of p53 has been directly linked to its ability to regulate cell cycle arrest and apoptosis (Guo et al., 2000; Ito et al., 2001; Luo et al., 2000), as well as senescence (Pearson et al., 2000). It had been hypothesized on the basis of in vitro data that p53 acetylation enhances its DNA binding through the relief of negative regulation of DNA binding exerted by the C-terminal region (Gu and Roeder, 1997; Liu et al., 1999; Sakaguchi et al., 1998). However, more recent in vivo studies show that lysine acetylation of p53 does not result in any enhancement of its DNA binding ability but, rather, promotes its recruitment of coactivators, leading to histone acetylation and transcriptional activation of target genes (Barlev et al., 2001).

While the molecular mechanisms of p53 acetylation-dependent coactivator recruitment are not known, notably, these p53-associating coactivators contain evolutionarily conserved bromodomains, which function as acetyl-lysine (AcK) binding domains (Dhalluin et al., 1999; Hudson et al., 2000; Jacobson et al., 2000; Marmorstein and Berger, 2001; Owen et al., 2000; Winston and Allis, 1999; Zeng and Zhou, 2001). The bromodomain, first reported in the *Drosophila* protein brahma (Haynes et al., 1992; Tamkun et al., 1992), is present in a large number of chromatin-associated proteins and nuclear histone acetyltransferases (Jeanmougin et al., 1997). The biological importance of the bromodomain/AcK recognition has further been demonstrated by the role of the bromodomain in tethering transcriptional HATs to specific chromosomal sites (Brownell and Allis, 1996; Manning et al., 2001; Travers, 1999) and in the assembly and activity of multiprotein chromatin remodeling complexes, including SAGA and SWI/SNF (Agalioti

*Correspondence: ming-ming.zhou@mssm.edu
[4]These authors contributed equally to this work.

et al., 2002; Brown et al., 2001; Hassan et al., 2002; Sterner et al., 1999), as well as in HIV-1 transcriptional activation (Dorr et al., 2002; Mujtaba et al., 2002).

To understand the role of lysine acetylation in p53 function, we examined possible involvement of the bromodomain in acetylation-mediated p53 association with the transcriptional coactivators. Our study, reported here, shows that the bromodomain of the coactivator CBP binds specifically to p53 at the C-terminal acetylated K382. This bromodomain-mediated action is responsible for p53 recruitment of CBP in vivo upon DNA damage, a molecular interaction that is crucial for p53-induced transcriptional activation of the cyclin-dependent kinase inhibitor p21 in cell cycle arrest. We further determined the three-dimensional structure of the CBP bromodomain in complex with a K382-acetylated p53 peptide by nuclear magnetic resonance (NMR) spectroscopy. Our structural and mutational analyses provide the detailed structural basis for this molecular mechanism of coactivator recruitment that is essential for p53 transcriptional regulation in DNA damage control.

Results

CBP Bromodomain Recognizes p53 Acetylated at K382 In Vitro

To test whether p53 acetylation-dependent recruitment of CBP involves the CBP bromodomain, we performed NMR titration of CBP bromodomain binding to synthetic p53 peptides derived from three lysine acetylation sites. As shown in 2D ^{1}H-^{15}N heteronuclear single quantum coherence (HSQC) spectra, addition of p53 peptides acetylated at K373 or K320 resulted in little, if any, chemical shift perturbations of any protein residue (Figure 1A). On the contrary, several protein residues exhibited major chemical shift perturbations as a function of concentration of a p53 peptide containing AcK382, indicating interactions between the protein and the peptide. This binding is dependent upon K382 acetylation of the peptide with a K_D of ~50 μM, as estimated from NMR titration. None of the p53 peptides showed any significant binding to the homologous bromodomain from PCAF (Jeanmougin et al., 1997) (data not shown). Notably, the p53 AcK373 and AcK382 peptides have the same sequence except that the acetylated lysine is in a different position, underscoring the selective nature of CBP bromodomain/p53 AcK382 recognition.

To examine the specificity of CBP bromodomain/p53 binding, we performed an in vitro binding assay using GST-fusion bromodomains and a biotinylated p53 AcK382 peptide that was immobilized onto streptavidin-agarose beads. Only the CBP bromodomain but not those from PCAF or transcriptional intermediary factor 1β (TIF1β, also known as KAP-1) (Friedman et al., 1996) formed interactions with the p53 peptide (Figure 1B). These results confirm that the CBP bromodomain can specifically interact with p53 acetylated at K382.

CBP and p53 Association In Vivo Requires the Bromodomain Interaction

We next assessed the biological relevance of CBP bromodomain/p53 binding in cell transfection experiments. The CBP bromodomain transfected in 293T cells was properly expressed (Figure 2A). Expression of p53 transfected in p53 null 10.1 mouse embryo fibroblasts (MEF, $p53^{-/-}$) cells was markedly induced after UV-C irradiation (Figure 2B), agreeing with a similar effect reported previously (Barlev et al., 2001). Interestingly, we observed that p53 acetylation at K382 was dependent upon the degree of the UV exposure (data not shown) and detected as early as 2 hr and peaked at 8 hr after UV-C exposure at 50 J/m^2 (Figure 2B). Under the optimized condition, the bromodomain of CBP formed a stable complex with lysine-acetylated p53 (Figure 2C). Mutation of K373 to alanine did not alter K382 acetylation, nor did it affect p53 association with the CBP bromodomain. However, a single K382A or double K373A/K382A mutation completely abolished the p53/CBP bromodomain association (Figure 2C), confirming that the CBP bromodomain interacts with p53 by recognizing the acetylated K382 site in the cell.

It is reported that the N-terminal region of p53 interacts with effector proteins, including Mdm2 and CBP, and that stress-induced phosphorylation in the region frees p53 from association with these proteins (Avantaggiati et al., 1997; Gu and Roeder, 1997; Haupt et al., 1997; Kubbutat et al., 1997; Lill et al., 1997; Scolnick et al., 1997). To determine whether p53 N-terminal region association with CBP is a prerequisite for p53 acetylation, we examined N-terminal deletion effect on p53/CBP binding. Strikingly, a p53 deletion mutant (deleting residues 13–52) was well expressed in the transfected 10.1 cells and acetylated at K382 regardless of UV irradiation (Figure 2D). This is in a sharp contrast to the full-length p53, which was expressed at a very low level and underwent a marked induction upon UV-C irradiation (Figures 2B and 2D). Moreover, the expressed, K382-acetylated p53 deletion mutant formed a stable complex with GST-CBP bromodomain immobilized on glutathione-sepharose resin (Figure 2D). These results suggest that lysine acetylation of p53 is not likely dependent upon its N-terminal region interaction with CBP but may be controlled by regulatory events involving the N-terminal region that precede the C-terminal lysine acetylation after UV-C irradiation.

We further examined this CBP/p53 interaction in the context of the full-length proteins. In 10.1 cells, the transfected p53 formed a stable complex with the endogenous CBP upon UV-C treatment, peaking at 8 hr after the exposure (Figure 3A). The N-terminal deletion mutant of p53, acetylated at K382 with or without UV-C irradiation, also associated with the endogenous CBP (Figure 3B). The UV-dependent CBP/p53 association was further confirmed in COS-7 cells by coexpressing HA-tagged CBP and Flag-tagged p53 (Figure 3C). Although p53 expression was markedly increased upon UV treatment, the UV-induced p53 acetylation at K382 resulted in an at least 10-fold enhancement of the CBP/p53 complex formation. Mutation of K382 to alanine drastically reduced p53 binding to CBP to a minimal level similar to that observed without UV treatment. These results argue that despite possible other protein-protein interactions between CBP and p53, the bromodomain-acetyl-lysine interaction is the major force that promotes these two proteins to form a stable complex upon UV treatment.

It has been reported that p53 lysine acetylation in

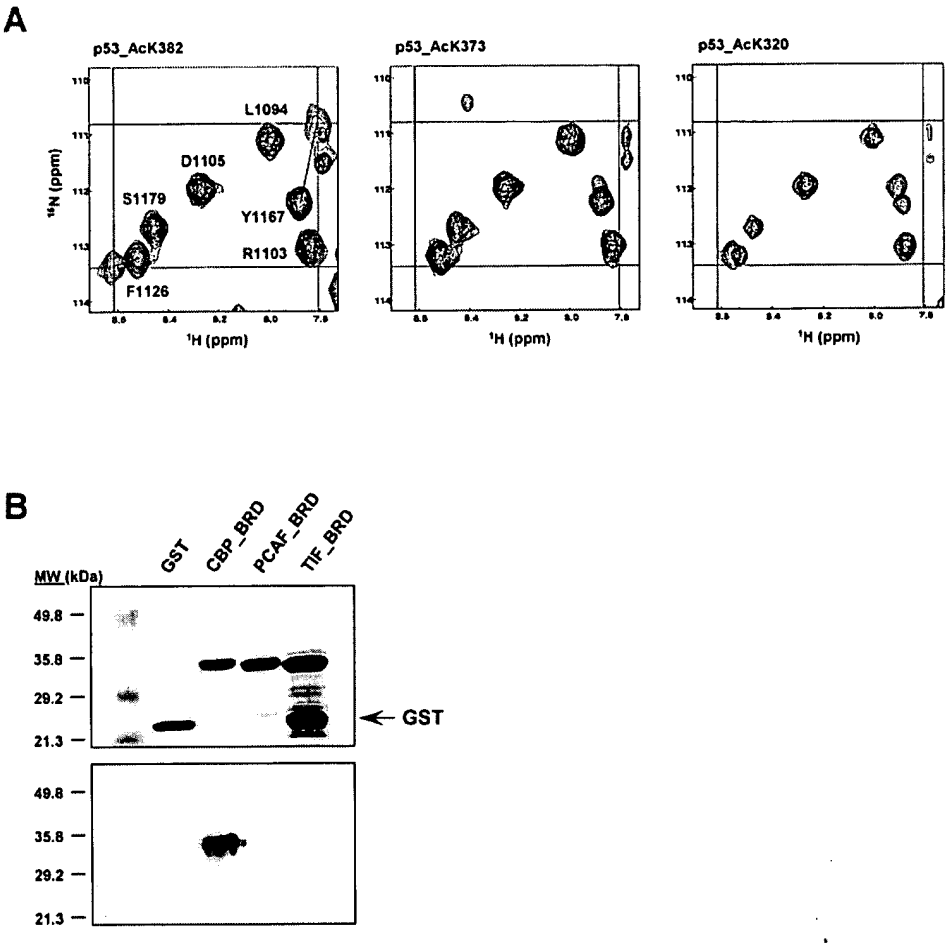

Figure 1. Recognition of Lysine-Acetylated p53 by the CBP Bromodomain

(A) CBP bromodomain binding to p53 peptides acetylated at K382 (SHLKSKKGQSTSRHK-AcK-LMFK) (left), K373 (SHLKSK-AcK-GQSTSRHK-K-LMFK) (middle), or K320 (SSPQPK-AcK-KPLDGE). Superimposition of the 2D ^{15}N HSQC spectra of the CBP bromodomin depicts differences of protein backbone resonances between the free form (black) or in the presence of a p53 peptide (red). Protein-to-peptide molar ratio was kept at 1:3.

(B) Binding of the purified GST-bromodomains of CBP, PCAF, and TIF1β (top) to a biotinylated p53 AcK382 peptide bound to streptavidin-agarose beads was determined by Western blotting using anti-GST-antibody (bottom).

response to stress signals is carried out by CBP/p300 (Gu and Roeder, 1997; Liu et al., 1999; Sakaguchi et al., 1998), two coactivator HATs that are highly homologous in sequence and size. Indeed, we showed that the recombinant and purified GST-fusion p53 or its N-terminal truncation mutant can be effectively acetylated at K382 by the HAT domain of CBP or p300 in vitro (Figure 3D). To address the question whether p300 also interacts with the acetylated p53 after UV-C treatment, we examined the endogenous p53 interactions with CBP or p300 in NIH/3T3 cells. As expected, the endogenous p53 formed a stable complex with the endogenous CBP in a K382 acetylation-dependent manner, which was effectively blocked by the transfected CBP bromodomain (Figure 3E). However, while p300 also weakly interacted with p53, this interaction was not dependent upon lysine acetylation, nor affected by the transfected CBP bromodomain. These data suggest that p53/p300 association likely does not involve a bromodomain-acetyl-lysine interaction, which seems consistent with the recent notion that these two homologous coactivators may function differently in cells (Giordano and Avantaggiati, 1999).

p53-Induced p21 Activation Requires the CBP Bromodomain/p53 AcK382 Interaction

To understand functional importance of the bromodomain-mediated CBP/p53 association, we investigated p53-induced p21 activation in 10.1 cells using a luciferase assay. UV-C treatment of the 10.1 cells transfected with p53 resulted in nearly a 7-fold enhancement of p21 luciferase activity (Figure 4A, lane 2). This p53-mediated p21 activation was dropped to a 5- or 2-fold increase in the cells transfected with a K373A or a K382A mutant, respectively (lanes 3 and 4), and almost completely disappeared with a K373A/K382A double mutant (lane 5). Notably, while expression of wild-type or mutant p53 upon UV-C treatment was enhanced to a similar level, the degree of p21-elevated expression agrees with that of its activation, which is dependent upon p53 acetylation at K382. The ratio of p21 expression level be-

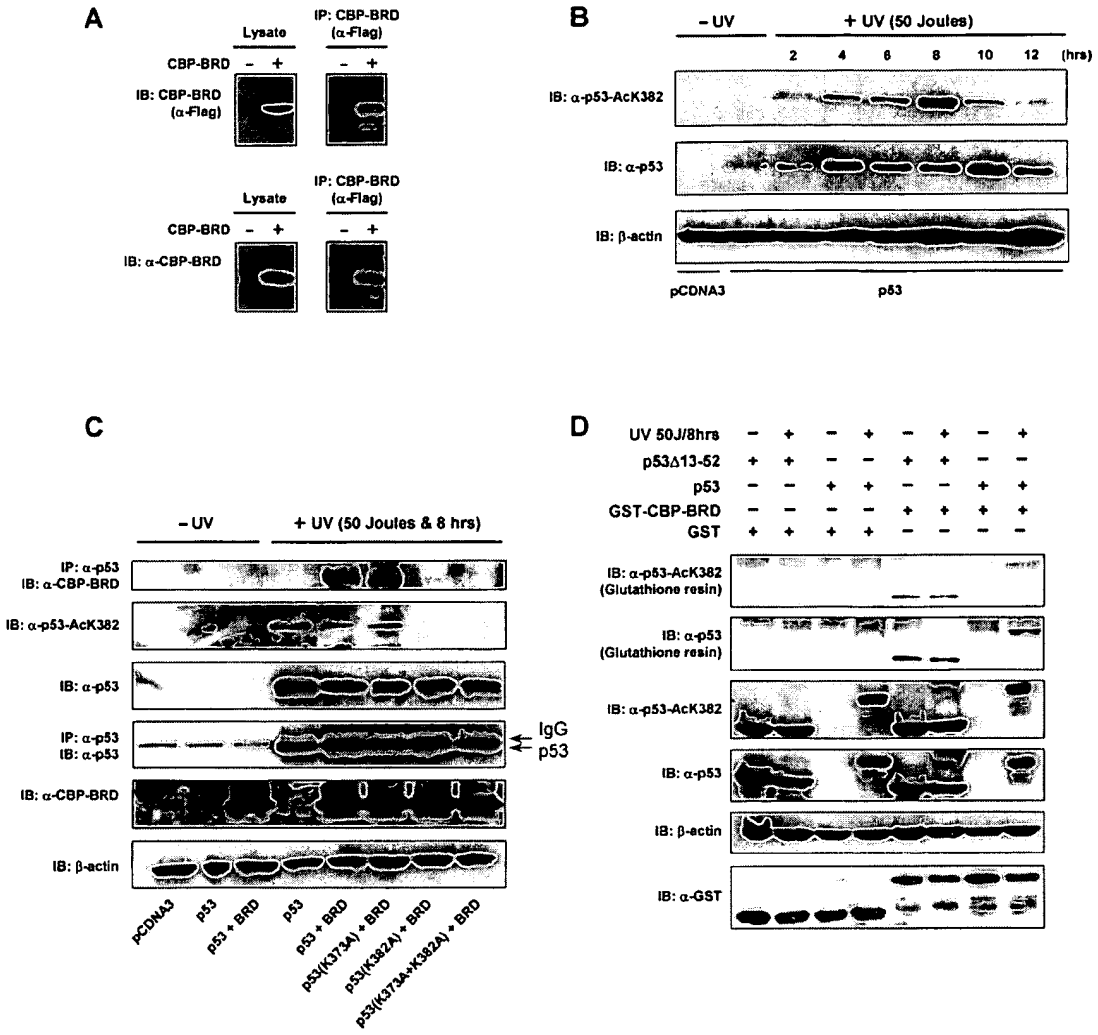

Figure 2. CBP Bromodomain Binding to Lysine-Acetylated p53 In Vivo

(A) Expression of the CBP bromodomain in 293T cells was assessed by Western analysis of cell lysates (left) or immunoprecipitate (right) using CBP bromodomain- or Flag-specific antibodies.

(B) Kinetics of K382 acetylation of p53 in the 10.1 cells following UV treatment was analyzed by Western blots using antibodies specific for p53 or p53 AcK382.

(C) Binding of CBP bromodomain to p53 or p53 mutants in 10.1 cells was examined by Western blotting analysis using antibodies specific to p53, p53-AcK382, and the CBP bromodomain.

(D) Effect of p53 N-terminal deletion on CBP bromodomain binding. p53 or the p53 deletion mutant in the transfected 10.1 cells treated with UV-C irradiation was assessed for their binding to GST-CBP bromodomain bound to glutathione-sepharose beads by Western blotting analysis.

tween UV-treated and nontreated 10.1 cells that were transfected with the wild-type, K373A, K382A, or K373A/K382A mutant is 3:1, 2.5:1, 1.6:1, or 1.1:1, respectively (Figure 4B). Remarkably, both the p53-induced p21 activation and the K382 acetylation dependence largely disappeared when the cells were cotransfected with the CBP bromodomain (Figures 4A and 4B, lanes 6–10). This inhibitory effect was not observed with the structurally homologous bromdomain of PCAF or TIF1β (Figure 4C), which was expressed at a comparable level (Figure 4D). Although we cannot rule out possible other functions of CBP, these data imply that the bromodomain from CBP but not that of PCAF or TIF1β selectively competes against CBP/p53 binding in cells, agreeing with our in vitro binding results (Figure 1C). Collectively, our data argue that p53-mediated p21 activation likely requires acetylation of p53 at K382 (to a lesser extent at K373) and the subsequent bromodomain-mediated p53/CBP association at AcK382.

Role of CBP Bromodomain/p53 AcK382 Association in Cell Cycle Arrest

To assess whether bromodomain-mediated CBP/p53 association is functionally important to p53-induced cell cycle arrest, we analyzed the cell cycle profile of the 10.1 cells transfected by p53 by flow cytometry analysis. As shown in Figure 4E, UV exposure of the 10.1 cells transfected with wild-type p53 resulted in a significant increase of cell population in G1 phase from ~20% to ~35%. Cells transfected with the K373A mutant showed

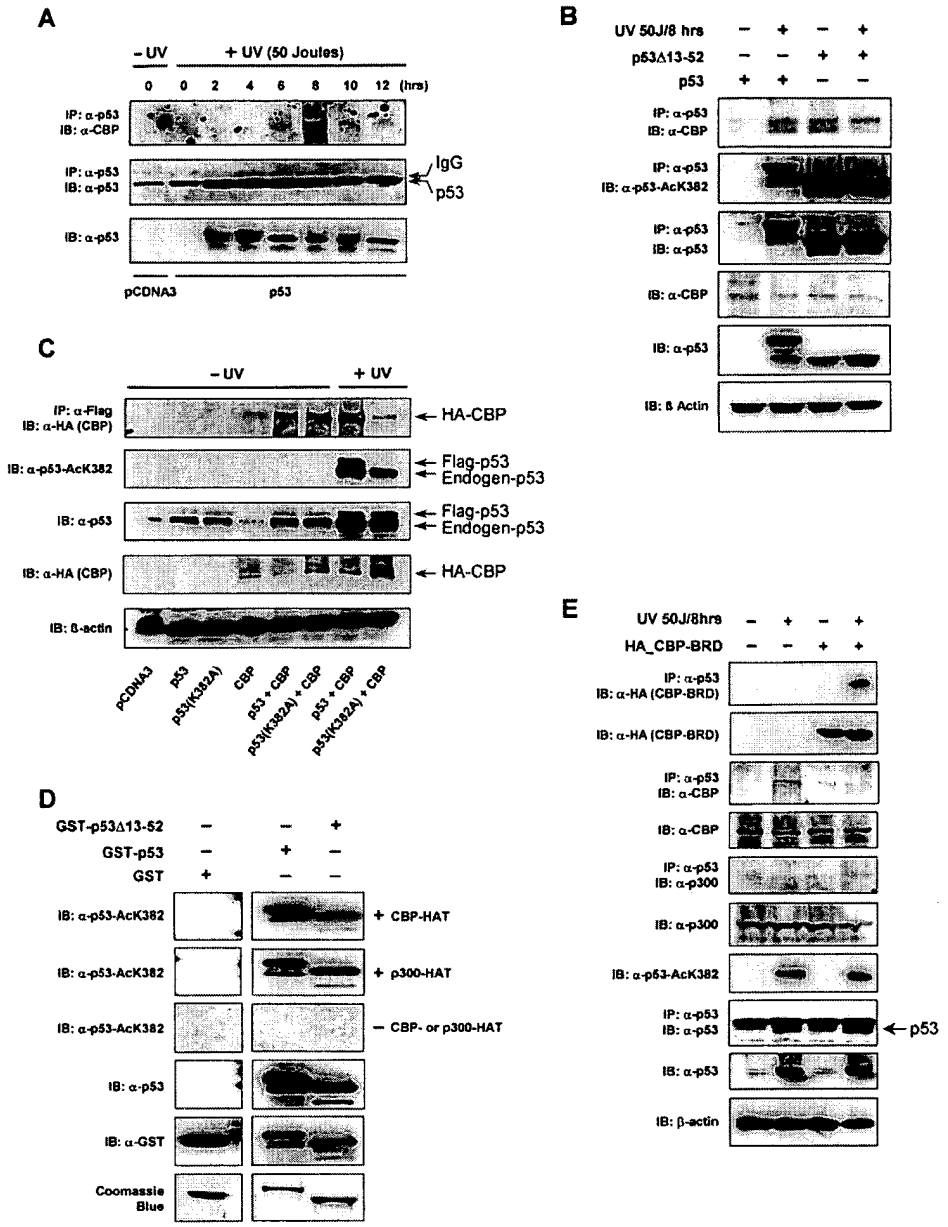

Figure 3. Association of the Endogenous CBP and p53 in 10.1 Cells

(A) Endogenous CBP binding to p53 in the 10.1 cells following UV-C irradiation. Expression of the transfected p53 and CBP/p53 binding were demonstrated by Western analysis.

(B) Effect of p53 N-terminal deletion on p53 binding to the endogenous CBP was assessed in the 10.1 cells transfected with p53 and p53 N-terminal deletion mutant and treated with UV-C p53 acetylation at K382.p53 binding to CBP was determined by Western blotting using antibodies specific for p53, p53-AcK382, or CBP bromodomain.

(C) Effects of K382A mutation on p53 association with the full-length CBP in COS-7 cells. The cells were transfected with the HA-tagged full-length CBP alone or with the Flag-tagged, wild-type p53 or mutant p53. Protein expression, p53 acetylation at K382, and CBP/p53 binding was examined by Western analysis using specific antibodies to p53, p53 AcK382, HA-tag, or Flag-tag.

(D) In vitro acetylation of K382 in p53 and p53 N-terminal deletion mutant by the HAT domain of CBP or p300 was assessed by Western blotting analysis using p53 AcK382 antibody.

(E) Acetylation-dependent endogenous p53 and CBP or p53 and p300 interactions in NIH/3T3 cells. Expression of p53, CBP, or p300, p53 acetylation at K382, and CBP/p53 binding upon UV-C irradiation was assessed in Western blotting by various specific antibodies.

a similar effect, whereas cells transfected with the K382A or K373A/K382A mutant exhibited no increase, if not a decrease. Notably, the 10.1 cells transfected with just the control vector pCDNA3 also showed a decreased G1 phase population upon UV-C exposure, similar to the effects with K382A and K373A/K382A mutants. Remarkably, this K382-dependent cell growth arrest by p53 was completely diminished when cotransfected

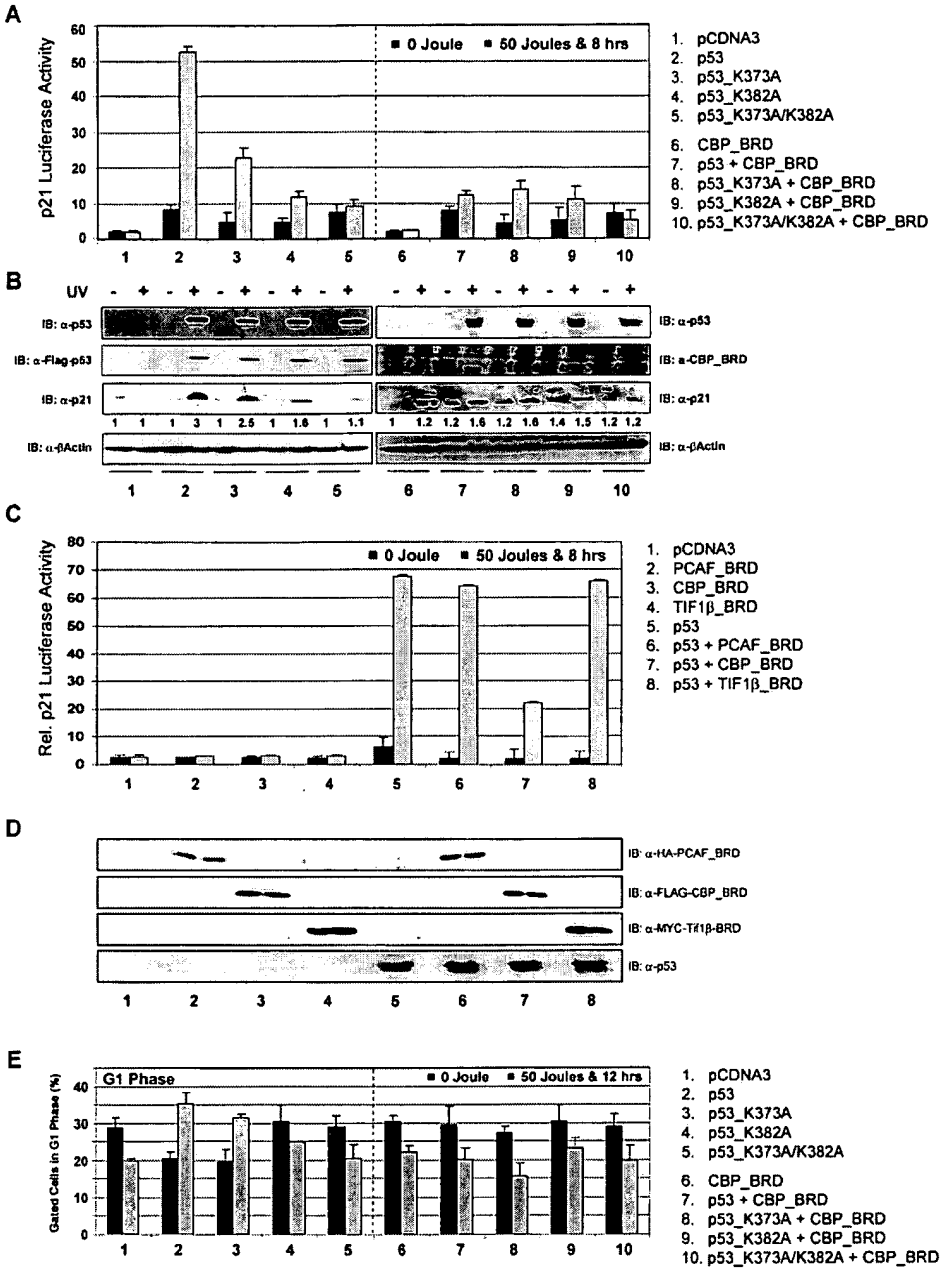

Figure 4. Functional Role of the CBP Bromodomain in CBP/p53 Association

(A) Effect of CBP bromodomain on p53-induced p21 activation in 10.1 cells after UV treatment. p21 activity of the 10.1 cells transfected with p53 or p53 mutant together with p21 luciferase and β-galactosidase, with or without CBP bromodomain, was measured in a luciferase-based assay. Mean values of the luciferase activities represent at least three independent cell transfections.

(B) Western blotting analysis assessing protein expression in the transfected 10.1 cells. Note that numerals below the p21 blot represent ratio of p21 expression in the cells transfected with p53, with or without CBP bromodomain, to that in the cells transfected with only the empty vector pCDNA3. The signals were quantitated using Kodak 1D Digital Image Analysis Software.

(C) Assessing effects of cotransfected bromodomains on p53-induced p21 activation in the 10.1 cells. The cell transfections and p21 luciferase activity analysis were same as described in (A).

(D) Western blots assessing expression of various bromodomains and p53 in the transfected 10.1 cells with or without UV-C treatment.

(E) Effect of the CBP bromodomain on cell cycle distribution induced by p53 in the 10.1 cells transfected with Us9-GFP, wild-type, or mutant p53, with or without the CBP bromodomains. The DNA content of the gated GFP-positive cells in G1 phase was determined by PI staining and FACS analysis. Average values of the DNA content of the cell cycle phases in each different experiment represent at least three independent transfection trials.

with the CBP bromodomain (Figure 4E, lanes 7–10). Transfection of the CBP bromodomain alone had an effect on cell cycle arrest similar to that of the control (Figure 4E, lanes 1 and 6). Finally, it appears that UV-C treatment of 10.1 cells transfected with the wild-type or mutant p53, with or without the CBP bromodomain, did not affect cell population in S or G2/M phase (data not shown). Taken together, our results demonstrate that p53 acetylation at K382 (to a much lesser extent, if any, at K373) in response to UV irradiation is responsible for p53-induced p21 activation and cell growth arrest and that the CBP bromodomain/p53 AcK382 binding is a key interaction for p53 acetylation-dependent coactivator recruitment essential for p53 transcriptional activity.

Structure of the CBP Bromodomain/p53 Peptide Complex

To understand the structural basis of CBP bromodomain/p53 recognition, we solved the three-dimensional structure of the CBP bromodomain in complex with a lysine-acetylated p53 peptide (residues 367–386) by NMR. The structure for the protein (residues 1081–1196) and the AcK382 peptide (residues 381–385) complex was well defined by the NMR data (Figure 5A, Table 1). The structure of the CBP bromodomain consists of a left-handed four-helix bundle (helices α_Z, α_A, α_B, and α_C) (Figure 5B) and is similar to those of the bromodomains from PCAF (Dhalluin et al., 1999), GCN5 (Hudson et al., 2000; Owen et al., 2000), and the double bromodomain module of $TAF_{II}250$ (Jacobson et al., 2000). The majority of the conformational differences among the bromodomains involve the ZA and BC loops that comprise the acetyl-lysine binding site. The corresponding regions in PCAF were shown to undergo conformational changes to accommodate peptide binding (Mujtaba et al., 2002). In contrast to the extended conformation of the Tat peptide in the PCAF bromodomain complex (Mujtaba et al., 2002), the p53 peptide, which lies across a pocket formed between the ZA and BC loops in the CBP bromodomain, adopts a β turn-like conformation with the acetylated K382 being at the beginning of the turn (Figure 5B). The side chain of the acetyl-lysine intercalates into the protein hydrophobic cavity and interacts with V1115, L1122, Y1125, and I1128 of the ZA loop and Y1167, V1174, and F1177 of the BC loop (Figure 5C). While K(AcK-1) contacts Y1167 of the protein, a large number of intermolecular NOEs were observed for two hydrophobic residues C-terminal to the acetyl-lysine. Particularly, L(AcK+1) shows numerous interactions with V1115, L1120, and I1122 in the ZA loop, V1174 and F1177 in the BC loop, whereas M(AcK+2) contacts largely Y1167 and V1174 of the BC loop. Most of these p53 binding residues are highly conserved in the bromodomain family except for L1120, which belongs to a two amino acid insertion in the ZA loop unique to CBP and a few closely related homologs in the bromodomain family (Figure 5D). Collectively, these specific interactions confer a selective association between the CBP bromodomain and p53.

Specificity of CBP Bromodomain and p53 Recognition

To determine functional importance of CBP bromodomain residues in p53 binding, we examined binding of bromodomain mutants to a biotinylated p53 AcK382 peptide immobilized onto streptavidin-agarose beads (Figure 6A). These residues are grouped according to their mutation effects on the complex formation: (1) point mutation of I1120, I1122, Y1125, I1128, or F1177 to alanine impaired up to ~50% of bromodomain/p53 peptide binding; (2) proteins containing a mutation of V1115A, P1123G, N1163A, or V1174A showed an 80% or greater reduction in the binding; (3) substitution of Y1167 or N1168 to alanine almost abolished the p53 peptide binding; (4) because of the relatively weak effect of I1120A or I1122A mutation, loss of p53 binding by the I1120-G1121-I1122 deletion mutant is likely due to local structural perturbations caused by the deletion in the ZA loop. This reasoning may explain an 80% reduction in p53 binding with P1123G (Figure 6A); and (5) a dramatic reduction in p53 binding by A1164V likely resulted from introduction of a bulky amino acid in the acetyl-lysine binding pocket, which interferes with the bromodomain/p53 interaction. These results agree with the intermolecular interactions observed in the structure of the bromodomain/p53 peptide complex (Figure 5C) and confirm that (1) both Y1167 and N1168 are essential for acetyl-lysine recognition; (2) V1115 is important for binding to both the acetyl-lysine and L(AcK+1); (3) V1174 is critical for recognition of possibly all three key amino acid residues AcK382, L(AcK+1) and M(AcK+2) in the p53 peptide; and (4) the residues at the two amino acid insertion of L1120-G1121, unique to the CBP bromodomain, make important contributions to the CBP/p53 association by direct interactions with AcK382 and L(AcK+1) and by defining the ZA loop conformation that is required for p53 binding.

To verify further the molecular determinants in the p53 sequence for CBP bromodomain binding, we tested mutant p53 peptides in a competition assay, in which a nonbiotinylated p53 peptide competed against a biotinylated p53 AcK382 peptide immobilized onto streptavidin-agarose beads for binding to the CBP bromodomain. As anticipated, the acetylated but not the nonacetylated K382 peptide of p53 effectively blocked the resin-immobilized p53 peptide from binding the bromodomain (Figure 6B, lanes 2 and 3). However, two p53 peptides acetylated at K373 or K320 showed almost no competition against p53 AcK382 peptide in bromodomain binding (Figure 6B, lanes 4 and 5 versus lane 3), confirming that the latter interaction is of higher affinity and specificity, consistent with the NMR binding data (Figure 1A). Alanine substitution of F(AcK+3) or M(AcK+2) in the p53 AcK382 peptide only slightly weakened its binding to the bromodomain (Figure 6C, lanes 6 and 7). Conversely, change of H(AcK−2) (lane 10), K(AcK−1) (lane 9), or L(AcK+1) (lane 8) to alanine caused a ~40%–70% reduction or a nearly complete loss of bromodomain binding. These mutation results confirm that AcK382 and L(AcK+1) are important in stabilizing the CBP bromodomain/p53 complex, agreeing with the extensive intermolecular interactions observed for these residues in the structure (Figure 5C) and the complementary mutational data of the protein (Figure 6A). This clear preference for a bulky hydrophobic residue at AcK+1 explains as to why the CBP bromodomain binds AcK382 but not AcK373 or AcK320 site in p53, the latter of which contains a Gly or Lys at AcK+1. Finally, the

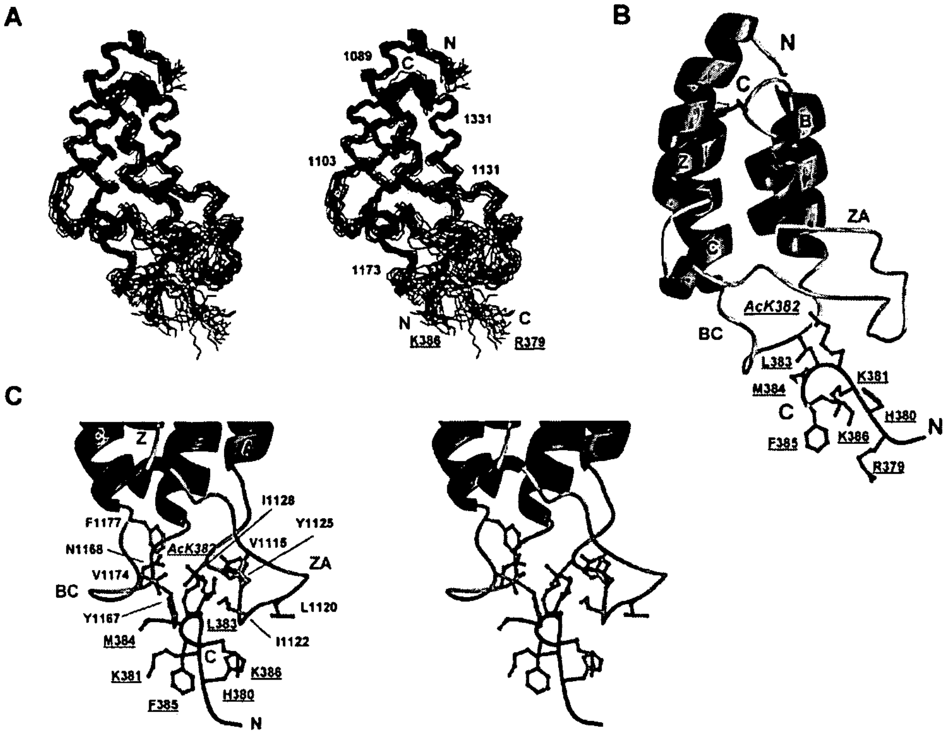

D

```
           1104            1114     1124         1134   1164       1174
            |               |.       .|           |     *|  **       |
                                                                     *
hsCBP      QD....PESLPFRQ.PVDPQLLGIPDYFDIVKNP...MD  ...  NAWLYNRK..TSRVYKFC
mmCBP      QD....PESLPFRQ.PVDPQLLGIPDYFDIVKNP...MD  ...  NAWLYNRK..TSRVYKYC
ceCBP      SE.....DAAPFRV.PVDAKLLNIPDYHEIIKRP...MD  ...  NAWLYNRK..NSKVYKYG
hsP300     QD....PESLPFRQ.PVDPQLLGIPDYFDIVKSP...MD  ...  NAWLYNRK..TSRVYKYC
scBDF1-1   .......DARPFLQ.PVDPVKLDIPFYFNYIKRP...MD  ...  NSIKFNGP..NAGISQMA
scBDF1-2   KH...ASYNYPFLE.PVDPVSMNLPTYFDYVKEP...MD  ...  NCYTFNPD..GTIVNMMG

hsPCAF     HQ.....SAWPFME.PVKRTE..APGYYEVIRSP...MD  ...  NCKEYNAP..ESEYYKCA
scGCN5     HA.....AAWPFLQ.PVNKEE..VPDYYDFIKEP...MD  ...  NCRMYNGE..NTSYYKYA
hsGCN5     HP.....SAWPFME.PVKKSE..APDYYEVIRFP...ID  ...  NCREYNPP..DSEYCRCA
mmGCN5     HP.....SAWPFME.PVKKSE..APDYYEVIRFP...ID  ...  NCREYNPP..NSEYCRCA
ttP55      HK....QS.WPFLD.PVNKDD..VPDYYDVITDP...ID  ...  NAKIYNQP..DTIYYKAA
sSNF2α     SS..GRQLSEVFIQLPSRK.E..LPEYYELIRKP...VD  ...  NAQTFNLE..GSQIYEDS
hsBRG1     SS.SGRQLSEVFIQLPSRK.E..LPEYYELIRKP...VD  ...  NAQTFNLE..GSLIYEDS

hsTAF2d1   L.....PNTYPFHT.PVNAKV..VKDYYKIITRP...MD  ...  NSATYNGP..KHSLTQIS
hsTAF2d2   AV....PDSWPFHH.PVNKKF..VPDYYKVIVNP...MD  ...  NSVKYNGP..ESQYTKTA
hsTIF1α    .......MSLAFQD.PVPLT...VPDYYKIIKNP...MD  ...  NCAEFNEP.DSEVANAGI
mmTIF1α    .......MSLAFQD.PVPLT...VPDYYKIIKNP...MD  ...  NCAEFNEP.DSEVANAGI
hsTIF1β    ............PCRPLHQLAT.DSTF.SLDQ.PGGTLD  ...  Q...FNKL.TEDKADVQS
mmTIF1β    ............PCRPLHQLAT.DSTF.SMEQ.PGGTLD  ...  Q...FNKL.TEDKADVQS
hsTIF1γ    .......LSIEFQE.PVPAS...IPNYYKIIKKP...MD  ...  NCERFNEMMKVVQVYADT
ggPB1-1    EQ..GRLLCELFIRAPKRRN...QPDYYEVVSQP...ID  ...  Q.LLFNNA...KAYYKPD
ggPB1-2    ..PSGRLISELFQKLPSKVQ...YPDYYAIIKEP...ID  ...  NAKTYNEP..GSQVFKDA
ggPB1-3    QG...QLISEPFFQLPSKKK...YPDYYQQIKTP...IS  ...  NAKRYNVP..NSAIYKRV
ggPB1-4    GT..QRRLCDLFMVKPSKKD...YPDYYKIILEP...MD  ...  NARHYNEE..GSQVYNDA
ggPB1-5    TDKRGRRLSAIFLRLPSRSE...LPDYYITIKKP...VD  ...  NACTYNEP..ESLIYKDA
           ______________________________________       __________________
                         ZA loop                              BC loop
```

Figure 5. NMR Structure of the CBP Bromodomain/p53 AcK382 Peptide Complex

(A) Stereoview of the backbone atoms (N, Cα, and C′) of 25 superimposed NMR structures of the CBP bromodomain (black) (showing residues 1085–1196) bound to the p53 AcK382 peptide (blue) (showing residues 379–386). For clarity, p53 residues are underlined.

(B) Ribbons (Carson, 1991) representation of the average minimized NMR structure of the CBP bromodomain/p53 peptide complex.

(C) Stereoview of the p53 binding site in the bromodomain showing side chains of the protein (green) and peptide (blue) residues that are directly involved intermolecular interactions.

(D) Sequence alignment of bromodomains highlighting amino acid variations in the ZA and BC loops. Bromodomains are grouped according to sequence similarities. Sequence numbers of CBP are shown above the sequence. Absolutely and highly conserved residues in bromodomains are colored in red and blue, respectively. Residues in the CBP or PCAF bromodomain that interact with p53 or HIV-1 Tat peptide, as shown by intermolecular NOEs, are underlined. Similarly, the residues of the yeast GCN5 bromodomain that directly contact the histone H4 peptide, as defined in the crystal structure, are also underlined. Residues in CBP bromodomain important for p53 binding, as determined by the mutational analysis, are highlighted by asterisk.

Table 1. Summary of NMR Structural Statistics

Total Experimental Restraints	2093	
Total NOE distance restraints[a]	2045	
Protein		
Total ambiguous	34	
Total unambiguous	1910	
Intraresidue	612	
Interresidue		
Sequential ($\|i - j\| = 1$)	475	
Medium ($2 \leq \|i - j\| \leq 4$)	435	
Long range ($\|i - j\| > 4$)	388	
Peptide	30	
Intermolecular	71	
Hydrogen bond restraints	48	
Final energies (kcal·mol^{-1})		
E_{Total}	456.0 ± 26.5	
E_{NOE}	68.1 ± 9.7	
$E_{Dihedral}$	0.6 ± 0.3	
E_{L-J}[b]	−550.6 ± 85.3	
	Protein/Peptide Complex[f]	Secondary Structure
Ramachandran plot (%)		
Most favorable region	67.9 ± 2.9	91.0 ± 2.7
Additionally allowed region	25.4 ± 2.8	8.2 ± 2.6
Generously allowed region	5.0 ± 2.0	0.8 ± 0.4
Disallowed region	1.7 ± 0.9	0.0 ± 0.0
Cartesian coordinate RMSDs (Å)[c]		
Backbone atoms (N, Cα, and C′)[d]	0.78 ± 0.12	0.39 ± 0.07
Heavy atoms[d]	1.35 ± 0.13	0.87 ± 0.06
Backbone atoms (N, Cα,and C′)[e]	0.55 ± 0.15	
Heavy atoms[e]	1.83 ± 0.50	
Backbone atoms (N, Cα, and C′)[f]	0.80 ± 0.12	0.52 ± 0.10
Heavy atoms[f]	1.39 ± 0.11	1.04 ± 0.06

[a]Of the total 2045 NOE-derived distance restraints, only 67 were obtained by using ARIA program, of which 34 are classified as ambiguous NOEs. The latter NOE signals in the NMR spectra match with more than one proton atom in both the chemical shift assignment and the final NMR structures.
[b]The Lennard-Jones potential was not used during any refinement stage.
[c]None of these final structures exhibit NOE-derived distance restraint violations greater than 0.3 Å or dihedral angle restraint violations greater than 5°.
[d]Protein residues 1085–1196.
[e]Peptide residues 381–385.
[f]Protein residues 1085–1196 and peptide residues 381–385.

mutational analysis data and few intermolecular NOEs observed for H(AcK−2) and K(AcK−1) in the NMR spectra suggest that while these residues N-terminal to AcK382 are functionally important for p53/CBP bromodomain binding, they are likely structurally dynamic in the complex.

Discussion

Growing evidence from in vivo studies demonstrates that stress-induced lysine acetylation of p53 play an important role in p53 stabilization and activation as a transcription factor (Barlev et al., 2001; Ito et al., 2001, 2002; Li et al., 2002). These studies show that acetylation-induced p53 activation in its transcriptional regulation in response to DNA damage does not result from an increase of its DNA binding activity as hypothesized previously (Gu and Roeder, 1997; Liu et al., 1999; Sakaguchi et al., 1998) but rather from its recruitment of coactivators and subsequent histone acetylation (Barlev et al., 2001). While multiple acetylation sites within the C-terminal tail of p53 have been reported, i.e., K320, K373, and K382 (to a lesser extent K372 and K381), specific effects of single or combined acetylation of these lysine residues on p53 activity remain elusive. Our study presented here provides the structural understanding of the molecular mechanism by which p53 recruits the coactivator CBP but not p300 upon UV-induced DNA damage via an interaction between its acetylated K382 and the bromodomain of CBP.

Our study provides several lines of evidence to support that the CBP bromodomain and p53 AcK382 interaction is functionally important for p53 function in response to cellular stress. First, our data suggest that the N-terminal region of p53 plays a negative role in its C-terminal acetylation by CBP upon DNA damage, agreeing with the notion that upon DNA damage, p53 becomes extensively phosphorylated within its N-terminal activation domain, which triggers its dissociation from the negative regulator Mdm2, resulting in p53 stabilization and activation as a transcription factor (Fuchs et al., 1998b; Haupt et al., 1997; Kubbutat et al., 1997; Momand and Zambetti, 1997). Second, our in vitro and in vivo binding results demonstrate that the specific CBP bromodomain/p53 AcK382 binding is a major force for

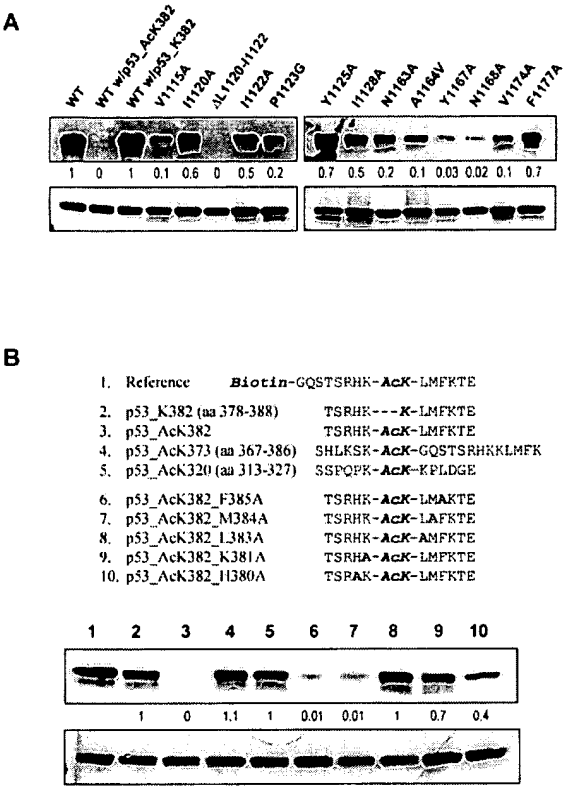

Figure 6. Mutational Analyses of CBP Bromodomain Binding to p53

(A) Effect of point mutation of CBP bromodomain residues on p53 peptide binding. Western blot with GST antibody shows GST-CBP bromodomain binding to the biotinylated p53 AcK382 peptide bound to streptavidin-agarose beads (top). Relatively equal amount of proteins was used in each binding experiment (bottom). Mutants highlighted in red exhibited markedly reduced binding to the p53 peptide. Mutational effects on the protein/peptide binding were quantitated.

(B) Mutational analysis of p53 peptide residues, assessed in a competition assay as described in Experimental Procedures. Mutant p53 peptides that showed a major reduction in binding to the bromodomain are indicated in red.

the endogenous p53 and CBP association after DNA damage. Third, our data confirm that acetylation at K382 (to a much less extent at K373) is responsible for p53-induced p21 activation and cell growth arrest in G1 phase but not S or G2/M phase (El-Deiry et al., 1995; Tang et al., 1998). This K382 acetylation effect is exerted through its interaction with the CBP bromodomain, which can be effectively blocked by the transfected CBP bromodomain but not by the homologous bromodomain of PCAF or TIF1β. Finally, our kinetics data demonstrate the dynamic nature of p53 acetylation and activation in response to stress signals and enabled us to systematically evaluate the biological importance of CBP bromodomain/p53 AcK382 interaction in p53 functions.

Our observation of acetylation-induced p53 expression, also reported previously (Barlev et al., 2001), agrees with the idea that acetylation promotes p53 stability by inhibiting its ubiquitnation by Mdm2 on the same C-terminal lysine residues p53 (Li et al., 2002) and that Mdm2/HDAC1-mediated deacetylation of p53 is required for its degradation (Ito et al., 2002). These observations that the single or double mutants of K382 and/or K373, which abrogates both acetylation and ubiquitnation at these sites, exhibit UV-induced increased stability similar to that of wild-type p53 suggest that this acetylation-induced stability likely results from collaboratively multiple C-terminal residues, i.e., K320, K373, and K382 (to a lesser extent K372 and K381).

Our finding of p53/CBP association via a bromodomain/AcK382 binding also provides new insights into p53 functions in cellular senescence or apoptosis in response to oncogenic transformation or DNA damage. It has been shown that in these processes the tumor suppressor PML controls the targeting of p53 and CBP into the PML nuclear bodies where a p53-PML-CBP complex is formed (Pearson et al., 2000). The formation of such a trimeric complex, which is required for p53-induced senescence or apoptosis, is dependent upon acetylation at K382 (Pearson et al., 2000). Our results presented here imply that the effect of K382 acetylation on p53 association with CBP and PML in the PML nuclear bodies is likely exerted through its specific interaction with the bromodomain of CBP.

In addition to p53, CBP interacts with or acetylates a large number of cellular proteins, thus playing an important role in a wide variety of cellular processes (Giordano and Avantaggiati, 1999; Vo and Goodman, 2001). Chromosomal translocation between the *MLL* (mixed-lineage leukemia) gene and *CBP* has been reported to cause acute myeloid leukemia (Ayton and Cleary, 2001; Lavau et al., 2000; Liedman and Zeleznik-Le, 2001; Sobulo et al., 1997). Notably, it has been recently shown that in the MLL-CBP fusion protein, which consists of the N-terminal portion of MLL fused in frame to parts of CBP, consisting of its bromodomain and HAT domain, are minimally necessary and sufficient for developing acute myeloid leukemia—deletion of either the BRD or HAT domain of CBP completely abolishes the transforming activity of MLL-CBP (Lavau et al., 2000; Sobulo et al., 1997). Although the biological ligand(s) of the CBP bromodomain in the MLL-CBP fusion protein may or may not be p53, the new structural knowledge of ligand specificity of the CBP bromodomain reported here should facilitate identification and investigation of its biological ligand(s) in MLL-CBP-induced leukemogenesis.

The new structure of the CBP bromodomain/p53 AcK382 peptide complex extends our knowledge on ligand selectivity of the bromodomain family. Structural comparison of the CBP bromodomain/p53 AcK382 peptide (SHLKSKKGQSTSRHK-AcK-LMFK), the PCAF bromodomain/HIV-1 Tat AcK50 peptide (SYGR-AcK-KRRQR) (Mujtaba et al., 2002), and the GCN5p bromodomain/histone H4 AcK16 peptide (A-AcK-RHRKILRNSIQGI) (Owen et al., 2000) complexes reveals that the mechanism of acetyl-lysine recognition is conserved in all three bromodomain/ligand complexes. The acetyl-lysine binding involves nearly identical sets of conserved residues in the different bromodomains, corresponding to V1115, Y1167, N1168, and V1174 in CBP. However, each bromodomain does recognize different sets of amino acid residues flanking the AcK to achieve their specificity. For instance, PCAF bromodomain makes specific interactions with Y(AcK−3), R(AcK+3), and Q(AcK+4) on both sides of AcK50 in Tat, whereas the yeast GCN5p bromodomain has a few contacts with H(AcK+2) and

(AcK+3) at the AcK16 site in histone H4. These intermolecular interactions are distinctly different from those of the CBP bromodomain, which recognizes L(AcK+1), K(AcK−1), and H(AcK−2) at the AcK382 site in p53. Specifically, V763 in PCAF interacts directly with Y(AcK−3) in HIV-1 Tat (Mujtaba et al., 2002), whereas mutation of the corresponding I1128 to alanine in CBP has only a partial reduction in p53 peptide binding. Moreover, E756 in PCAF, which is important for interactions with R(AcK+3) and Q(AcK+4) at the AcK50 in Tat, is changed to L1119 followed by the unique two amino acid insertion in the CBP bromodomain. The hydrophobic residues near the two amino acid insertion are directly involved in CBP bromodomain binding to the L(AcK+1) and H(AcK−2) at the AcK382 site in p53. These distinct intermolecular interactions confer CBP bromodomain's recognition of AcK382 over AcK373 or AcK320 site in p53. Finally, because of these different modes of ligand recognition, the conformation of the bound peptide in CBP and PCAF bromdomains is also different—the p53 peptide forms a β turn-like conformation, whereas the HIV-1 Tat peptide adapts an extended conformation (Mujtaba et al., 2002). Taken together, these structural features of bromodomain/ligand complexes reinforce the notion that differences in ligand selectivity attribute to a few but important differences in bromodomain sequences, mostly in the ZA loop.

In summary, we show in this study that the bromodomain of the coactivator CBP binds specifically to p53 at the C-terminal transiently acetylated K382 upon UV-C irradiation. This bromodomain action is responsible for acetylation-dependent p53/CBP association in vivo, which is required for activation of the cyclin-dependent kinase inhibitor p21 in p53-induced cell cycle arrest. Our three-dimensional structure of the CBP bromodomain in complex with a lysine 382-acetylated p53 peptide together with complementary mutational analyses provides the detailed structural understanding for this selective molecular recognition and suggests that evolutionary changes of amino acid compositions in the ZA loop contribute directly to differences in ligand specificity of different bromodomains. Our findings underscore a specific bromodomain/acetyl-lysine interaction as a key step in p53 acetylation-dependent coactivator recruitment that is essential for the activation of p53 transcriptional regulation in DNA damage control.

Experimental Procedures

Sample Preparation and Plasmid Constructs

The bromodomain of CBP (residues 1082–1197) was expressed in *Escherichia coli* BL21(DE3) cells in the pET15b vector (Novagen). Isotope-labeled proteins were prepared from cells grown on a minimal medium containing $^{15}NH_4Cl$ with or without $^{13}C_6$-glucose in H_2O or 75% ^2H_2O. The protein was purified by nickel-IDA affinity chromatography, followed by thrombin cleavage to remove an N-terminal poly-His-tag. GST-fusion bromodomains of CBP (residues 1082–1197), PCAF (residues 712–832), and TIF1β (residues 702–812) were expressed in *E. coli* in the pGEX4T3 vector (Pharmacia) and purified with a glutathione-sepharose column. NMR spectra of the recombinant CBP, PCAF, and TIF1β were acquired to ensure proper protein folding. The acetyl-lysine-containing peptides were ordered from BioSynthesis, Inc. (Lewisville, TX). The CBP bromodomain was also subcloned into HA- (Clontech) or Flag-tagged (Stratagene) vectors. HA-tagged p53, p21 minimal promoter-driven luciferase construct, and β-galactosidase (β-gal expression vector) were described previously (Fuchs et al., 1998a). The expression constructs for human Flag-tagged p53 and mutants and CBP (pRSV-HA-CBP) are same as those described previously (Kwok et al., 1996; Nakamura et al., 2000).

In Vitro Protein-Peptide Binding Assay and Mutational Analysis

Site-directed mutagenesis of CBP was performed with the QuikChange kit (Stratagene). DNA sequencing confirmed the desired mutations. GST-bromodomains of CBP, PCAF, or TIF1β (10 μM) were incubated with an N-terminal biotinylated p53 AcK382 peptide (50 μM) in a 50 mM Tris buffer (pH 7.5) containing 50 mM NaCl, 0.1% BSA, and 1 mM DTT at 22°C for 2 hr. Streptavidin-agarose beads were added to the mixture and washed in the Tris buffer containing 500 mM NaCl and 0.1% NP-40. Proteins eluted from the beads were separated by SDS-PAGE and visualized in Western blot by anti-GST antibody and horseradish-peroxidase-conjugated goat anti-rabbit IgG. Peptide competition assay was performed by incubating a nonbiotinylated peptide with the CBP bromodomain and the biotinylated p53 AcK382 peptide. The molar ratio of the biotinylated and nonbiotinylated peptides in the mixture was kept at 1:2.

In Vivo p53 and CBP/p300 Binding Analysis

Mouse embryonic fibroblast 10.1 cells were propagated in Dulbecco's modified Eagle medium with 10% fetal bovine serum and penicillin-streptomycin (Life Technologies) in a humidified atmosphere of 5% CO_2. COS-7, 293T, and NIH/3T3 cells were maintained in 10% fetal calf serum. Transfections were performed using lipofectamine-plus reagent (Life Technologies) or the calcium phosphate method (Fuchs et al., 1998a). Plasmid DNAs of 1.0–2.5 μg were used in cell transfections. The transfected 10.1 cells were subject to UV-C irradiation of 50 J/m^2 36 hr after transfection and harvested 2–12 hr later. Protein expression was examined by Western blotting using monoclonal antibodies to HA (Roche Diagnostics), Flag (Stratagene), or β actin (Sigma), as well as rabbit polyclonal antibodies to CBP bromodomain, p53, and AcK382 of p53 (Trevigen). Western blots for endogenous p53, CBP, and p300 in NIH/3T3 cells were performed by specific antibodies from Santa Cruz Biotech.

Transcriptional Activation Assay

The 10.1 cells, transfected with p53 (2.5 μg), p21 luciferase (0.5 μg), and β-galactosidase (0.5 μg) with and without the CBP bromodomain (1.0 μg) were irradiated by UV-C and harvested as described above. The cell extracts were assayed for luciferase activity using a luciferase assay (Promega). Luciferase activity derived from p53-induced p21 activation was normalized to a cotransfected vector expressing β-galactosidase.

Cell Cycle Analysis

Cell cycle analysis of the 10.1 cells, transfected with Us9-GFP, wild-type, or mutant p53 with or without the CBP bromodomain was performed on Calibur flow cytometer (Becton Dickinson) using GFP and PI staining. Cells were treated with the UV-C irradiation, harvested after 12 hr by trypsinization, washed with PBS, and fixed in chilled 70% ethanol in PBS buffer. One hour before acquiring the data, cells were washed again with PBS and stained with PI. The data were acquired and analyzed using CellQuest software.

In Vitro HAT Assay

In vitro HAT acetylation was done using a procedure described previously (Lavau et al., 2000). The purified GST, GST-p53, or GST-p53 mutant was incubated with the HAT domain of p300 (residues 1195–1707) (Upstate Biotech) or CBP (residues 1174–1850) in a 50 mM Tris buffer (pH 8.0) containing 2% glycerol, 0.1 mM EDTA, and 1 mM dithiotheritol and acetyl-CoA for 1 hr at 30°C. Acetylation of p53 was assessed by Western analysis using p53 AcK382 antibody.

NMR Spectroscopy

NMR samples contained a protein/peptide complex of ~0.5 mM in 100 mM phosphate buffer (pH 6.5) containing 5 mM perdeuterated DTT and 0.5 mM EDTA in $H_2O/^2H_2O$ (9/1) or ^2H_2O. All NMR spectra were acquired at 30°C on a Bruker 500 or 600 MHz NMR spectrometer. The ^1H, ^{13}C, and ^{15}N resonances of the protein were assigned

by triple-resonance NMR spectra collected with a $^{13}C/^{15}N$-labeled and 75% deuterated protein bound to an unlabeled peptide (Yamazaki et al., 1994). The distance restraints were obtained in 3D ^{13}C- or ^{15}N-NOESY spectra (Clore and Gronenborn, 1994). Slowly exchanging amides, identified in 2D ^{15}N-HSQC spectra recorded after a H_2O buffer was changed to a ^2H_2O buffer, were used with structures calculated with only NOE distance restraints to generate hydrogen-bond restraints for final structure calculations. The intermolecular NOEs were detected in ^{13}C-edited (F_1), $^{13}C/^{15}N$-filtered (F_3) 3D NOESY spectrum (Clore and Gronenborn, 1994).

Structure Calculations

Structures of the CBP bromodomain/p53 peptide complex were calculated with a distance geometry-simulated annealing protocol using the X-PLOR program (Brunger, 1993). Long-range NOE assignments were assisted by model structures generated by homology modeling with the program Modeller (Sali and Blundell, 1993), using the PCAF bromodomain structure as a template (Dhalluin et al., 1999; Mujtaba et al., 2002). Manually assigned NOE-derived distance restraints were used to calculate initial structures. ARIA (Nilges and O'Donoghue, 1998)-assigned distance restraints agree with structures calculated using only the manually determined NOE distance restraints. Ramachandran plot analysis of the final structures was performed with Procheck-NMR program (Laskowski et al., 1996).

Acknowledgments

We thank Drs. T. Mukhopadhyay for p53 constructs; M. Ott and E. Verdin for polyclonal antibodies to CBP bromodomain; A. Beavis for Us9-GFP construct; H.W. Snoeck for assistance in flow cytometry analysis; and T. Buschmann for technical advice. This work was supported by grants from the National Institutes of Health to M.-M.Z. (CA87658 and GM66531) and to Z.R. (CA80058).

Received: April 8, 2003
Revised: December 15, 2003
Accepted: December 16, 2003
Published: January 29, 2004

References

Agalioti, T., Chen, G., and Thanos, D. (2002). Deciphering the transcriptional histone acetylation code for a human gene. Cell *111*, 381–392.

Alarcon-Vargas, D., and Ronai, Z. (2002). p53-Mdm2—the affair that never ends. Carcinogenesis *23*, 541–547.

Attardi, L.D., Lowe, S.W., Brugarolas, J., and Jacks, T. (1996). Transcriptional activation by p53, but not induction of the p21 gene, is essential for oncogene-mediated apoptosis. EMBO J. *15*, 3693–3701.

Avantaggiati, M.L., Ogryzko, V., Gardner, K., Giordano, A., Levine, A.S., and Kelly, K. (1997). Recruitment of p300/CBP in p53-dependent signal pathways. Cell *89*, 1175–1184.

Ayton, P.M., and Cleary, M.L. (2001). Molecular mechanisms of leukemogenesis mediated by MLL fusion proteins. Oncogene *20*, 5695–5707.

Barlev, N.A., Liu, L., Chehab, N.H., Mansfield, K., Harris, K.G., Halazonetis, T.D., and Berger, S.L. (2001). Acetylation of p53 activates transcription through recruitment of coactivators/histone acetyltransferases. Mol. Cell *8*, 1243–1254.

Brown, C.E., Howe, L., Sousa, K., Alley, S.C., Carozza, M.J., Tan, S., and Workman, J.L. (2001). Recruitment of HAT complexes by direct activator interactions with the ATM-related Tra1 subunit. Science *292*, 2333–2337.

Brownell, J.E., and Allis, C.D. (1996). Special HATs for special occasions: linking histone acetylation to chromatin assembly and gene activation. Curr. Opin. Genet. Dev. *6*, 176–184.

Brunger, A.T. (1993). X-PLOR version 3.1: a system for X-Ray crystallography and NMR, version 3.1 (New Haven, CT: Yale University Press).

Carson, M. (1991). Ribbons 2.0. J. Appl. Crystallogr. *24*, 958–961.

Clore, G.M., and Gronenborn, A.M. (1994). Multidimensional heteronuclear nuclear magnetic resonance of proteins. Methods Enzymol. *239*, 349–363.

Dhalluin, C., Carlson, J.E., Zeng, L., He, C., Aggarwal, A.K., and Zhou, M.-M. (1999). Structure and ligand of a histone acetyltransferase bromodomain. Nature *399*, 491–496.

Dorr, A., Kiermer, V., Pedal, A., Rackwitz, H.-R., Henklein, P., Schubert, U., Zhou, M.-M., Verdin, E., and Ott, M. (2002). Transcriptional synergy between Tat and PCAF is dependent on the binding of acetylated Tat to the PCAF bromodomain. EMBO J. *21*, 2715–2733.

El-Deiry, W.S., Tokino, T., Velculescu, V.E., Levy, D.B., Parsons, R., Trent, J.M., Lin, D., Mercer, W.E., Kinzler, K.W., and Vogelstein, B. (1993). WAF1, a potential mediator of p53 tumor suppression. Cell *75*, 817–825.

El-Deiry, W.S., Tokino, T., Waldman, T., Oliner, J.D., Velculescu, V.E., Burrell, M., Hill, D.E., Healy, E., Rees, J.L., Hamilton, S.R., et al. (1995). Topological control of p21WAF1/CIP1 expression in normal and neoplastic tissues. Cancer Res. *55*, 2910–2919.

Friedman, J.R., Fredericks, W.J., Jensen, D.E., Speicher, D.W., Huang, X.P., Neilson, E.G., and Rauscher, F.J., III. (1996). KAP-1, a novel corepressor for the highly conserved KRAB repression domain. Genes Dev. *10*, 2067–2078.

Fuchs, S.Y., Adler, V., Pincus, M.R., and Ronai, Z. (1998a). MEKK1/JNK signaling stabilizes and activates p53. Proc. Natl. Acad. Sci. USA *95*, 10541–10546.

Fuchs, S.Y., Fried, V.A., and Ronai, Z. (1998b). Stress-activated kinases regulate protein stability. Oncogene *17*, 1483–1490.

Giordano, A., and Avantaggiati, M.L. (1999). p300 and CBP: partners for life and death. J. Cell. Physiol. *181*, 218–230.

Gu, W., and Roeder, R.G. (1997). Activation of p53 sequence-specific DNA binding by acetylation of the p53 C-terminal domain. Cell *90*, 595–606.

Guo, A., Salomoni, P., Luo, J., Shih, A., Zhong, S., Gu, W., and Paolo Pandolfi, P. (2000). The function of PML in p53-dependent apoptosis. Nat. Cell Biol. *2*, 730–736.

Hassan, A.H., Prochasson, P., Neely, K.E., Galasinski, S.C., Chandy, M., Carrozza, M.J., and Workman, J.L. (2002). Function and selectivity of bromodomains in anchoring chromatin-modifying complexes to promoter nucleosomes. Cell *111*, 369–379.

Haupt, Y., Maya, R., Kazaz, A., and Oren, M. (1997). Mdm2 promotes the rapid degradation of p53. Nature *387*, 296–299.

Haynes, S.R., Dollard, C., Winston, F., Beck, S., Trowsdale, J., and Dawid, I.B. (1992). The bromodomain: a conserved sequence found in human, *Drosophia* and yeast proteins. Nucleic Acids Res. *20*, 2603.

Hudson, B.P., Martinez-Yamout, M.A., Dyson, H.J., and Wright, P.E. (2000). Solution structure and acetyl-lysine binding activity of the GCN5 bromodomain. J. Mol. Biol. *304*, 355–370.

Hupp, T.R., and Lane, D.P. (1994). Allosteric activation of latent p53 tetramers. Curr. Biol. *4*, 865–875.

Ito, A., Lai, C.H., Zhao, X., Saito, S., Hamilton, M.H., Appella, E., and Yao, T.P. (2001). p300/CBP-mediated p53 acetylation is commonly induced by p53-activating agents and inhibited by MDM2. EMBO J. *20*, 1331–1340.

Ito, A., Kawaguchi, Y., Lai, C.H., Kovacs, J.J., Higashimoto, Y., Appella, E., and Yao, T.P. (2002). MDM2-HDAC1-mediated deacetylation of p53 is required for its degradation. EMBO J. *21*, 6236–6245.

Jacobson, R.H., Ladurner, A.G., King, D.S., and Tjian, R. (2000). Structure and function of a human TAFII250 double bromodomain module. Science *288*, 1422–1425.

Jeanmougin, F., Wurtz, J.M., Douarin, B.L., Chambon, P., and Losson, R. (1997). The bromodomain revisited. Trends Biochem. Sci. *22*, 151–153.

Ko, L.J., and Prives, C. (1996). p53: puzzle and paradigm. Genes Dev. *10*, 1054–1072.

Kubbutat, M.H., Jones, S.N., and Vousden, K.H. (1997). Regulation of p53 stability by Mdm2. Nature *387*, 299–303.

Kwok, R.P., Laurance, M.E., Lundblad, J.R., Goldman, P.S., Shih, H., Connor, L.M., Marriott, S.J., and Goodman, R.H. (1996). Control of cAMP-regulated enhancers by the viral transactivator Tax through CREB and the co-activator CBP. Nature *380*, 642–646.

Laskowski, R.A., Rullmannn, J.A., MacArthur, M.W., Kaptein, R., and Thornton, J.M. (1996). AQUA and PROCHECK-NMR: programs for checking the quality of protein structures solved by NMR. J. Biomol. NMR *8*, 477–486.

Lavau, C., Du, C., Thirman, M., and Zeleznik-Le, N. (2000). Chromatin-related properties of CBP fused to MLL generate a myelodysplastic-like syndrome that evolves into myeloid leukemia. EMBO J. *19*, 4655–4664.

Levine, A.J. (1997). p53, the cellular gatekeeper for growth and division. Cell *88*, 323–331.

Li, M., Luo, J., Brooks, C.L., and Gu, W. (2002). Acetylation of p53 inhibits its ubiquitination by Mdm2. J. Biol. Chem. *277*, 50607–50611.

Liedman, D., and Zeleznik-Le, N. (2001). Retroviral transduction model of mixed lineage leukemia fused to CREB binding protein. Curr. Opin. Hematol. *8*, 218–223.

Lill, N.L., Grossman, S.R., Ginsberg, D., DeCaprio, J., and Livingston, D.M. (1997). Binding and modulation of p53 by p300/CBP coactivators. Nature *387*, 823–827.

Liu, L., Scolnick, D.M., Trievel, R.C., Zhang, H.B., Marmorstein, R., Halazonetis, T.D., and Berger, S.L. (1999). p53 sites acetylated in vitro by P/CAF and p300 are acetylated in vivo in response to DNA damage. Mol. Cell. Biol. *19*, 1202–1209.

Luo, J., Su, F., Chen, D., Shiloh, A., and Gu, W. (2000). Deacetylation of p53 modulates its effect on cell growth and apoptosis. Nature *408*, 377–381.

Manning, E.T., Ikehara, T., Ito, T., Kadonaga, J.T., and Kraus, W.L. (2001). p300 forms a stable, template-committed complex with chromatin: role for the bromodomain. Mol. Cell. Biol. *21*, 3876–3887.

Marmorstein, R., and Berger, S.L. (2001). Structure and function of bromodomains in chromatin-regulating complexes. Gene *272*, 1–9.

Miyashita, T., and Reed, J.C. (1995). Tumor suppressor p53 is a direct transcriptional activator of the human bax gene. Cell *80*, 293–299.

Momand, J., and Zambetti, G.P. (1997). Mdm-2: "big brother" of p53. J. Cell. Biochem. *64*, 343–352.

Mujtaba, S., He, Y., Zeng, L., Farooq, A., Carlson, J.E., Ott, M., Verdin, E., and Zhou, M.-M. (2002). Structural basis of lysine-acetylated HIV-1 Tat recognition by P/CAF bromodomain. Mol. Cell *9*, 575–586.

Nakamura, S., Roth, J.A., and Mukhopadhyay, T. (2000). Multiple lysine mutations in the C-terminal domain of p53 interfere with MDM2-dependent protein degradation and ubiquitination. Mol. Cell *20*, 9391–9398.

Nilges, M., and O'Donoghue, S. (1998). Ambiguous NOEs and automated NOE assignment. Prog. NMR Spectrosc. *32*, 107–139.

Owen, D.J., Ornaghi, P., Yang, J.C., Lowe, N., Evans, P.R., Ballario, P., Neuhaus, D., Eiletici, P., and Travers, A.A. (2000). The structural basis for the recognition of acetylated histone H4 by the bromodomain of histone acetyltransferase gcn5p. EMBO J. *19*, 6141–6149.

Pearson, M., Carbone, R., Sebastiani, C., Cioce, M., Fagioli, M., Saito, S., Higashimoto, Y., Appella, E., Minucci, S., Pandolfi, P.P., et al. (2000). PML regulates p53 acetylation and premature senescence induced by oncogenic Ras. Nature *406*, 207–210.

Prives, C., and Hall, P.A. (1999). The p53 pathway. J. Pathol. *187*, 112–126.

Sakaguchi, K., Herrera, J.E., Saito, S., Miki, T., Bustin, M., Vassilev, A., Anderson, C.W., and Appella, E. (1998). DNA damage activates p53 through a phosphorylation-acetylation cascade. Genes Dev. *12*, 2831–2841.

Sali, A., and Blundell, T. (1993). Comparative protein modelling by satisfaction of spatial restraints. J. Mol. Biol. *234*, 779–815.

Scolnick, D.M., Chehab, N.H., Stavridi, E.S., Lien, M.C., Caruso, L., Moran, E., Berger, S.L., and Halazonetis, T.D. (1997). CREB-binding protein and p300/CBP-associated factor are transcriptional coactivators of the p53 tumor suppressor protein. Cancer Res. *57*, 3693–3696.

Sobulo, O.M., Borrow, J., Tomek, R., Reshmi, S., Harden, A., Schlegelberger, B., Housman, D., Doggett, N.A., Rowley, J.D., and Zeleznik-Le, N.J. (1997). MLL is fused to CBP, a histone acetyltransferase, in therapy-related acute myeloid leukemia with a t(11;16)(q23,p13.3). Proc. Natl. Acad. Sci. USA *94*, 8732–8737.

Sterner, D.E., Grant, P.A., Roberts, S.M., Duggan, L.J., Belotserkovskaya, R., Pacella, L.A., Winston, F., Workman, J.L., and Berger, S.L. (1999). Functional organization of the yeast SAGA complex: distinct components involved in structural integrity, nucleosome acetylation, and TATA-binding protein interaction. Mol. Cell. Biol. *19*, 86–98.

Tamkun, J.W., Deuring, R., Scott, M.P., Kissinger, M., Pattatucci, A.M., Kaufman, T.C., and Kennison, J.A. (1992). brahma: a regulator of *Drosophila* homeotic genes structurally related to the yeast transcriptional activator SNF2/SWI2. Cell *68*, 561–572.

Tang, H.Y., Zhao, K., Pizzolato, J.F., Fonarev, M., Langer, J.C., and Manfredi, J.J. (1998). Constitutive expression of the cyclin-dependent kinase inhibitor p21 is transcriptionally regulated by the tumor suppressor protein p53. J. Biol. Chem. *273*, 29156–29163.

Travers, A. (1999). Chromatin modification: how to put a HAT on the histones. Curr. Biol. *9*, 23–25.

Vo, N., and Goodman, R.H. (2001). CREB-binding protein and p300 in transcriptional regulation. J. Biol. Chem. *276*, 13505–13508.

Vogelstein, B., Lane, D., and Levine, M.J. (2000). Surfing the p53 network. Nature *408*, 307–310.

Wang, Y., and Prives, C. (1995). Increased and altered DNA binding of human p53 by S and G2/M but not G1 cyclin-dependent kinases. Nature *376*, 88–91.

Winston, F., and Allis, C.D. (1999). The bromodomain: a chromatin-targeting module? Nat. Struct. Biol. *6*, 601–604.

Yamazaki, T., Lee, W., Arrowsmith, C.H., Mahandiram, D.R., and Kay, L.E. (1994). A suite of triple resonance NMR experiments for the backbone assignment of 15N, 13C, 2H labeled proteins with high sensitivity. J. Am. Chem. Soc. *116*, 11655–11666.

Yin, Y., Liu, Y.X., Jin, Y.J., Hall, E.J., and Barrett, J.C. (2003). PAC1 phosphatase is a transcription target of p53 in signalling apoptosis and growth suppression. Nature *422*, 527–531.

Zeng, L., and Zhou, M.-M. (2001). Bromodomain: an acetyl-lysine binding domain. FEBS Lett. *513*, 124–128.

Zhao, R., Gish, K., Murphy, M., Yin, Y., Notterman, D., Hoffman, W.H., Tom, E., Mack, D.H., and Levine, A.J. (2000). Analysis of p53-regulated gene expression patterns using oligonucleotide arrays. Genes Dev. *14*, 981–993.

Accession Numbers

Coordinates for the three-dimensional structure of the CBP bromodomain/p53 peptide complex have been deposited in the Brookhaven Protein Data Bank under the accession code 1JSP.